Plug Repairs of Marine Glass Fiber / Vinyl Ester Laminates Subjected to Uniaxial Tension

by

Alexandros Michelis

Bachelor of Science in Marine Engineering
Hellenic Naval Academy, 1999

Submitted to the Department of Mechanical Engineering
in Partial Fulfillment of the Requirements for the Degrees of

Naval Engineer

and

Master of Science in Mechanical Engineering

at the
Massachusetts Institute of Technology
June 2009

Signature of Author .....
Department of Mechanical Engineering
May 8, 2009

Certified by .....
James H. Williams, Jr.
School of Engineering Professor of Teaching Excellence
Thesis Supervisor

Certified by .....
Mark S. Welsh
Professor of the Practice of Naval Construction and Engineering
Thesis Supervisor

Accepted by .....
David E. Hardt
Ralph E. and Eloise F. Cross Professor of Mechanical Engineering
Chairman, Department Committee on Graduate Students

Plug Repairs of Marine Glass Fiber / Vinyl Ester Laminates Subjected to Uniaxial Tension

by

Alexandros Michelis

Submitted to the Department of Mechanical Engineering,
on May 8, 2009 in Partial Fulfillment of the
Requirements for the Degrees of Naval Engineer and
Master of Science in Mechanical Engineering

Abstract

Glass fiber/vinyl ester composite laminates are currently being used and proposed for the hulls, bulkheads, and superstructures of large ships. This thesis examines the effectiveness of the repair of such laminates using glass fiber/vinyl ester chopped strand mat plugs to fill circular holes.

The stress distributions around circular holes in various glass fiber/vinyl ester woven roving laminates subjected to uniaxial tension are calculated before and after repairs using plug materials of different fiber volume fractions. The orthotropic laminates ranged from balanced to unidirectional woven rovings, and the chopped strand mat plug fiber volume fractions ranged from 0 to 0.40.

The effectiveness of the plug in reducing the laminate stresses increased monotonically with increasing fiber volume fraction, reducing the maximum laminate stress to about 60% of the unrepaired laminate stress at a plug fiber volume fraction of 0.40.

Thesis Supervisor: James H. Williams, Jr
Titles: School of Engineering Professor of Teaching Excellence, Charles F. Hopewell Faculty Fellow, Professor of Writing and Humanistic Studies

Thesis Supervisor: Mark S. Welsh
Title: Professor of the Practice of Naval Construction and Engineering

Acknowledgments

I wish to express my deepest appreciation to the following:

- My thesis supervisor, Professor James H. Williams Jr., for his invaluable mentoring, guidance, support and patience.
- My thesis supervisor, Professor Mark S. Welsh, for his advice and support.
- My wife, Garyfallia Aikaterini Vlachou, for her love, understanding, patience and support.
- My parents, Nikolaos Michelis and Eleni Micheli, and my sister, Maria Micheli, for their love and concern.
- The Hellenic Navy for the financial support of my graduate studies at MIT.

I am also grateful for the financial contribution of the DDG-1000 Program Manager (NAVSEA PMS 500) and the technical guidance of the DDG-1000 Ship Design Manager (NAVSEA 05D).

Table of Contents

List of Figures

List of Tables

1. Introduction

1.1 General

1.1.1 Application of composites to naval surface ships

The use of fiber-reinforced polymer (FRP) composite materials in naval surface ships has its roots in the effort of the marine industry to optimize ship designs in terms of weight, damage tolerance, and cost. The aim is to construct the entire ship or parts of the ship's structure as lightweight and corrosion resistant as possible, without compromise to structural strength and durability, and at the lowest overall cost.

The application of FRP composites meets this challenge because certain types of composites, such as glass-reinforced plastic (GRP), combine good mechanical properties with low weight and excellent corrosion resistance. Studies show that a patrol boat (up to 55 m long and 300 tons displacement) made of GRP has a structural weight that is 10% less than a comparable aluminum boat and more than 35% less than a comparable steel boat [1-3]. For larger ships, like corvettes (~85 m long and 1200 tons displacement), the structural weight savings could be as much as 30%, with a full-load displacement reduction up to 21 % [2]. The lower structural weight allows naval ship designers to increase the military payload and to achieve higher speed [1-5].

A key parameter in the assessment of FRP composite use in naval surface ships is cost. In general, the construction cost of a composite patrol boat is estimated to be about 30% higher than of an equivalent steel boat [2]. On the other hand, a comparative analysis conducted by Goubalt and Mayes [3] suggested that the operating cost of a composite patrol boat is less than of a similar steel design, resulting in a lower life-cycle cost. In particular, the reduced maintenance cost due to the corrosion resistance of composites and the lower fuel consumption due to the reduced structural weight could effectively mean a life-cycle cost of a composite patrol boat of 6% less than for an equivalent steel boat [3]. For corvettes, life-cycle cost savings of up to 15% could be achieved [2].

In surface ship building, FRP composites can be utilized for the construction of both primary and secondary structures [1, 2]. A summary of these structures where FRP composite materials can be applied is listed in Table 1 [1, 2].

Table 1: Ship structures for potential application of FRP composites [1, 2, 6].

Structure Classification	Structure Type
Primary	- Hulls and hovercraft skirts - Superstructures - Masts - Propulsion systems (propulsors and propulsion shafts)
Secondary	- Funnels and stacks - Bulkheads, decks, doors and hatches - Enclosures and shields - Rudders and stabilizing flaps - Machinery and engine components - Engine and equipment foundations - Heat exchangers and pressure vessels - Piping - Ventilation ducts - Deck gratings

1.1.1.1 Material characteristics of glass fiber / vinyl ester composites used in naval surface ships

The majority of composites used in marine applications are based on glass fibers, with some exceptions in which carbon fibers are utilized either for local strengthening of the structure or occasionally for the complete hull construction [1-3, 5-16]. Glass fibers come in two main types: E-glass and S-glass fibers. E-glass fibers are typically used in ship building, while S-glass fibers are used in the aerospace industry for special applications requiring higher performance [17]. S-glass has approximately 35% higher strength, better fatigue resistance, and better retention of mechanical properties at

elevated temperatures than E-glass [6, 18]. A summary of typical properties of E-glass and carbon fibers can be seen in Table 2 [7].

Table 2: Summary of typical properties of E-glass and carbon fibers [7].

Fiber Material	Density [g/cm^3]	Tensile Strength [MPa]	Tensile Modulus [GPa]	Ultimate Elongation [%]	1995 Cost [$/lb]
E-Glass (24 oz WR)	2.60	3450	72.45	4.8	1.14
Carbon-PAN	1.76	2415-4830	227-393	0.38-2.0	12

Relative to carbon fibers, E-glass is a material exhibiting high strength, low stiffness and low cost [18]. Glass strands may be chopped into short lengths (5 mm to 50 mm) for direct use in spray-up laminating, or may be treated with an emulsion or powder binder and bound together into a loose fabric with more or less random fiber orientation, resulting in a material called chopped-strand mat (CSM) [4, 8]. "The grades of CSM commonly used in ship fabrication have weights in the range 300 g/m^2 to 900 g/m^2" [8]. A variation of mat is the continuous stand mat, which has longer strands than CSM, and thus possesses improved mechanical properties compared to CSM [18]. Glass strands can also be combined to form rovings, which can be woven into a coarse fabric called woven roving (WR). Laminates made of mat are only 33-50% as strong as fabric laminates of comparable thickness [18].

WR material is usually of plain weave with a balanced or biased configuration. Specifically, a balanced fabric has an equal distribution of fibers along the warp and weft directions, while a biased configuration has an unequal fiber distribution in the warp and weft directions, based on the desired properties of the final product. Weights of WR commonly employed in hand or automated laminating of ship and boat hulls range from 200 to 900 g/m^2, although weights up to 4000 g/m^2 may be employed [8]. As an example, DF1400 WR of weight 1350 g/m^2 is used for the monocoque hull construction of the Huon Class minehunting vessels of the Royal Australian Navy [19]. For marine structural applications, a 50% **glass fiber** weight fraction is preferred for WR [17]. WR alternating

with layers of mat is also a common marine construction material, which is often referred to as a pair [9]. The use of mat between consecutive plies of WR provides better interlaminar shear strength in laminates than a pure WR configuration [6, 20]. As an example, Duomat® 1230 (1230 g/m^2, WR 920 and CSM 300, stitched) and Duomat® 1960 (1960 g/m^2, WR 1500 and CSM 450, stitched) are used for the construction of the superstructure and deck skins, respectively, of the Huon Class minehunters [19].

In warship designs and large marine structures, mostly balanced or nearly balanced WR and unidirectional tapes are utilized, while CSM is used scarcely [6, 21]. Most U.S. Navy construction uses only WR [6]. The use of a CSM layer on the outer surface of the ship hull is recommended as a protective barrier from water ingress to the underlying WR layers [11, 22]. According to Chalmers [4], "fibers can now be woven or knitted into three-dimensional arrangements giving an almost unlimited choice of strength paths, constrained only by the necessity for wetting-out the fibers with resin, and by the cost of the initial loom set-up."

Polyester and **vinyl ester** are the most widely used resin systems in marine applications [1, 6, 16, 17, 22]. **Vinyl ester** in particular is becoming very popular in marine construction because it demonstrates good structural performance combined with excellent corrosion and chemical resistance, and excellent resistance to water absorption [6, 15-18, 22]. **Vinyl ester** falls between polyester and epoxy in terms of cost and performance [17, 18]. It exhibits higher failure strain, up to 6-9%, compared to 2-3% for common polyesters [8, 20, 23]. GRP composites with **vinyl ester** matrices have significantly better delamination strength (>25%) compared to laminates with an isophthalic polyester resin matrix [10].

Additionally, **glass fiber / vinyl ester** composites exhibit improved toughness compared to **glass fiber** / polyester composites, not only due to the tougher matrix, but also because **vinyl ester** composites do not suffer from debonds and subcritical cracks after curing to the extent that polysester-based composites do [15, 24]. Typical processing methods for **vinyl ester** composites are hand lay-up, Resin Transfer Molding (RTM), Vacuum Assisted Resin Transfer Molding (VARTM) and filament winding. The disadvantage of **vinyl ester** compared to polyester resins is its higher cost [7, 16, 18], but

this is not an overriding drawback when higher material cost can be justified by enhanced performance.

1.1.1.2 Construction of surface ship hulls with FRP composites

The composite structures employed in naval ship hull construction can be divided into the following four major categories [1, 2, 7, 8, 11]:

- Framed single skin construction.
- Corrugated construction.
- Monocoque (frame-less) construction.
- Sandwich construction.

Examples of a framed single skin construction, a corrugated construction and a monocoque construction for a minehunting vessel hull design are shown in Figure 1.

The framed single skin is the most common construction form for the manufacturing of hulls, decks and bulkheads in large and small GRP hulls. In the framed single skin construction, the hull consists of a thin FRP laminate shell stiffened with longitudinal and transverse frames. The hull thickness is about 10 mm to 15 mm. The stiffeners are usually of a "hat" section type and are formed by involving the lay-up of strips of reinforcements (prepregs) over trapezoidal foam formers. The presence of the stiffeners effectively reduces the unsupported span of shell or deck panels and provides torsional stability under lateral or compressive loads. As a result, the framed single skin hull displays adequate stiffness combined with excellent impact and underwater blast resistance.

Another type of stiffening has the form of corrugations on the outer shell, resulting in a corrugated structure. The corrugations are aligned in the direction of dominant in-plane or bending stress. This kind of structure provides a number of advantages compared to a conventional framed single skin design. Firstly, it displays higher stiffness and strength, resulting in substantial weight saving. At the same time, it has 25% lower construction cost because there is no need for separate fabrication of stiffeners. Finally, it improves the reliability and impact resistance of the structure by eliminating most of the bonded stiffener attachments.

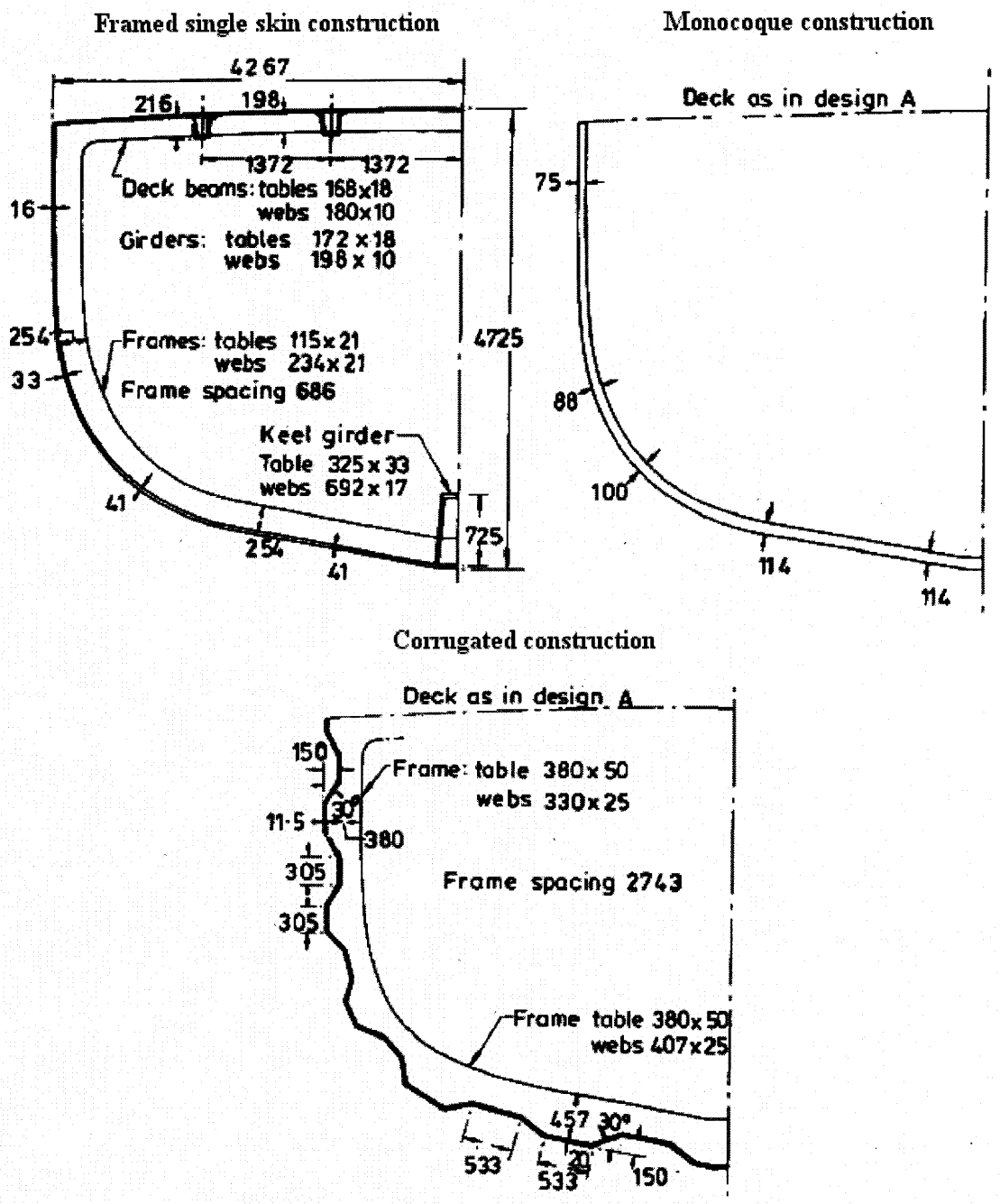

Figure 1: Alternative minehunting vessel hull designs [8]. (Dimensions in mm)

The monocoque construction does not make use of a hull framing system in order to achieve the required hull stiffness. Instead, it consists of a thick laminate hull without the addition of longitudinal and transverse frames. In this case, designers are able to design a structure that can withstand hull-bending and hydrostatic loads by varying the thickness of the composite laminate from ~50 mm near the main deck to ~180 mm at the

keel of the ship [19]. In some applications the thickness of the laminate can reach values up to 230 mm [6]. Decks and main bulkheads also contribute to the overall stiffness of the hull structure. Although this type of hull construction is suitable for automated construction, it carries a large weight penalty. Monocoque hulls can be more than 10% heavier than similar framed single-skin designs.

The sandwich construction consists of thin FRP face skins over a thick core of medium density polyvinyl chloride foam or polyurethane foam or end grain balsa. The skins provide high stiffness and strength to the structure, while the core provides high shear resistance and low total weight [1, 2, 7, 8, 11, 23]. The sandwich construction can be monocoque, without additional stiffening, or framed. A monocoque sandwich construction provides smooth surfaces on both sides of the hull [23]. As an example, monocoque sandwich composites are utilized for the construction of yacht hulls that participate in the America's Cup. In this application, thin and stiff skins, combined with relatively thick cores, provide the required hull stiffness. On the other hand, framed sandwich construction permits the use of softer skins and core materials.

1.1.1.3 Construction of surface ship superstructures with FRP composites

Beyond hull manufacturing, FRP composites are utilized for the construction of superstructures of naval surface ships [1, 2]. In more conservative approaches, only elements of the superstructure, such as the helicopter hangar or the masts, are manufactured with composite materials.

A comparison between traditional superstructures made of steel or aluminum and composite superstructures reveals that the latter offers a number of advantages [1, 2, 5]. The use of FRP composites instead of steel lowers the structural weight of the superstructure and provides better corrosion resistance and fatigue performance. Compared to aluminum, FRP composites provide better corrosion resistance, fatigue performance and fire resistance.

It is estimated that composite superstructures are 30% to 40% lighter than equivalent steel structures [1]. Depending on the type of composite and the amount of steel framing, the weight savings in a single skin composite structure stiffened by a steel frame, can reach values up to 70% [2, 5]. The lower topside weight translates into better

stability and seakeeping performance of the design, while increasing the payload, endurance and speed [5]. In contrast, composite superstructures are about 30% heavier than similar aluminum structures [2]. The corrosion and fatigue resistance of FRP composites means that less maintenance and fewer repairs of the structure are required. Høyning and Taby [5] proposed the use of FRP composites instead of aluminum for deckhouses and superstructures, because in the case of fire, aluminum without fire insulation tends to loose strength, conduct heat from space to space, and melt. However, the use of FRP composites increases the manufacturing cost of the superstructure by 18% to 50% [1, 2]. Studies have shown that the cost of a composite superstructure with applied radar signature reduction is 40% higher than the cost of a similar steel structure [5].

Other estimates indicate an increase in the cost for composite superstructures of medium-sized frigates up to 140% [2, 5]. This can be a prohibitive factor for the use of composites when low acquisition cost is a requirement for the design. On the other hand, "the key parameters in the cost comparison can change significantly if the weight saving obtained by composites is used to optimize the hull shape and thereby increase speed or reduce the cost of the machinery, reduce fuel consumption, or increase fuel or weapon capacity" [5]. Finally, the radar cross-section of composite superstructures, which is an extremely important attribute for naval ships, is reduced significantly [5, 14, 21]. GRP does not provide proper electromagnetic reflection properties on its own, but its surface "can be made reflective without adding weight of significant cost" [5].

The thickness of the laminate in composite superstructures, made with framed single skin construction, varies roughly from 3 mm to 25 mm [3]. The U.S. Navy has evaluated and demonstrated successfully the Seemann Composites Resin Injection Molding Process (SCRIMP) for the fabrication of hat-stiffened panels with skin thicknesses of ~8 mm and ~14.5 mm [13]. These panels can be utilized for the construction of composite deckhouse, mast and foundation structures. Studies have showed that a sandwich construction consisting of glass fiber / polyester face skins, with thickness of 2 mm to 4 mm, and balsa core, with thickness of 40 mm to 60 mm, could effectively be used for the construction of composite superstructures [5].

1.1.2 Repair schemes for composites and their application to the marine industry

1.1.2.1 Introduction to impact damage and repair of marine composites

A marine composite structure can be damaged in service due to mechanical loading or environmental conditions [1]. In particular, the marine structures are highly susceptible to impact damage throughout their lifetime (slamming due to waves and concentrated impacts) [17, 25]. Impact damage of composites is a combination of three types of damage: fracture of fibers, delaminations between laminas and through-thickness splits along the fibers [11]. The impact resistance of marine composites depends on "the toughness of the resin matrix, the quality of the fiber-matrix interface bond, and the toughness of the fibers" [17]. Under ideal conditions, GRP laminates can absorb elastically up to 15 times more impact energy than similar steel or aluminum plates [21]. "However, fabricated GRP structures are likely to have less overall impact strength than equivalent steel or aluminum structures in which large amounts of energy can be absorbed by plastic deformation."

The impact can be both of low and high velocity, while the resulting damage can be of penetrating or non-penetrating nature [10]. Low-velocity impact damage can occur either locally, such as a weight being dropped onto a surface, or from more general collision between objects (for example, impact of the hull with a floating object). Beyond the conventional cases of impact damage, a case of special interest for naval applications is the battle inflicted high velocity impact damage. This special category of impact damage includes damage due to projectiles and fragments. Warships may also be damaged by explosions, either underwater or air blast (mine detonations, explosions close to the structure from artillery shells, blasts from incoming missiles destroyed by the ship's hard-kill system, or pressure waves from nuclear explosions) [5].

The purpose of any repair depends on the level to which the composite structure properties need to be restored. In particular, the objective of repair can be identified as follows:

- Restoration of surface profile.
- Restoration of static strength and stiffness.
- Restoration of fatigue performance and long-term durability.

Depending on the type, repair environment and structural significance of the composite structure, the implemented repair may display the following characteristics [1, 26]:

- Minimum weight penalty.
- Simple application process and tooling.
- Use of readily available and easily storable repair materials.
- Removal as little sound material as possible.
- Minimum degradation or damage of the region surrounding the area under repair.
- Minimum downtime of equipment.
- Minimum total cost.

The repair schemes can be classified based on their structural or non-structural nature. Table 3 provides a summary of this classification [1]. The repair of minor surface damage is not crucial unless aesthetic reasons apply or the long-term degradation of the properties of the composite structure must be considered. On the other hand, the repair of delaminations, broken fibers and joint failures is crucial when the structural integrity or the water-tightness of the vessel is compromised. A non-structural repair, such as a cosmetic repair, can be performed in an uncontrolled environment, but structural repairs demand a strict control of the environmental conditions [27].

Although suggested requirements for bonded repair are enclosed area, temperature and humidity control, and isolation of the cleaned surface of the laminate prior to bonding, it is most favorable that the repair be conducted outdoors under realistic shipyard conditions and even under bad weather conditions. This is extremely important for repairs related to the structural integrity and survival of a ship deployed far from its base or a repair facility, where depot level repairs can be performed. In naval applications, the repairs are desired to be of field level, with quick application, undertaken directly on the ship (on site), and in a situation where skilled personnel and / or adequate facilities are unavailable. This level of repair becomes more significant when it concerns battle damage repairs on warships.

Table 3: Description of damage types [1].

Damage Type	Repair Classification	Damage Description
Non-structural	Mark and Monitor	This approach is undertaken when the nature of the damage does not warrant any form of repair. With this technique, it is necessary to record all information about the nature of the damage in order to be able to compare any worsening of the defect while the structure is subjected to operational loading.
	Cosmetic	Cosmetic repairs are designed to repair localized surface defects to the original profile and to prevent moisture ingress.
	Temporary	Temporary repairs are to be conducted only when there are operational reasons that prevent the recommended repair approach. These types of repairs must be made permanent at the next designated maintenance period.
Structural	Minor	Structural minor restoration of the structure to full serviceability, requiring though increased inspection frequencies to ensure that the repair remains effective.
	Major	Major restoration of the composite structure to its original integrity.

1.1.2.2 Nondestructive evaluation of damage in marine composites

Damage assessment is an important step prior to repair. It involves a series of inspections and evaluations in order to determine the extent of the damage. In the case of damaged composites, the accurate detection of the damaged region is a complex task because the damaged area can extend internally into the laminate via delamination beyond the region identified visually. For example, in a military aircraft, a projectile of 23 mm in diameter can leave a hole 25 mm in diameter surrounded by a 15 mm or larger delaminated strip [28]. Thus, accurate and reliable damage assessment methods are required in order to detect and evaluate the damage, and to assess the quality of the performed repair, without harming the composite structure.

Several nondestructive evaluation (NDE) methods are available for damage assessment on composites in aerospace applications [17, 29, 30], but only a fraction of them is applicable to marine composites [31]. The main restrictions are the increased thickness of marine composite structures compared to the thickness of the composites utilized in aerospace industry, and the distinctive characteristics of marine composite structures (structure's geometry, type of construction, and accessibility of the site to be inspected). The large thickness of marine composites, which can reach the extreme value of ~200 mm at the keel of a composite hull, especially makes the inspection of the structure by NDE methods a challenging task [19]. The primary NDE methods used by the marine industry (beyond visual inspection) are [19, 29, 31]:

- Ultrasonic pulse-echo.
- Infrared thermography.
- Automated coin tapping.

1.1.2.3 Repair schemes for marine composites

Several of the most common repair schemes for marine structures are the following:

- Patch (lap) repair and flush patch repair.
- Scarf repair or step repair.
- Resin infusion repair.

Patch and scarf repairs are intended to "restore the load path removed by the damage, ideally, without significantly changing the original load distribution" [26]. Patch repairs are used for repairing minor structural damage to small marine crafts with hulls thinner than 10 mm, or for repairing secondary structures (decks or superstructures) on large composite ships, when a scarf repair is not applicable [1]. In the patch repair technique, the repair material can be applied either on one or both sides of the composite structure. A patch repair can be easily and quickly applied while the boat is dockside or at sea. Patches rarely recover more than 70% of the original strength. Flush patch repairs are a special category of a patch repair in which the patches are placed inside the hole created by the removal of the damaged area.

A scarf repair is the most common type of composite repair for marine applications reviewed by the various repair manuals [27, 32-34]. It can be single-sided, double-sided or a partial-repair, depending on the type and the extent of inflicted damage, and it may include the addition of extra applies over the scarf region (doubler). A scarf repair is more structurally efficient than a patch repair; it can restore up to 90% of the original stiffness and strength of the original structure [1]. Compared to a patch repair, it demands a more complex application requiring special skills, and is more expensive and time-consuming.

A step repair is a type of scarf repair. In a scarf repair the damaged laminate is removed and the edges of the sound laminate are tapered back at a shallow angle ($\theta<5°$), while in a step repair a rectangular stepped surface is created by cutting into the composite to a set depth and peeling out material within this area along the level of the laminate. When applied in thick laminates, scarf and step repairs have the disadvantage of requiring removal of a large amount of sound material around the damaged region because of the shallow scarf angles required [26].

The resin infusion repair method is a relatively new technique [1]. It is utilized for the restoration of minor structural damage in single-skin laminates and for repairing disbonds between the skin and core of sandwich composites [1, 26, 27]. The resin infusion repair procedure involves the injection of a compatible thermosetting resin into the delaminated or disbonded region, directly (if the damaged area is exposed) or through injection holes [26]. The process often requires preheating of the damaged area, and pressure and temperature application, in order to improve the mating of the delaminated surfaces. For the repair of delaminations in hull laminates and debonding of the internal stiffener frames, Trask, Turton and Lay [35] and Elliott and Trask [36] recommended a resin infusion repair technique similar to that employed by the SCHRIMP resin transfer molding process. By utilizing this technique, "typically, 1 m section of debonded stiffener could be fully repaired in five hours by two technicians, without an extended period out of service and with minimal technical support other than that which can be carried on site."

1.1.2.4 Alternative repair schemes for marine composites

The American Bureau of Shipping (ABS) [32] and United States Navy [33] demonstrated a repair in way of through bolt failure on single-skin laminates in the form of a plug combined with a partial scarf. In particular, the proposed repair process included the following steps [32, 33]:

- Removal of the damaged laminate around the bolt hole to a diameter at least 50 mm.
- Addition of a backing plate on one side of the hole and securing of it with either screws or resin putty.
- Filling the hole with resin putty.
- Introduction of a single side scarf repair made of GRP on the side of the plate without the backing plate, with chopped strand mat as a first ply.
- Removal of the backing plate and addition of a backup ply on the far side of the hole.

According to the Design Standard of the UK Navy [27], in GRP marine structures, plug repairs could be applied either for minor repair of localized impact damage of the hull that does not exceed 50 mm in diameter or for the repair of holes created by the extraction of core plug samples from the hull for testing. The plug material was the epoxy system UW43 (potting resin, manufacturer: Wessex Resins). It could be applied alone or in combination with a patch consisting of up to seven plies of chopped strand mat and woven roving. The repair procedure offered by the Design Standard of the UK Navy for the application of plug repair for the minor repair of localized impact damage is provided in Table 4 [27].

Wegman and Tullos [37] recommended the use of the plug concept as part of repair schemes applied in special cases:

- For the repair of non-structural composite laminates containing minor damage, they suggested the use of an adhesive plug combined with two plies of glass cloth applied to the external face of the laminate.
- For the repair of non-structural composite laminates containing major damage, they proposed the use of a plug made from the same material as the parent laminate combined with two plies of glass cloth applied to the external face of

the laminate. In this case, the plug was ~0.8 mm smaller on all sides than the hole in the original panel and the remaining cavity was filled with a paste adhesive.

Table 4: Repair procedure for application of plug repair for minor repair of localized impact damage of hull that does not exceed 50 mm in diameter [27].

Step 1	The damaged area is prepared with a bevel of 10^{o} to 15^{o}. The overlap area on the surface surrounding the damage is rubbed down until the glass fibers are exposed. Grease and dust are cleaned off by using a good detergent.	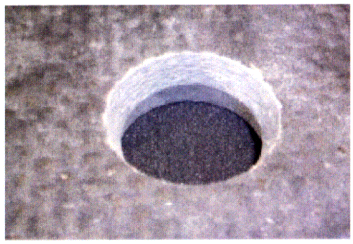
Step 2	A former (backing plate) following the contour of the structure is secured to the laminate. A wax parting agent must be used on the former to ensure a smooth, polished surface is attained.	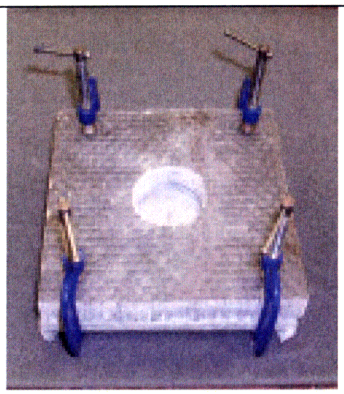
Step 3	The UW43 resin system is applied. After the setting of the resin, the outer surface of the repair may be sanded as necessary.	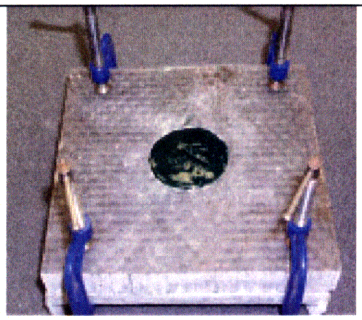

Baker, Dutton and Kelly [26] proposed plug repair techniques for minor repairs such as minor depressions and indentations, skin damage and core replacement in honeycomb panels, and fastener hole elongation. Particularly, they suggested, along with Baker [38], the use of the plug concept as a repair method for the following cases:

- In the case of lightly loaded sandwich composites with honeycomb panels where the composite skin has been penetrated, potted repairs could be applied in order to stabilize the skin and to seal the damaged region. The potting compound could be a compatible resin mixed with either chopped **glass fibers** or ultrafine glass sphere fillers.
- Damage to attachment holes, such as minor hole elongation or wear, could be repaired by filling the hole with a potting compound, provided the bearing loads are low.

An alternative approach was to plug the cavity with glass cloth / epoxy prepeg or wet lay-up [26, 38].

Armstrong, Bevan and Cole [17] recommended the application of the plug repair scheme in the form of a potted repair in the case of a small hole found in a sandwich composite with honeycomb core. The hole could be filled with a potting compound in order to prevent water ingression until a permanent repair could be applied.

Vaidya, Basappa, Mathew and Sands [39] investigated the concept of the plug repair scheme, alone or combined with doublers, as a repair method for S2-glass / **vinyl ester** laminates manufactured by using the VARTM technique and bearing damage "in the form of clean hole representative of perforation type of impact."

Damaged and repaired specimens made of S2-glass / **vinyl ester** were subjected to fatigue flexural loading. One of the repair schemes considered was plugging the hole with epoxy mixed with either micro-balloons or E-glass chopped strand mat. The performed fatigue tests revealed that for a specimen with a hole 12.7 mm in diameter filled with a micro-balloon / epoxy plug, the fatigue life efficiency was 85.14% of the pristine sample, compared to 37.97 % of the same specimen with unfilled hole. For a specimen with a hole 25.4 mm in diameter filled with micro-balloon / epoxy plug, the fatigue life efficiency was 57.55 % of the pristine sample, compared to 37.26 % for the same specimen with an unfilled hole. Furthermore, they demonstrated that samples repaired with the combination of a plug made of micro-balloon / epoxy plug and carbon / epoxy doublers bonded on both sides of the clean hole could exceed the fatigue efficiency of the undamaged sample.

Hundman and Horn [40] examined the effect of bonding a solid plug in a centrally located hole on the stress concentration around the hole in a composite plate, in order to evaluate the repaired strength of damaged composite panels subjected to in-plane loads. Their theoretical analysis was based on Lekhnitskii's theoretical solutions [41]. They also conducted finite element analyses and experimental testing in order to evaluate the bonded plug repair concept and to validate and refine their analytical predictions.

Both the plate and plug were made of Hercules AS4 graphite fibers in a polyetheretherketone (PEEK) thermoplastic matrix, using the same stacking sequence. The plugs were bonded into the circular cutouts of the plates by utilizing either PEEK adhesive layers melted with the application of eddy currents or room temperature curing epoxy paste adhesive (ATACS 4103). They concluded that the plug concept could be an effective method of reducing stress concentrations around holes in repaired composite panels by 50% or more, depending on the application.

Vlattas and Soutis [42] measured the compressive strength of carbon fiber / epoxy laminates made of HTA/913C standard pre-preg with centrally located circular holes filled with solid plugs, made of the same material by using the same lay-up. The specimens were 215 mm in length, 50 mm in width and 3 mm thick (24 plies, $[(\pm 45/0_2)_3]_s$), and the drilled holes had a diameter of 10 mm. A standard high strength adhesive (Araldite 2011) was used for the bonding of the plug. By fitting the plug in the hole, the increase of the measured residual compressive strength was of the order of approximately 10%.

1.2 Definition of the problem and thesis overview

In general, a repair scheme used for non-structural or structural restoration of a composite structure should be the simplest and least intrusive. At the same time, a repair method should be able to restore structural stiffness and strain capability to the required level, without compromising other functions of the component or structure. The plug concept seems to be an attractive repair scheme in terms of application speed, simplicity, required skills and impact on the composite structure, but it is not clear if it can be utilized for other than cosmetic, minor or temporary repairs.

Numerous analytical solutions, finite element analyses and experimental data exist for patch and scarf repair schemes, especially for applications in the aerospace industry [26, 43-48]. Although some studies on the plug repair concept also exist [28, 39, 40, 42], the application of the plug repair scheme for the repair of **glass fiber / vinyl ester** marine composites has not been studied so extensively.

The main issue addressed in this thesis is whether a plug repair scheme, using **glass fiber / vinyl ester** chopped strand mat (CSM) as the plug material, can be applied for the repair of **glass fiber / vinyl ester** marine composites. The analyses to be conducted will examine the effect of a CSM plug on the stress distribution around a hole in a **glass fiber / vinyl ester** laminate, subjected to a uniaxial tensile stress. A reduction in the stresses around the hole due to the presence of the plug will translate into an increase in the strength of the damaged **glass fiber / vinyl ester** laminate. The aim is to investigate if the plug repair scheme can be utilized only as a temporary or cosmetic measure, or has the potential as a permanent repair, at least, for lightly loaded **glass fiber / vinyl ester** marine structures.

A potential procedure for the application of **glass fiber / vinyl ester** chopped strand mat plug repair on a damaged **glass fiber / vinyl ester** laminate is summarized in Table 5.

Table 5: Repair procedure for glass fiber / vinyl ester chopped strand mat plug repair applied in glass fiber / vinyl ester laminate.

Step 1	The damaged area of the **glass fiber / vinyl ester** laminate is removed by cutting a circular hole in the plate. The sound material inside and around the hole is first sanded and then cleaned of dust and other contaminants.	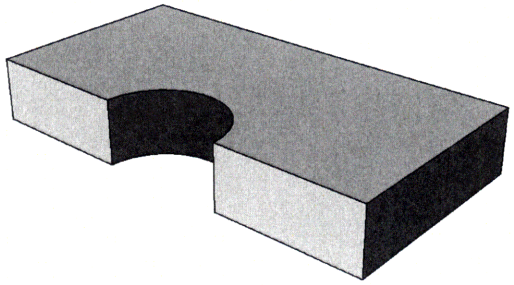
Step 2	A backing plate is secured with screws or resin putty on the laminate.	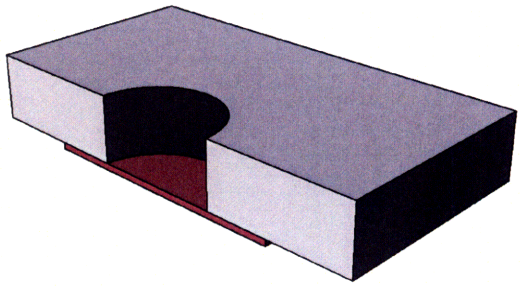
Step 3	The hole is filled with **glass fiber / vinyl ester** chopped strand mat.	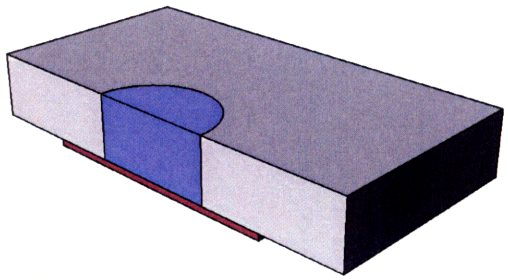
Step 4	The backing plate is removed after the curing of the **glass fiber / vinyl ester** chopped strand mat plug.	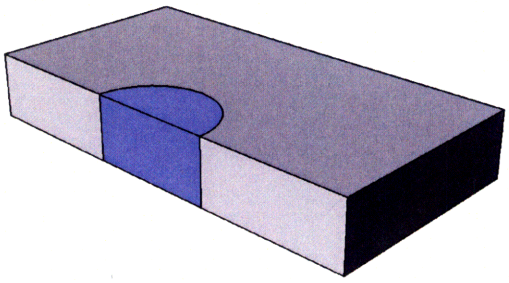

2. Analytical approach of the plug repair scheme

2.1 Constitutive properties of glass fiber / vinyl ester woven roving and chopped strand mat materials

The first step in the present analysis is the calculation of the constitutive properties for the **glass fiber / vinyl ester** woven roving (WR) and chopped strand mat (CSM) materials. The analytical calculation of these properties is provided in Appendices A and B for the **glass fiber / vinyl ester** WR and the **glass fiber / vinyl ester** CSM, respectively. The WR is modeled as an orthotropic material, while the CSM as an isotropic.

A summary of the constitutive properties of the **glass fiber / vinyl ester** WR is given in Table 6, whereas a summary of the constitutive properties of the **glass fiber / vinyl ester** CSM is given in Table 7. The properties of all the laminates presented in Table 6 correspond to a 29.2% fiber volume fraction. In Table 6 and 7, E is the elastic modulus, G is the shear modulus, and v is the Poisson's ratio.

Table 6: Constitutive properties of glass fiber / vinyl ester woven roving (WR) laminates, where the listed fiber percentage corresponds to the x-direction.

Material	E_x [GPa]	E_y [GPa]	G_{xy} [GPa]	v_{xy}
Balanced WR	23.42	23.42	8.86	0.09
WR 60% biased	26.45	20.38	8.86	0.11
WR 70% biased	29.49	17.34	8.86	0.12
WR 80% biased	32.53	14.30	8.86	0.15
WR 90% biased	35.56	11.27	8.86	0.19
Unidirectional	38.60	8.23	8.86	0.26

Table 7: Constitutive properties of glass fiber / vinyl ester chopped strand mat (CSM) plugs.

Property	Fiber volume fraction V_f [%]												
	0	2	5	6	10	13	16	20	23	27	31	36	40
E [GPa]	3.40	4.00	4.66	5.38	6.16	6.99	7.90	8.88	9.95	11.13	12.42	13.86	15.48
G [GPa]	1.25	1.48	1.73	2.00	2.29	2.61	2.95	3.31	3.71	4.15	4.64	5.18	5.79
v	0.36	0.35	0.35	0.34	0.34	0.34	0.34	0.34	0.34	0.34	0.34	0.34	0.34

2.2 Lekhnitskii's theoretical solutions

The mathematical approach of the plug repair scheme that follows is based on Lekhnitskii's theoretical solutions [41]. Lekhnitskii offered a number of expressions that can be utilized to evaluate the stress distribution in an anisotropic homogeneous plate having an elliptical or circular opening and deformed by stresses applied along the plate edges. The plate was assumed to be infinite, so any effects of the external plate edge were disregarded. A summary of the cases presented by Lekhnitskii is provided in Table 8.

Table 8: Schematics of cases analyzed by Lekhnitskii's analytical solutions for plate with hole unfilled or filled with plug and subjected to in-plane loading [41].

	Cases	
1	**Tension applied in one direction on orthotropic plate with circular unfilled hole (Lekhnitskii [41], pp. 171-190)**	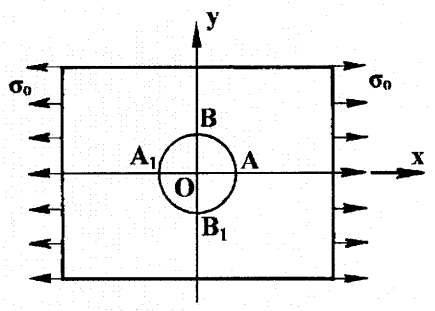

	Cases	
2	**Tension applied in one direction on orthotropic plate with circular plugged hole (Lekhnitskii [41], pp. 197-203)**	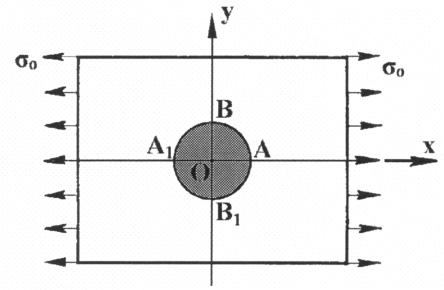
3	**Tension applied in two directions on orthotropic plate with circular plugged hole (Lekhnitskii [41], pp. 203-207)**	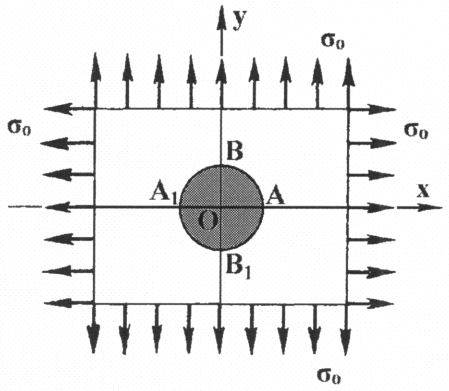
4	**Shear stress applied along edges of orthotropic plate with circular plugged hole (Lekhnitskii [41], pp. 207-211)**	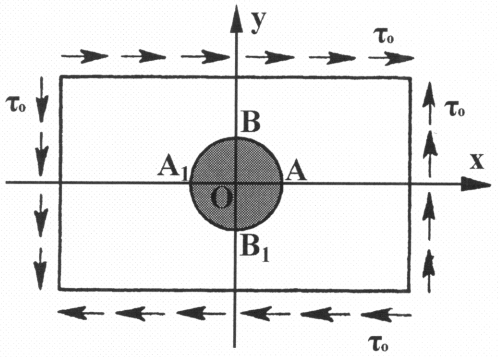
5	**In-plane bending of orthotropic plate with circular plugged hole (Lekhnitskii [41], pp. 212-216)**	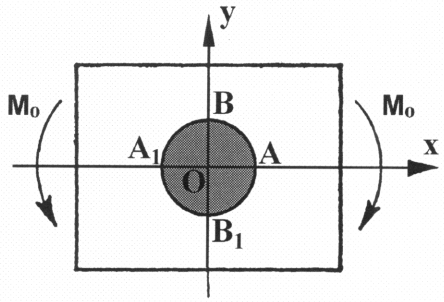

2.3 Glass fiber / vinyl ester composite plate with unfilled circular hole, subjected to tensile load

Let us first examine the stress field along the edge of an unfilled hole in an infinitely wide thin composite plate under a far-field tensile stress by considering the two-dimensional geometry in Figure 2. The plate is rectangular and corresponds to an orthotropic laminate made of **glass fiber / vinyl ester** woven roving. The applied stress is parallel to the plane of the plate and aligned with the x-direction, which is a principal material direction of the laminate. The uniformly distributed tensile stress σ_o acts along the two edges of the plate, as shown in Figure 2. For our analysis, we employ two coordinate systems, one Cartesian and one polar.

The origin of both coordinate systems is the center of the hole. In the Cartesian system, the axes x and y are the principal directions of elasticity of the woven roving. In the polar coordinate system, θ is the polar angle measured from the x axis and r is the radius measured from the center of the circular hole. The radius of the hole is a.

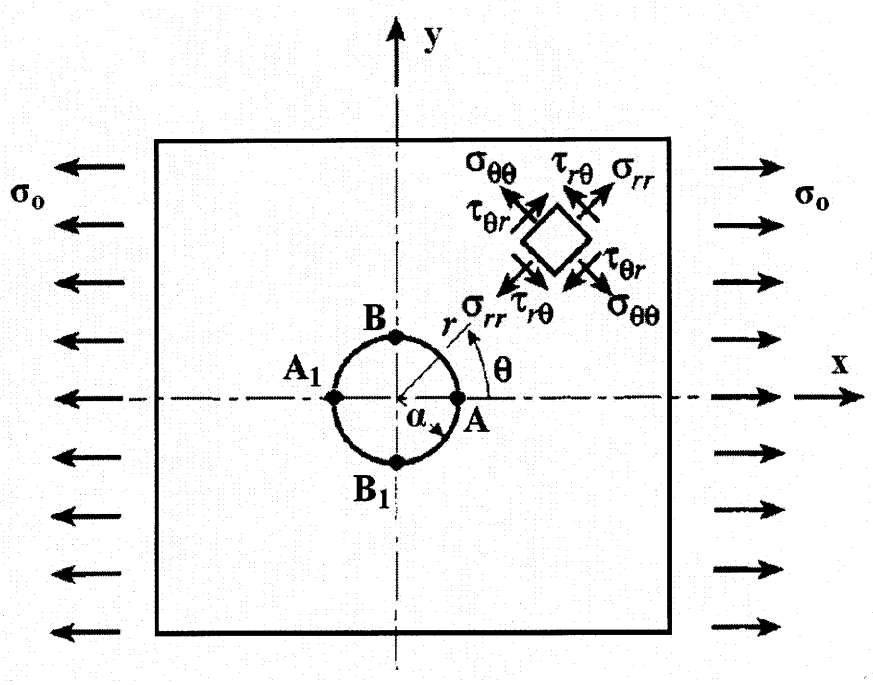

Figure 2: Two-dimensional plate with circular hole under uniaxial tensile stress.

The analysis considers the plate to be an elastic body obeying the generalized Hooke's law. The components of strain are linear functions of the components of stress.

The stress condition is plane stress, so the normal stress σ_{zz} and both out-of-plane shear stresses are zero. For a thin laminated plate in which the fibers are parallel to the x-y plane and the plate is loaded by uniformly distributed stresses along the edges, the plane-stress condition provides approximate results for the stresses with reasonable accuracy [49-51]. Thus, the stress field throughout the plate can be examined using the two-dimensional geometry of Figure 2.

For a homogeneous isotropic plate subjected to a uniaxial stress in the x-direction, the stresses around the unfilled hole in polar coordinates σ_{rr}, $\sigma_{\theta\theta}$, and $\tau_{r\theta}$ are given by [50]

$$\sigma_{rr} = \frac{1}{2}\sigma_o[(1-\frac{a^2}{r^2}) + (1+\frac{3a^4}{r^4} - \frac{4a^2}{r^2})\cos 2\theta] \tag{1}$$

$$\sigma_{\theta\theta} = \frac{1}{2}\sigma_o[(1+\frac{a^2}{r^2}) - (1+\frac{3a^4}{r^4})\cos 2\theta] \tag{2}$$

$$\tau_{r\theta} = -\frac{1}{2}\sigma_o(1-\frac{3a^4}{r^4} + \frac{2a^2}{r^2})\sin 2\theta \tag{3}$$

The stresses around the unfilled hole in the Cartesian coordinate system σ_{xx}, σ_{yy}, and τ_{xy} can be expressed in terms of the stresses in polar coordinates σ_{rr}, $\sigma_{\theta\theta}$, and $\tau_{r\theta}$ as [50]

$$\sigma_{xx} = \sigma_{rr}\cos^2\theta + \sigma_{\theta\theta}\sin^2\theta - 2\tau_{r\theta}\sin\theta\cos\theta \tag{4}$$

$$\sigma_{yy} = \sigma_{rr}\sin^2\theta + \sigma_{\theta\theta}\cos^2\theta + 2\tau_{r\theta}\sin\theta\cos\theta \tag{5}$$

$$\tau_{xy} = (\sigma_{rr} - \sigma_{\theta\theta})\sin\theta\cos\theta + \tau_{r\theta}(\cos^2\theta - \sin^2\theta) \tag{6}$$

At the boundary of the hole (r=a), Equations (1)-(3) give

$$\sigma_{rr}(r=a) = 0 \tag{7}$$

$$\sigma_{\theta\theta}(r=a) = \sigma_o(1-2\cos 2\theta) \tag{8}$$

$$\tau_{r\theta}(r=a) = 0 \tag{9}$$

If Equations (7)-(9) are substituted into Equations (4)-(6), expressions for the stresses in Cartesian coordinates ate the edge of the hole are obtained

$$\sigma_{xx}(r=a)=\sigma_{\theta\theta}\sin^2\theta \tag{10}$$

$$\sigma_{yy}(r=a)=\sigma_{\theta\theta}\cos^2\theta \tag{11}$$

$$\tau_{xy}(r=a)=-\sigma_{\theta\theta}\sin\theta\cos\theta \tag{12}$$

Equations (10)-(12) show that the stresses in Cartesian coordinates σ_{xx}, σ_{yy}, and τ_{xy} along the edge of the hole are a function only of the tangential stress $\sigma_{\theta\theta}$ and the angle θ.

2.4 Glass fiber / vinyl ester composite plate with unfilled circular hole, subjected to tension in one direction

In order to evaluate the stresses around the hole edge due to the applied remote tensile stress, Lekhnitskii's [41] analytical solution for the stress distribution in an orthotropic plate with a circular hole is used. The laminate's engineering constants in the formulation are the Young's modulus in the x-direction E_x, the Young's modulus in the y-direction E_y, the in-plane Poisson's ratio ν_{xy}, and the in-plane shear modulus G_{xy}. We also introduce the Young's modulus in the direction tangent to the hole E_θ.

The circumferential stress $\sigma_{\theta\theta}$, along the edge of an unfilled hole in an orthotropic laminate, subjected to a uniaxial stress in the x-direction, is given by Lekhnitskii [41] as

$$\sigma_{\theta\theta}=\sigma_o\frac{E_\theta}{E_x}[-k\cos^2\theta+(1+n)\sin^2\theta] \tag{13}$$

where

$$E_\theta=[\frac{\sin^4\theta}{E_x}+(\frac{1}{G_{xy}}-\frac{2\nu_{xy}}{E_x})\sin^2\theta\cos^2\theta+\frac{\cos^4\theta}{E_y}]^{-1} \tag{14}$$

$$k=\sqrt{\frac{E_x}{E_y}} \tag{15}$$

$$n=\sqrt{2(\frac{E_x}{E_y}-\nu_{xy})+\frac{E_x}{G_{xy}}} \tag{16}$$

and where E_x, E_y, G_{xy} and v_{xy} are laminate properties defined above.

By combining Equations (10), (11) and (13), we can evaluate the stresses σ_{xx} and σ_{yy}. The distribution of stress $\sigma_{\theta\theta}$, σ_{xx} and σ_{yy} will be symmetrical with respect to both principal directions x and y. Referring to Figure 2, at points A and A_1 of the hole boundary (where θ is 0^o and 180^o, respectively), $\sigma_{\theta\theta}$ will obtain the value

$$\sigma_{\theta\theta} = \sigma_o \frac{E_\theta}{E_x}(-k) = \sigma_o \frac{E_y}{E_x}(-k) = \sigma_o \frac{1}{k^2}(-k) = -\frac{\sigma_o}{k} \tag{17}$$

At points B ($\theta=90^o$) and B_1 ($\theta=270^o$), $\sigma_{\theta\theta}$ becomes

$$\sigma_{\theta\theta} = \sigma_o \frac{E_\theta}{E_x}(1+n) = \sigma_o \frac{E_x}{E_x}(1+n) = \sigma_o(1+n) \tag{18}$$

As Lekhnitskii notes, one of these values of tangential stress $\sigma_{\theta\theta}$ will be the largest in magnitude for the entire laminate, "but it is impossible to know beforehand which one without knowing the elastic constants." Depending on the material and the geometry examined, the largest stress could be either the tensile stress at points B and B_1, or the compressive stress at points A and A_1.

For a laminate made of **glass fiber / vinyl ester** balanced woven roving (WR) having engineering constants E_x = *23.76 GPa*, E_y = *23.76 GPa*, v_{xy} = *0.0914*, and G_{xy} =*8.86 GPa* as shown in Table 6, the distribution of stress $\sigma_{\theta\theta}$, σ_{xx}, and σ_{yy} around the hole edge is presented in Figure 3. Only the stress values corresponding to the arc AB (0^o-90^o) are plotted due to the aforementioned symmetry. As noted earlier, a balanced WR is a fabric that has an equal distribution of fibers along the warp and weft directions. In our case, the warp and weft directions of the WR are aligned with the coordinate axe x and y, respectively, and in a balanced laminate the percentage of fibers in the x-direction is equal to the percentage of fibers in the y-direction.

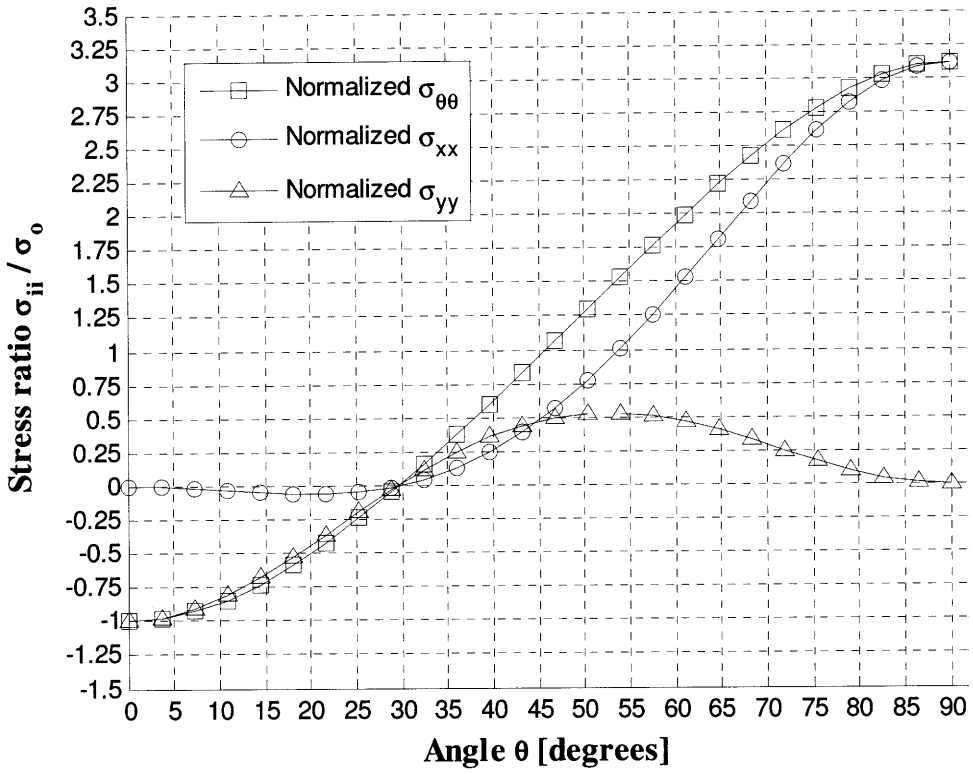

Figure 3: Stresses $\sigma_{\theta\theta}$, σ_{xx} and σ_{yy} around edge of circular unfilled hole in orthotropic laminate of glass fiber / vinyl ester balanced woven roving (WR) due to uniaxial tension σ_o in x-direction

As anticipated, the maximum $\sigma_{\theta\theta}$ and σ_{xx} stresses around the edge of the hole (r = a) are significantly higher than the applied stress. The largest absolute stress on the plate is the tensile stress at points B and B_1. The ratio of the greatest tensile stress to the greatest compressive stress is approximately three.

Konish and Whitney [52], Tan [53, 54] and Barbero [55] provide mathematical expressions for the calculation of the stress concentration factor (SCF) for an orthotropic plate of infinite width containing an elliptical or circular hole. For a balanced symmetric laminate under uniaxial in-plane loading, such as our case, the SCF $K_{t\infty}$ can be expressed in terms of laminate properties as [55]

$$K_{t\infty} = 1 + \sqrt{2(\sqrt{\frac{E_x}{Ey}} - \nu_{xy} + \frac{E_x}{2G_{xy}})} \tag{19}$$

For the balanced WR in Table 6, Equation (19) gives a stress concentration factor $K_{t\infty}$ equal to 3.11, which agrees with the result of Leknitskii's mathematical model ($\frac{\sigma_{\theta\theta}\max}{\sigma_o}$ =3.11). Note that the SCF for a homogeneous isotropic plate is 3.00.

Figure 4 shows the variation of the circumferential stress $\sigma_{\theta\theta}$ on an unfilled hole as a function of the angle θ for each of the woven roving laminates in Table 6. It is evident that the material of the laminate has significant effect on the magnitude of the maximum stress at the boundary of the hole. The smallest value of stress $\sigma_{\theta\theta}$ corresponds to the case of a balanced WR laminate.

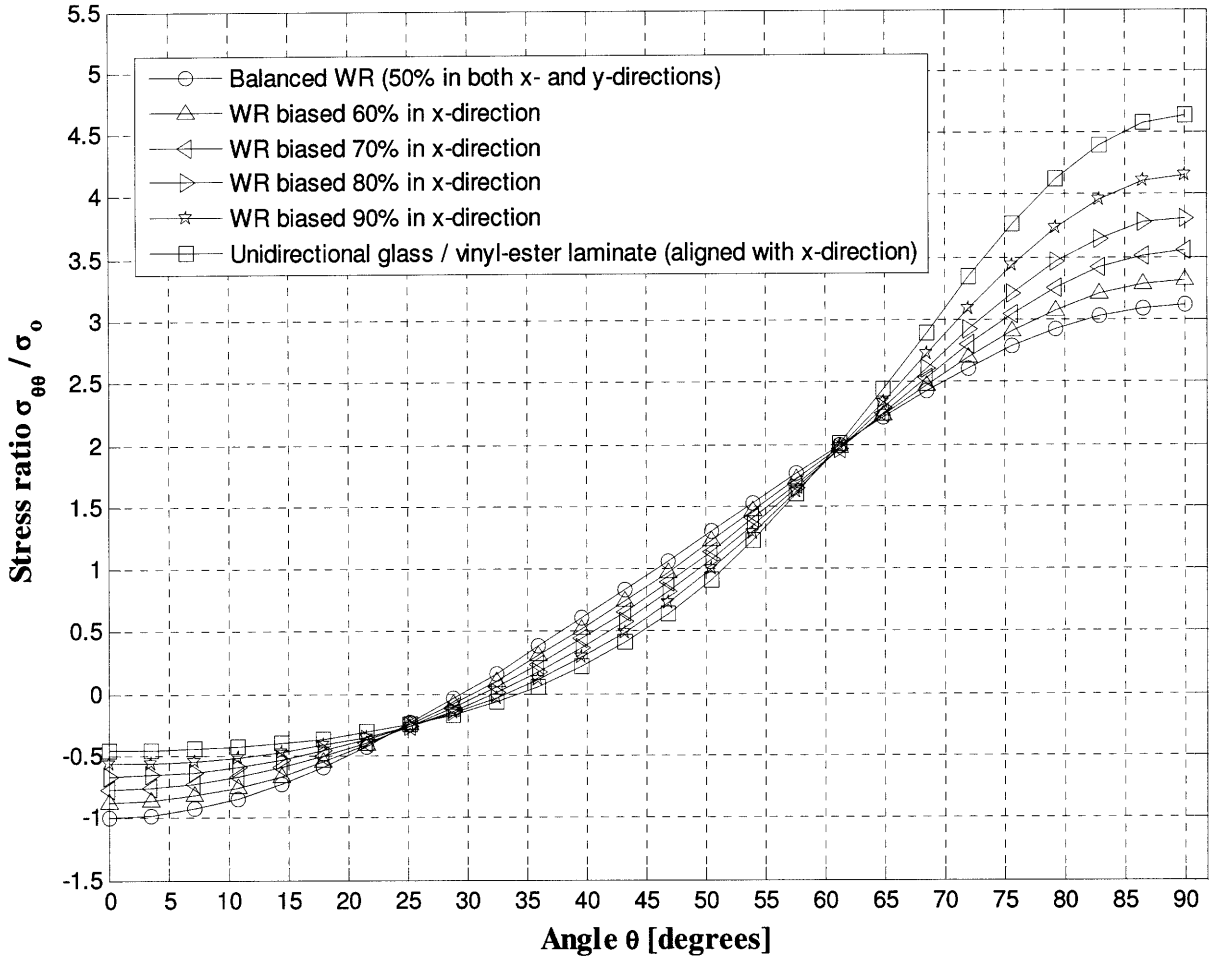

Figure 4: Stress $\sigma_{\theta\theta}$ around edge of unfilled hole for different types of glass fiber / vinyl ester woven roving (WR) laminates.

2.5 Glass fiber / vinyl ester laminate with circular hole filled with glass fiber / vinyl ester plug, subjected to tension in one direction

Consider the geometry in Figure 2 but containing a circular hole filled with a plug of **glass fiber / vinyl ester** chopped strand mat (CSM). Again, we make use of Lekhnitskii's analytical solutions and, in particular, the mathematical model for the stress distribution in an orthotropic plate with a circular filled hole. This model was derived by using a complex variables solution technique. In particular, Lekhnitskii superposed the stresses for a plate without a plug with those of an infinite plate with a hole. The

boundary conditions at the edge of the cutout were modified accordingly to represent the effect of the plug's presence. Lekhnitskii's solution assumed the same thickness of the laminate and plug, and perfect bonding between the plug and the hole boundary. It is expected that the introduction of the plug in a damaged plate will decrease the stresses around the hole.

The tangential stress $\sigma_{\theta\theta}$ in the laminate along the edge of the hole is given by [41]

$$\begin{aligned}\sigma_{\theta\theta} = \frac{\sigma_o}{\Delta}\frac{E_\theta}{E_x}\{&(\Delta - q_1)\sin^6\theta + [\Delta(n^2-2k) + (k+n)q_1 + (1+2k)q_2 \\ &-(2+k)(1+n)q_3]\sin^4\theta\cos^2\theta + [k^2\Delta - (1+2k)(k+n)q_2 + \\ &k(2+k)q_3 + k(1+n)q_4]\sin^2\theta\sin^2\theta\cos^4\theta - k^2 q_4\cos^6\theta\}\end{aligned} \tag{20}$$

where Δ, q_1, q_2, q_3, and q_4 are parameters given by

$$\begin{aligned}\Delta = &(q_{11}q_{22} + q_{11}'q_{22}')k + q_{22}(q_{66} + 2q_{12}') + (q_{11}q_{22}'k + q_{22}q_{11}')n \\ &-(q_{12} - q_{12}')^2 k\end{aligned} \tag{21}$$

$$q_1 = (q_{11} - q_{11}')q_{22}(n^2 - k) + [(q_{11} - q_{11}')q_{22} + (q_{12} - q_{12}')^2]kn - q_{22}(q_{12} - q_{12}') \tag{22}$$

$$q_2 = (q_{11} - q_{11}')q_{22} + q_{11}(q_{12} - q_{12}')k(1+n) \tag{23}$$

$$q_3 = (q_{11} - q_{11}')(q_{22}n + q_{22}'k) + q_{22}(q_{12} - q_{12}') + (q_{12} - q_{12}')^2 k \tag{24}$$

$$q_4 = -(q_{11} - q_{11}')q_{22}' + (q_{12} - q_{12}')[2q_{12} + q_{66} + q_{11}(k+n)] - (q_{12} - q_{12}')^2 \tag{25}$$

q_{11}, q_{12}, q_{22}, q_{16}, q_{26}, and q_{66} are independent elastic compliances and are expressed in terms of the engineering constants E_x, E_y, ν_{xy} and G_{xy} of the plate material as

$$q_{11} = \frac{1}{E_x} \tag{26}$$

$$q_{22} = \frac{1}{E_y} \tag{27}$$

$$q_{12} = -\frac{\nu_{xy}}{E_x} \tag{28}$$

$$q_{66} = \frac{1}{G_{xy}} \tag{29}$$

$$q_{16} = q_{26} = 0 \tag{30}$$

q_{11}', q_{12}', q_{22}', q_{16}', q_{26}', and q_{66}' are the elastic compliances of the plug and can be expressed in terms of the plug's engineering constants E_x', E_y', v_{xy}' and G_{xy}' as

$$q_{11}' = \frac{1}{E_x'} \tag{31}$$

$$q_{22}' = \frac{1}{E_y'} \tag{32}$$

$$q_{12}' = -\frac{\nu_{xy}'}{E_x'} \tag{33}$$

$$q_{66}' = \frac{1}{G_{xy}'} \tag{34}$$

$$q_{16}' = q_{26}' = 0 \tag{35}$$

Since in our analysis the plug material (CSM) is isotropic, the plug's constitutive properties become $E_x' = E_y' = E$, $v_{xy}' = v$ and $G_{xy}' = G$, where E, G, and v, are given in Table 7. Equations (31)-(34) therefore become

$$q_{11}' = q_{22}' = \frac{1}{E} \tag{36}$$

$$q_{12}' = -\frac{\nu}{E} \tag{37}$$

$$q_{66}' = \frac{1}{G} \tag{38}$$

By combining Equations (10), (11) and (20), we can compute the distribution of stresses σ_{xx} and σ_{yy} at the boundary of the hole for any given combination of laminate and plug material. For a laminate of **glass fiber / vinyl ester** balanced WR and plugs made of **glass fiber / vinyl ester** CSM of varying fiber volume fractions V_f, the distributions of σ_{xx}

and σ_{yy} around the boundary of the hole are plotted in Figure 5 and Figure 6, respectively. As in Figure 3, only the stresses corresponding to the arc AB (0^o-90^o) are plotted due to the symmetry with respect to both principal directions x and y. The engineering constants utilized for Figure 3 and Figure 4 are given in Table 6 and Table 7.

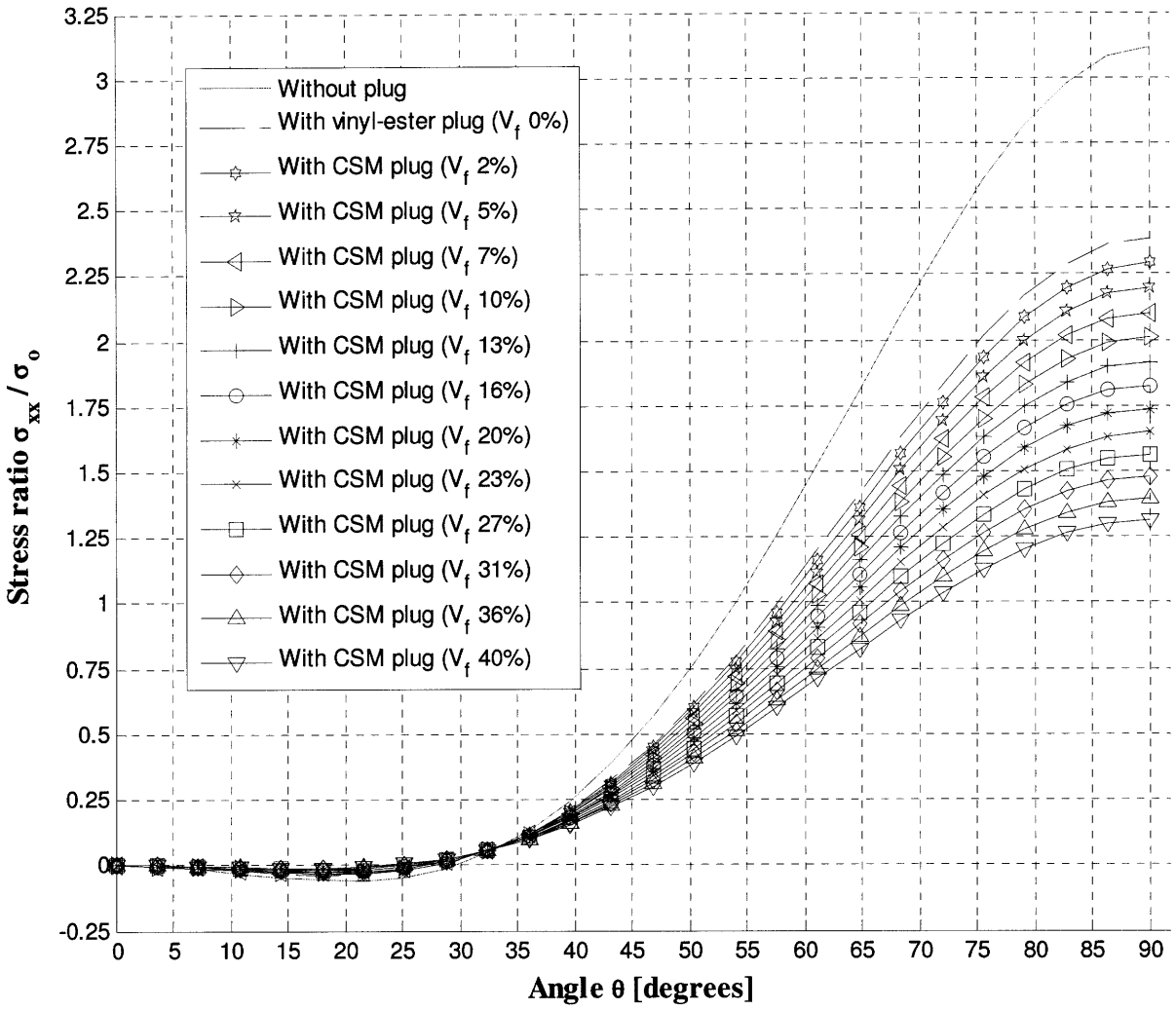

Figure 5: Stress σ_{xx} around hole in glass fiber / vinyl ester laminate of balanced woven roving containing various plugs, and subjected to uniaxial tension σ_o in x-direction.

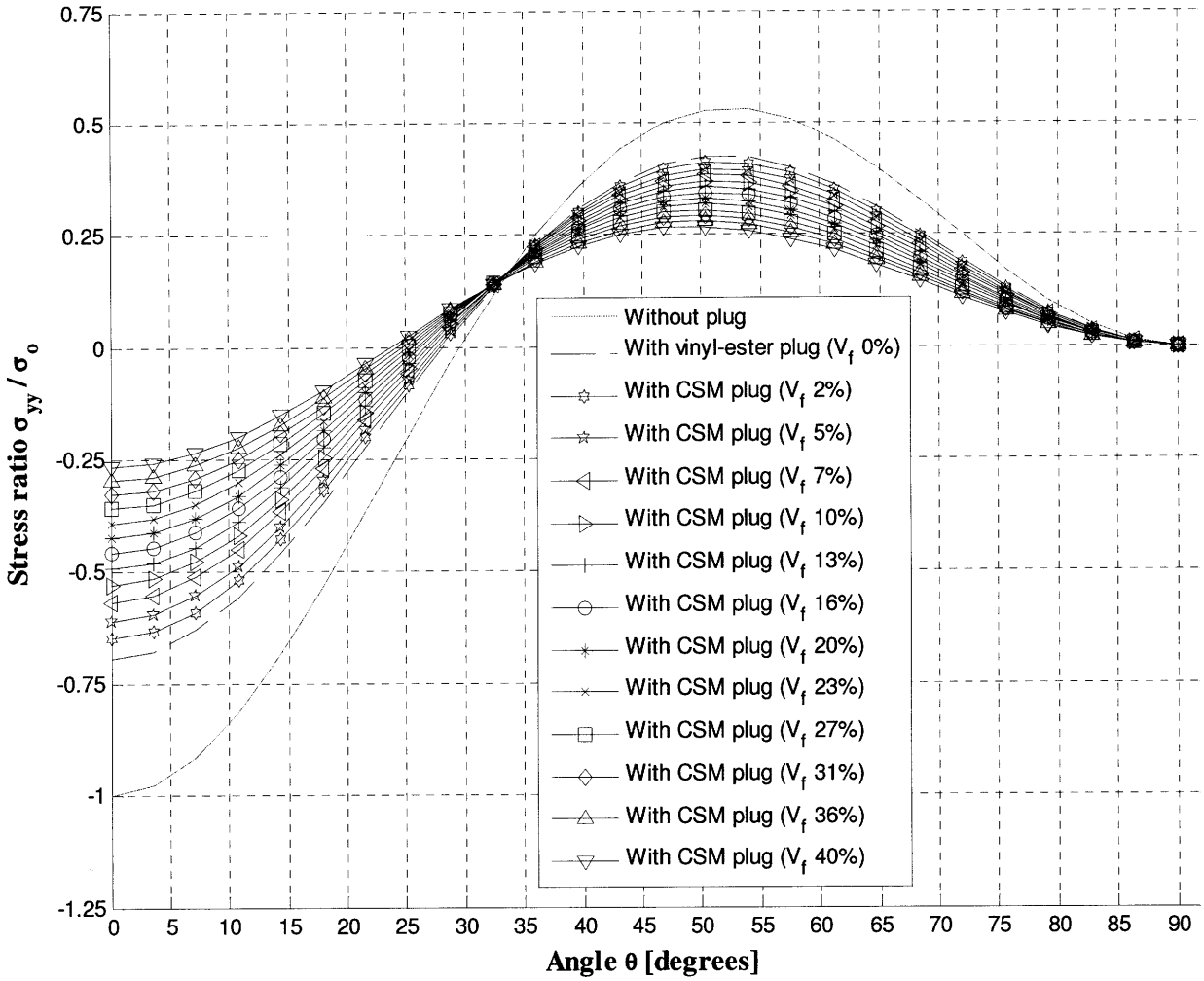

Figure 6: Stress σ_{yy} around hole in glass fiber / vinyl ester laminate of balanced woven roving containing various plugs, and subjected to uniaxial tension σ_o in x-direction.

Figure 5 and Figure 6 reveal that filling the hole with a plug of CSM has the beneficial effect of reducing the maximum stresses around the hole boundary. The introduction of the plug reduces considerably the magnitude of both the maximum tensile stress and the maximum compressive stress. As the fiber volume fraction V_f of the plug increases, the effect of the plug's presence in stress reduction also increases. In fact, by the introduction of a CSM plug with V_f =27%, the maximum tensile stress at the hole

boundary is reduced by 50%, while the introduction of a CSM plug with V_f =40% reduces the maximum tensile stress at the hole boundary by 58%. In this latter case σ_{xx} is only 31% higher than the applied tensile stress.

Figure 7 displays the effect of the increase of the percentage of **glass fiber** volume fraction in the CSM plug on the maximum tensile stress σ_{xx} around the edge of the hole for a laminate of balanced WR. Figure 8 and Figure 9 show the effect of the increase of the percentage of fiber volume fraction on the maximum stress σ_{yy} and minimum stress σ_{yy} (that is, the maximum compressive stress), respectively, around the edge of the hole for a laminate of balanced WR. Clearly, the increase in the fiber volume fraction in the CSM plug contributes to the overall reduction of all stresses in the vicinity of the filled hole.

Similar plots to Figure 5 through Figure 9 for different WR laminates, having varying biased fiber configurations, are provided in Appendix C.

Figure 10 displays the effect of the changes in the fiber volume fraction in the CSM plug on the maximum stress σ_{xx} around the edge of the hole for various laminates. Figure 11 and Figure 12 show the effect of changes in the fiber volume fraction in the CSM plug on the maximum stress σ_{yy} and minimum stress σ_{yy} (that is, the maximum compressive stress), respectively, around the edge of the hole for the same laminates. As can be clearly seen, an increase of the fiber volume fraction in the plug results in the general reduction of stresses around the edge of filled holes for all the laminates.

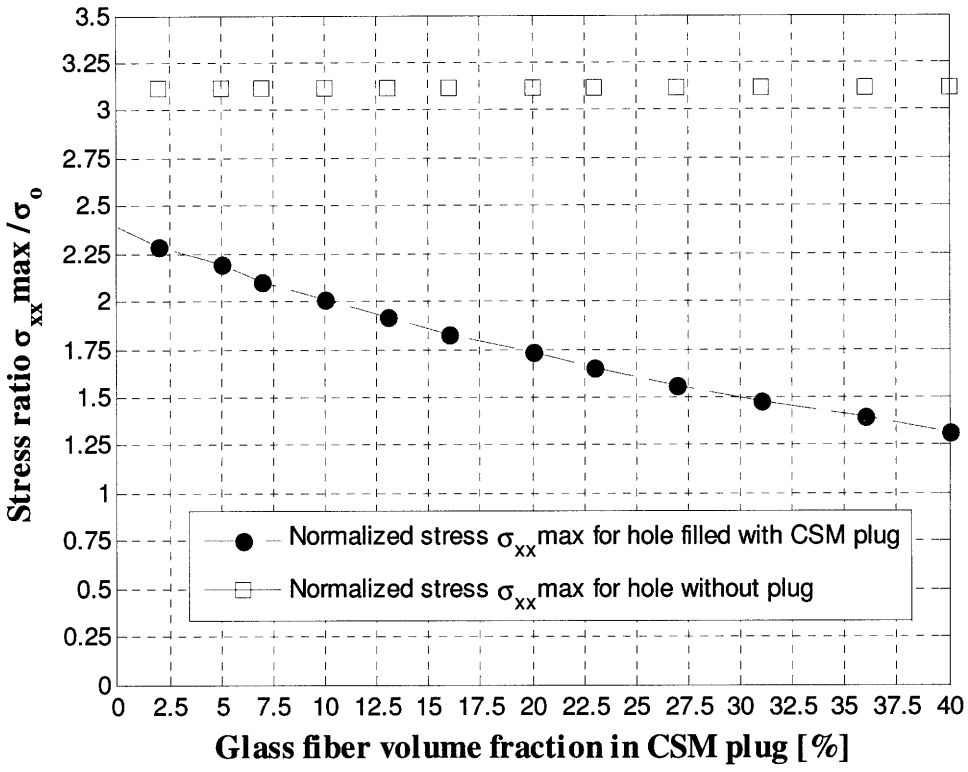

Figure 7: Normalized maximum stress σ_{xx} around edge of hole in laminate of glass fiber / vinyl ester balanced woven roving (WR) for various chopped strand mat (CSM) plugs, and subjected to uniaxial tension σ_o in x-direction.

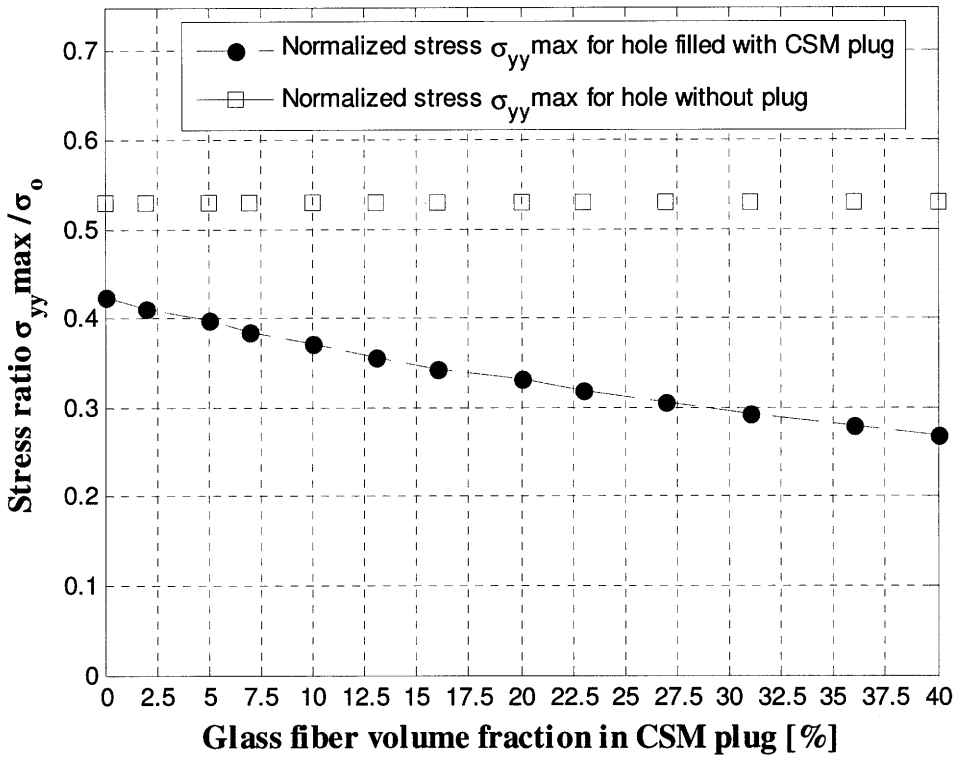

Figure 8: Normalized maximum stress σ_{yy} around edge of hole in laminate of glass fiber / vinyl ester balanced woven roving (WR) for various chopped strand mat (CSM) plugs, and subjected to uniaxial tension σ_o in x-direction.

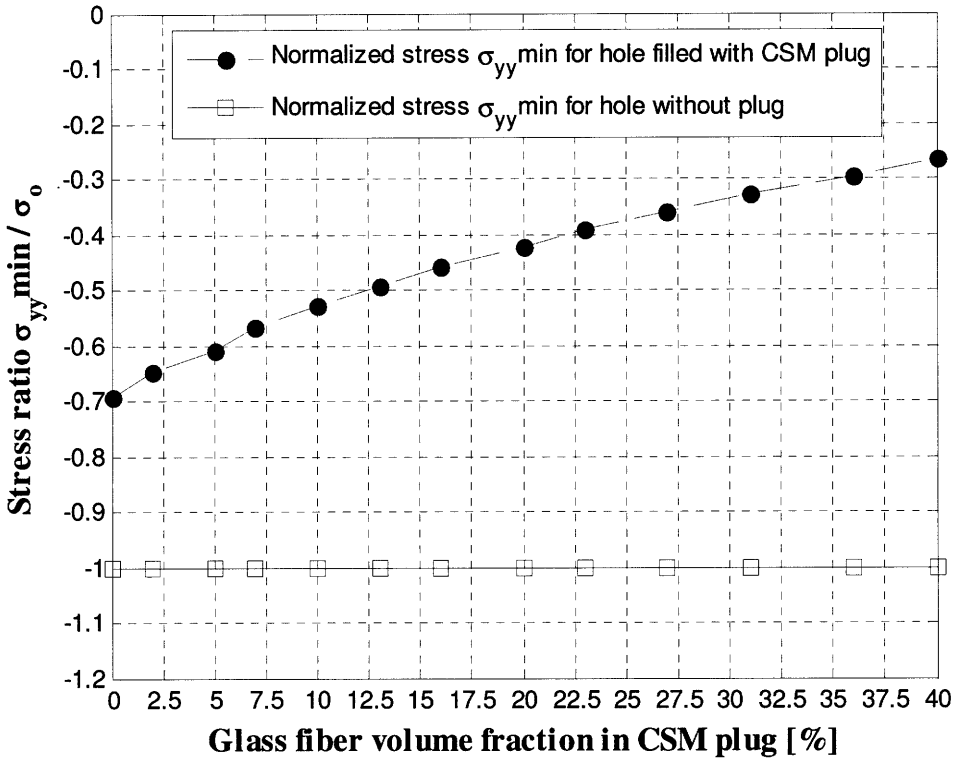

Figure 9: Normalized minimum stress σ_{yy} around edge of hole in laminate of glass fiber / vinyl ester balanced woven roving (WR) for various chopped strand mat (CSM) plugs, and subjected to uniaxial tension σ_o in x-direction.

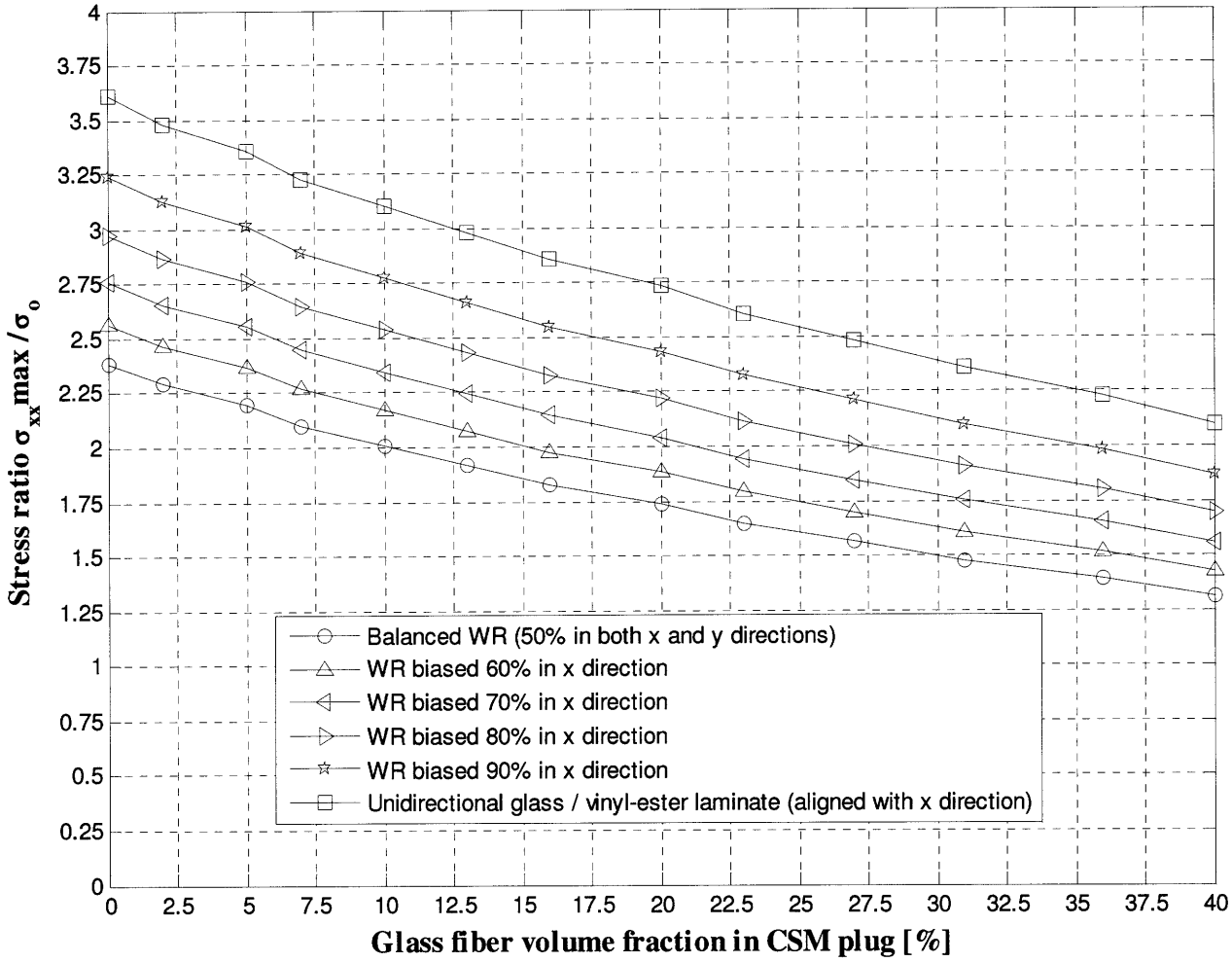

Figure 10: Normalized maximum stress σ_{xx} at hole in several laminates of woven roving (WR) for various chopped strand mat (CSM) plugs, subjected to uniaxial tension σ_o in x-direction.

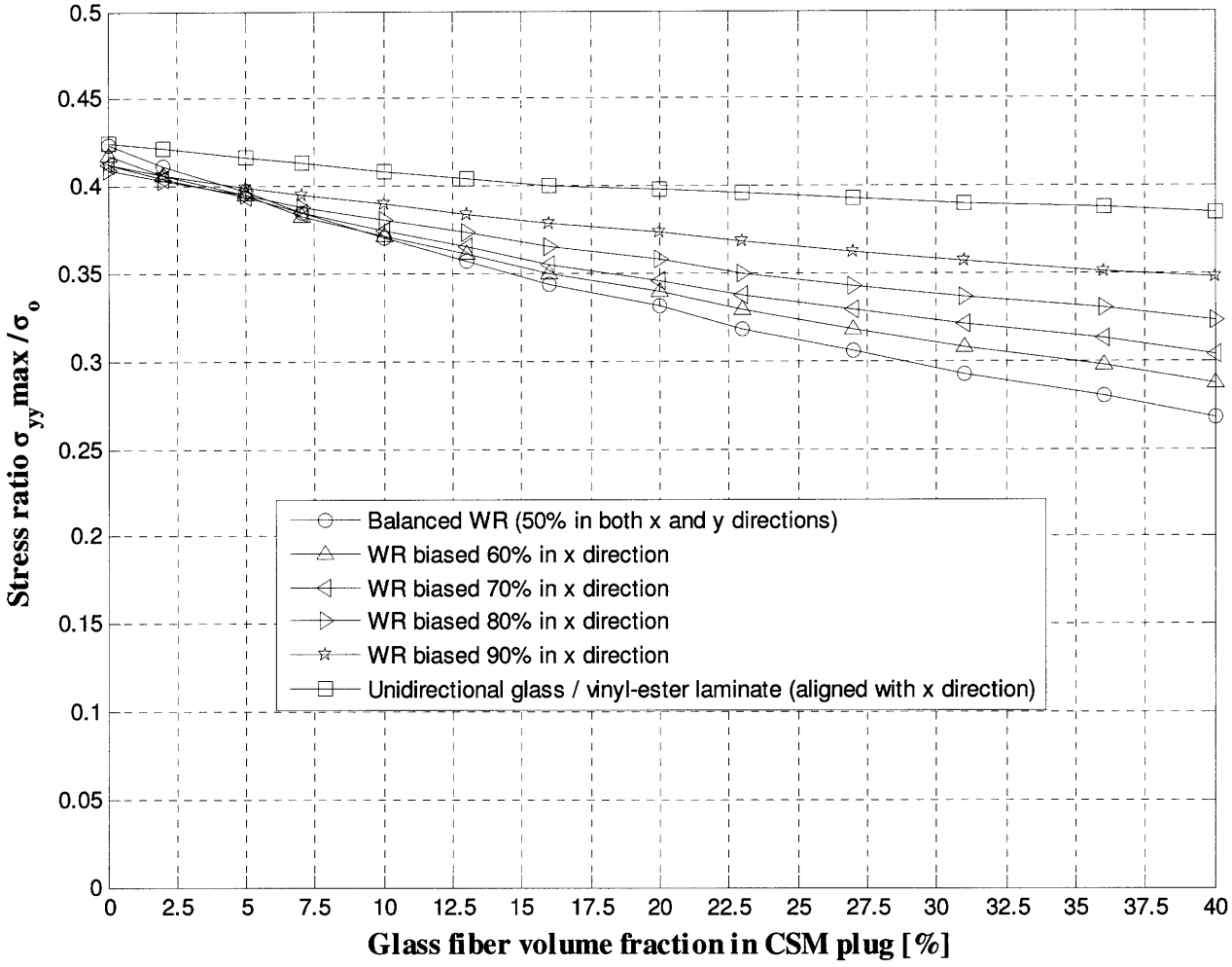

Figure 11: Normalized maximum stress σ_{yy} at hole in several laminates of woven roving (WR) for various chopped strand mat (CSM) plugs, subjected to uniaxial tension σ_o in x-direction.

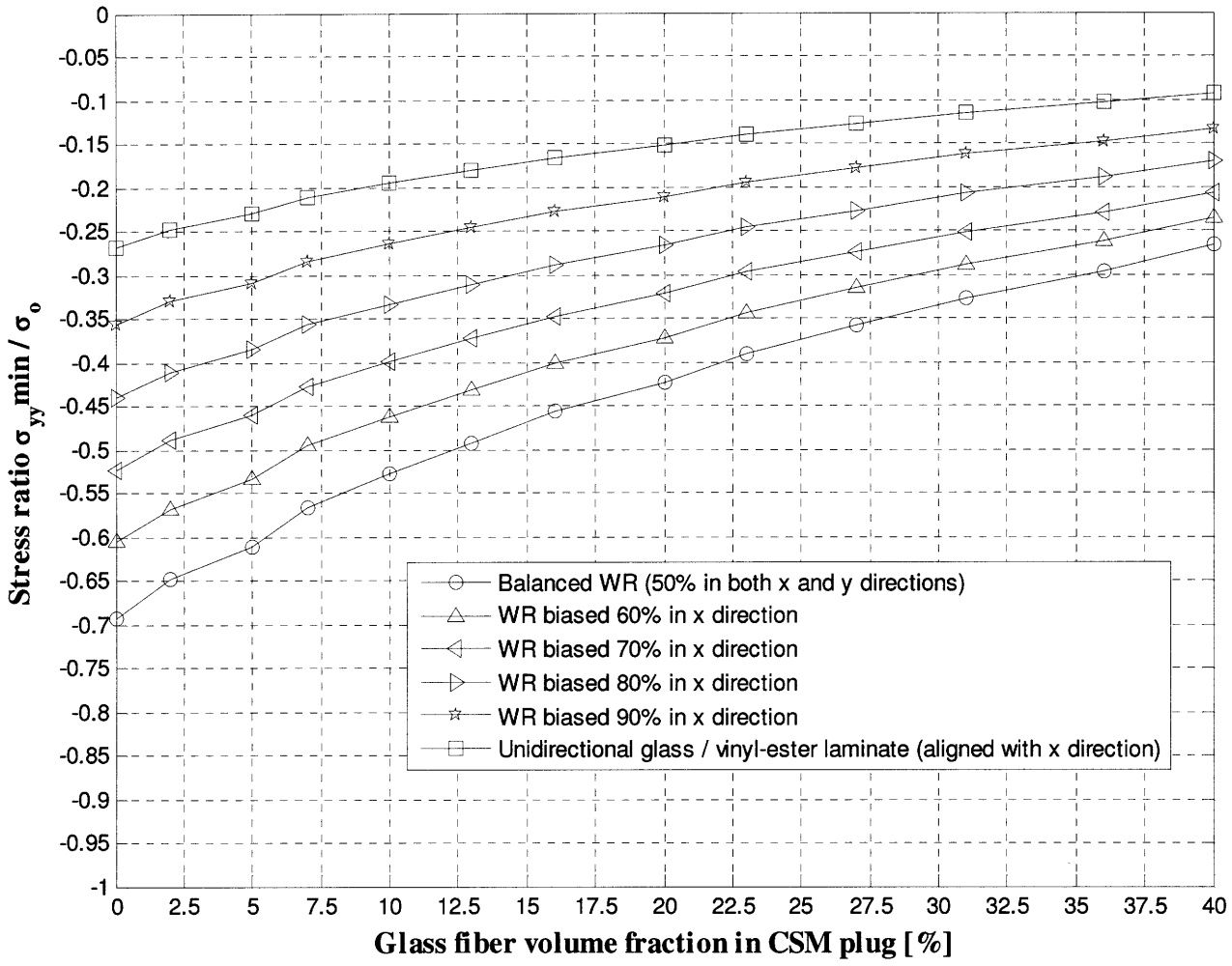

Figure 12: Normalized minimum stress σ_{yy} at hole in several laminates of woven roving (WR) for various chopped strand mat (CSM) plugs, subjected to uniaxial tension σ_o in x-direction.

2.6 The effect of plate thickness

The mathematical models presented in Sections 2.1 and 2.2 are plane stress, two-dimensional, models for laminates containing open and plugged holes. An important question arises as to the validity of these results as the laminate thickness increases, thereby introducing thickness effects and forcing a portion of the laminate into plain strain (Figure 13).

Sternberg and Sadowsky [56] performed a three-dimensional analysis on an isotropic plate that showed that the stress is slightly lower at the edge of the hole near surface of the plate and somewhat higher at the hole periphery near the mid-plane, both compared with the corresponding plane stress results. In particular, they showed that for an isotropic plate, with Poisson's ratio $v=0.3$, of thickness equal to 1.5 times the radius of the hole and subjected to uniaxial in-plane stress the maximum stress at the surface was 7% less than the maximum stress predicted by the two-dimensional model, while the maximum stress at the mid-plane was 3% higher than the corresponding two-dimensional value.

Folias and Wang [57] also presented an analytical solution for the three-dimensional stresses in an isotropic plate of arbitrary thickness weakened by a cylindrical hole. They provided several valuable observations and results [57]:

- The value of the SCF varies across the thickness of the isotropic plate and is a function of the ratio $\frac{hole\ radius}{plate\ thickness}=\frac{a}{t}$ and the Poisson's ratio v of the material of the plate.
- For ratios of $\frac{a}{t}>0.5$, the maximum stress occurs nearer the midplane of the plate than the free surface.
- For ratios of $\frac{a}{t}<0.5$, the maximum stress occurs nearer the free surface of the plate, approximately one-hole radius from the surface.

Using finite elements, Young and Lee [58] confirmed the observations of Sternberg and Sadowsky [56]. W.D. Pilkey and D.F. Pilkey [59] commented in their discussion of holes in thick isotropic elements that "the usual two-dimensional stress concentration factors are sufficiently accurate for design application to elements of arbitrary thickness." Kotousov and Wang [60] stated that there is no global criterion identifying what cases of plate thicknesses qualify as plane stress or plane strain and that the decision of whether a plate should be treated as thin or thick is largely empirical.

Based in these discussions, although the plane-stress solutions offered here are inadequate to provide information on the variation of stresses through the thickness of a laminate, these results should provide useful design guidelines.

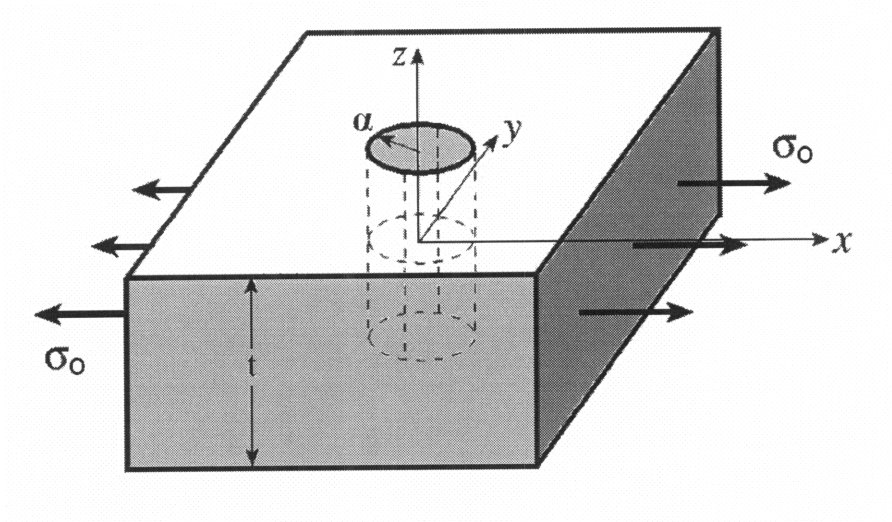

Figure 13: Schematic of three-dimensional plate with cylindrical hole under uniformly applied tensile stress.

3. Discussion, Conclusions, and Recommendations

3.1 Discussion and Conclusions

The performed analyses considered only the loading case of the laminate in which the applied stress was parallel to the plane of the plate and aligned with the *x*-direction (a principal material direction of the laminate), in part, because this case corresponded to the largest induced stresses at the hole boundary. The stress distribution around the hole is strongly influenced by the fiber orientation relative to the direction of the applied stress. The variation of the stress distribution around the hole for various angles φ between the principal material *x*-direction of the laminate and the direction of the tensile load can be seen in Figure 14 and Figure 15 for a **glass fiber / vinyl ester** laminate of balanced WR and a **glass fiber / vinyl ester** laminate of unidirectional composite, respectively. Clearly, the corresponding stresses at the hole boundary are the highest when the fibers are oriented parallel to the loading axis ($\varphi=0^{o}$).

Lekniitskii's analytical expressions apply for cases of infinite plates. If the damaged area is small compared to the size of the composite structure, then the stress results of the performed analysis can be employed for finite width plates [61]. For the case of a large damaged area compared to the size of the component, the obtained results can still provide useful design guidelines.

If the laminate is made of laminas of different orientation, then the calculation of the stress distribution at the hole boundary must be done on a lamina-by-lamina basis [62]. Further complications arise in the stress evaluation around the damaged region when the parameter thickness is introduced to the analysis, as discussed in Section 2.6.

Smith [8] recommended that the design allowable for stress and strain in a marine composite structure should not exceed 30% of the ultimate failure stress and strain, respectively. In **glass fiber** / polyester WR and CSM, it may be necessary to keep the tensile strain at 25% to 30% of the ultimate failure strain [15]. According to Plessis [22], a good design should ensure that FRP structures should never be stressed "above the 25% threshold of damage." Other more conservative references have specified that the sustained stress levels should not exceed 10% to 20% of the ultimate values [11].

Baley, Davies, Grohens and Dolto [15] have shown that safety factors proposed for marine composite structures, which varied from 4 to 6 for static loads and up to 10 for dynamic loads, were higher than those employed for similar metallic structures.

Based in these discussions, it appears that marine composite structures are designed with large safety factors or equivalently for low applied stresses and strains. Thus, it seems that the plug repair scheme can be utilized not only as a temporary repair or a repair for non-structural components, but also as a permanent repair, at least, for lightly loaded **glass fiber / vinyl ester** marine structures. Further, it may be employed for the repair of highly loaded **glass fiber / vinyl ester** marine structures, but only after the performance of a comprehensive stress analysis of the damaged region.

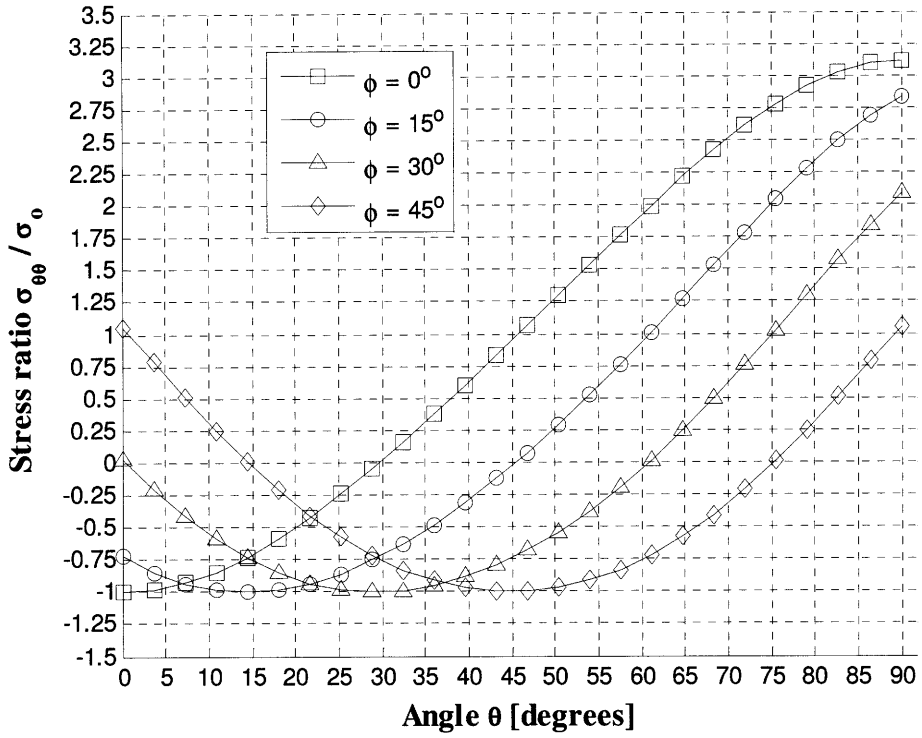

Figure 14: Stress $\sigma_{\theta\theta}$ around edge of unfilled hole in balanced glass fiber / vinyl ester woven roving (WR) laminate for various angles φ, where φ is the angle between the applied uniaxial tensile stress and the x-direction (principal material direction).

Note that, the introduction of the **glass fiber / vinyl ester** CSM plug considerably reduces the stresses in these analyses, partly because the laminate does not possess high moduli. In other words, it is the combination of the **glass fiber / vinyl ester** plug of relatively low stiffness with the **glass fiber / vinyl ester** laminate also of relatively low stiffness that provides the excellent stress reduction of the plug repair scheme in this thesis. If the laminates were made of higher performance fibers such as carbon fibers, then the performance of the **glass fiber / vinyl ester** plug in reducing the stresses at the hole boundary would be reduced significantly.

In conclusion, damage analysis of composite structures should be based on the investigation of the stress state around the damaged area. "Although current repair methodology tends to bypass the damage analysis step and design the repair based on past experience or similar structural damage" [63], the accurate evaluation of the stress

field in the vicinity of a damaged area can assist in identifying the most appropriate and cost-effective repair scheme. Thus, stress analyses as those performed in this thesis are valuable steps in the design and selection of the best repair techniques and materials.

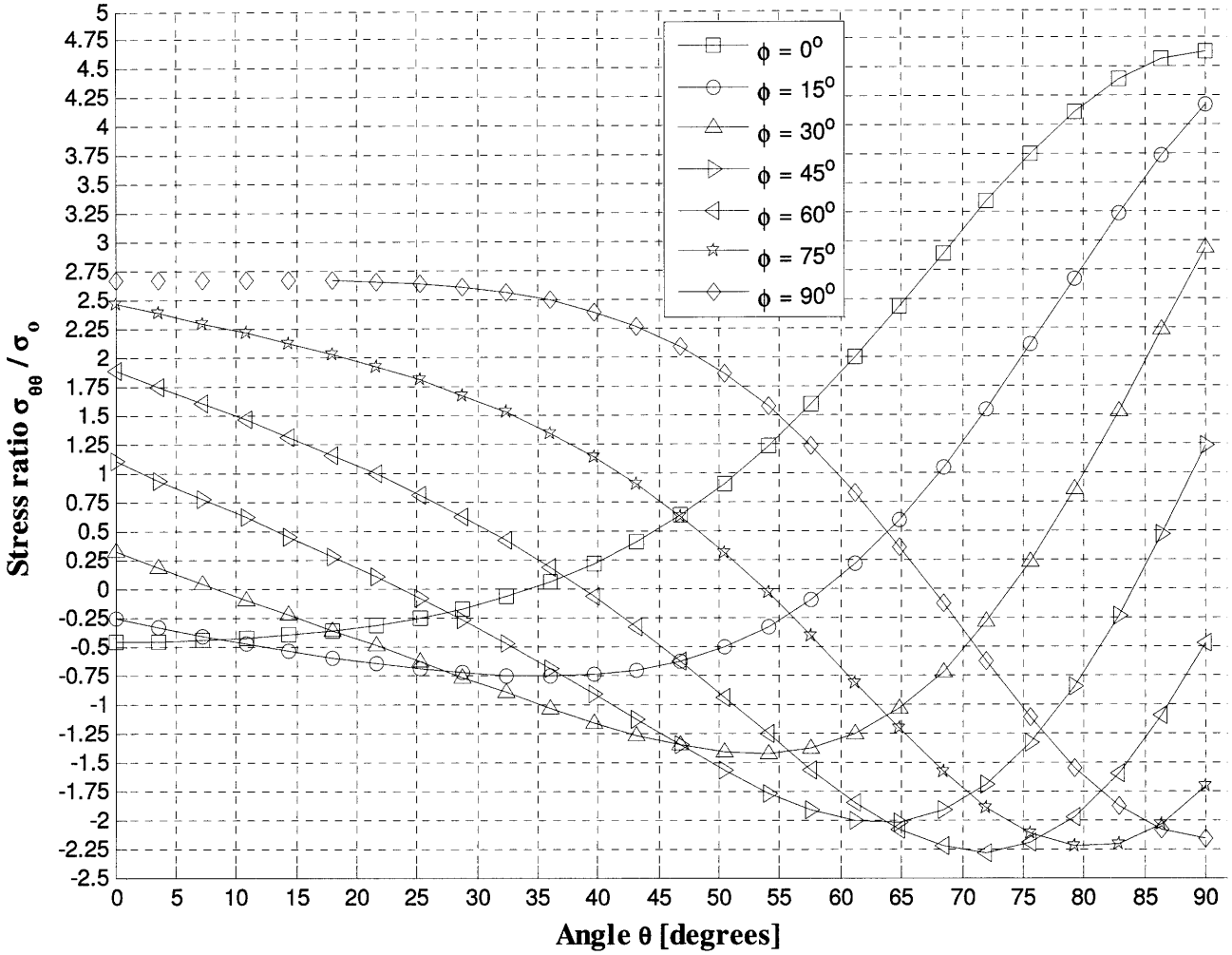

Figure 15: Stress $\sigma_{\theta\theta}$ around edge of unfilled hole in unidirectional glass fiber / vinyl ester laminate for various angles φ, where φ is the angle between the applied uniaxial tensile stress and the *x*-direction (principal material direction).

3.2 Recommendations

The strength and stiffness of a laminate vary depending on the loading conditions; they are different when the laminate is loaded in tension, compression or bending. Thus,

the behavior of the portrayed plug repair scheme should be investigated further under compression and bending, but also under combined loading. With respect to bending, a thorough analysis of the plug repair scheme is crucial, since composite panels in marine structures are "likely to be deflection limited rather than stress limited" due to the relatively low stiffness of **glass fiber / vinyl ester** composites compared to metals [11]. Fatigue and creep should also be considered. Experimental and finite element analyses should also be employed for further investigation of the plug repair scheme.

Finally, alternative repair schemes utilizing the plug concept appear to be attractive. In particular, the following repair schemes should be examined for application in marine **glass fiber / vinyl ester** laminates:

- The introduction of a CSM plug made of a different material from **glass fiber / vinyl ester**. For example, the use of chopped carbon fibers instead of chopped **glass fibers** in the CSM plug should be investigated.
- The application of thin cross-piled or unidirectional **glass fiber / vinyl ester** or carbon fiber / **vinyl ester** patches on top of the **glass fiber / vinyl ester** plug. In particular, a repair scheme of this form may be suitable for major structural repairs and could be more cost-effective than the traditional patch and scarf repairs applied in marine composites.

References

[1] A.P. Mouritz and C.P. Gardiner, "Marine Applications," ASM Handbook Vol. 21, ASM International Handbook Committee, ASM International, 2001.

[2] A.P. Mouritz, E. Gellert, P. Burchill and K. Challis, "Review of Advanced Composite Structures for Naval Ships and Submarines," Composite Structures, vol. 53, pp. 21-41, 387-394, 2001.

[3] P. Goubalt and S. Mayes, "Comparative Analysis of Metal and Composite Materials for the Primary Structures of a Patrol Craft," Naval Engineers Journal, vol. 108, no. 3, pp. 387-394, 1996.

[4] D.W. Chalmers, "The Potential for the Use of Composite Materials in Marine Structures," Marine Structures, vol. 7, pp. 441-456, 1994.

[5] B. Høyning and J. Taby, "Warship Design: The Potential for Composites in Frigate Superstructures," International Conference on Lightweight Construction - Latest Developments, 2000, London, RHINA, 2000.

[6] Use of Fiber Reinforced Plastics in the Marine Industry, SSC-360, Ship Structure Committee, 1990.

[7] Design Guide for Marine Applications of Composites, SSC-403, Ship Structure Committee, 1997.

[8] C. S. Smith, Design of Marine Structures in Composite Materials, Elsevier Science Publishing Co. Inc., 1990.

[9] A.W. Horsmon Jr., "Composites," Ship Design and Construction Vol. 1, T. Lamb, Ed., SNAME, 2003.

[10] O. Gullberg and K.A. Olsson, "Design and Construction of GRP Sandwich Ship Hulls," Marine Structures, vol. 3, pp. 93-109, 1990.

[11] R.A. Shenoi and J.F. Wellicome, Eds., Composite Materials in Maritime Structures Vol. 1 and 2, Cambridge Ocean Technology Series 5, Cambridge University Press, 1993.

[12] K. Galanis, "Hull Construction with Composite Materials for Ships over 100 m in Length," Thesis, Massachusetts Institute of Technology, 2002.

[13] M.O. Critchfield, T.D. Judy and A.D. Kurzweil, "Low-Cost Design and Fabrication of Composite Ship Structures," Marine Structures, vol. 7, pp. 475-494, 1994.

[14] S. Aksu, S. Cannon, C. Gardiner and M. Gudze, "Hull Material Selection for Replacement Patrol Boats – An Overview," DSTO-TN-0410, DSTO Aeronautical and Maritime Research Laboratory, Australia, 2002.

[15] C. Baley, P. Davies, Y. Grohens and G. Dolto, "Application of Interlaminar Tests to Marine Composites. A Literature Review," Applied Composite Materials, vol. 11, pp. 99-126, 2004.

[16] W.C. Tucker and T. Juska, "Marine Applications," Handbook of Composites, S.T. Peters, Ed., Chapman and Hall, pp. 916-930, 1998.

[17] K.B Armstrong, L.G. Bevan and W.F. Cole II, Care and Repair of Advanced Composites, 2nd ed., SAE International, pp. 19-25, 169-170, 209-226, 258-266, 2005.

[18] A.B. Strong, Fundamentals of Composites Manufacturing: Materials, Methods, and Applications, 2nd ed., Society of Manufacturing Engineers, pp. 115-122, 2008.

[19] N.S. John, I Grabovac, E. Gellert, Z. Shah Khan, A. Mouritz and P. Burchill, "Fibre-Resin Composite Research in Support of Current and Future Royal Australian Navy Vessels," International Conference, Lightweight Construction - Latest Developments, 2000, London, RHINA, 2000.

[20] R.J. Scott, Fiberglass Boat Design and Construction, 2nd ed., SNAME, pp. 39-106, 1996.

[21] D.W. Chalmers, "The Properties and Uses of Marine Structural Materials," Marine Structures, vol. 1, pp. 47-70, 1988.

[22] H.D. Plessis, Fibreglass Boats, 4th ed., Adlard Coles Nautical, 2006.

[23] P.G. Bergan, L. Buene, A.T. Echtermeyer and B. Hayman, "Assessment of FRP Sandwich Structures for Marine Applications," Marine Structures, vol. 7, pp. 457-473, 1994.

[24] B.A. Sjögren and L.A. Berglund, "The Effects of Matrix and Interface on Damage in GRP Cross-Ply Laminates," Composites Science and Technology, vol. 60, pp. 9-21, 2000.

[25] G. Dorey, "Impact Damage in Composites – Development, Consequences and Prevention," 6th ICCM and 2nd ECCM, Elsevier Applied Science, pp. 3.1-3.26, 1987.

[26] A. Baker, S. Dutton and D. Kelly, Composite Materials for Aircraft Structures, 2nd ed., AIAA, pp. 369-379, 2004.

[27] GRP Survey and Repair Requirements for HM Ships, Boats, Craft and Structures, Ministry of Defense, Defense Standard 02-752 Pt2, pp. 10-11, 46-49, UK, 2005.

[28] P. Berbinau, C. Filiou and C. Soutis, "Stress and Failure Analysis of Composite Laminates with an Inclusion under Multiaxial Compression-Tension Loading," Applied Composite Materials, vol. 8, pp. 307-326, 2001.

[29] T.S. Jones, "Nondestructive Evaluation Methods for Composites," Handbook of Composites, S.T. Peters, Ed., Chapman and Hall, pp. 838-856, 1998.

[30] M.M. Schwartz, Composite Materials: Properties, Nondestructive Testing, and Repair, Prentice Hall PTR, pp. 314-345, 1996.

[31] D. Panagiotidis, "Adhesively Bonded Composite Repairs in Marine Applications and Utility Model for Selection for Their Nondestructive Evaluations," Thesis, Massachusetts Institute of Technology, 2007.

[32] Rules for Materials and Welding, Part 2, Aluminum and Fiber Reinforced Plastics (FRP), Chapters 5-6, American Bureau of Shipping, pp. 117-130, 2006.

[33] USN Composite Repair Manual (draft), provided by NSWCCD.

[34] Navigation and Vessel Inspection Circular No. 8-87, U.S. Coast Guard, 1987.

[35] R. Trask, T. Turton and P. Lay, "Field Repair of Marine Composite Stiffeners Utilizing Resin Infusion," International Conference on Joining and Repair of Plastics and Composites, 1999, IMechE Conference Transactions, Professional Publishing Ltd, pp. 161-172, 1999.

[36] D.M. Elliott and R.S Trask, "Damage Tolerance and Repair of GFRP Warships," Journal of Thermoplastic Materials, vol. 14, pp. 201-212, 2001.

[37] R.F. Wegman and T.R. Tullos, Handbook of Adhesive Bonded Structural Repair, pp. 94-98, 1992.

[38] P.K. Malick, Ed., Composites Engineering Handbook, Marcel Dekker, Inc., pp. 748-750, 1997.

[39] U.K. Vaidya, G. Basappa, B. Mathew and J.M. Sands, "Flexural Fatigue Response of Repaired S2-Glass / Vinyl Ester Composites," 32nd International SAMPE Technical Conference, Vol. 32, Revolutionary Materials: Technology and Economics, pp. 788-801, 2000.

[40] T. Hundman and W.J. Horn, "Stress Analysis of an Orthotropic Plate with a Plugged Center Hole," AIAA/ASME/ASCE/AHS/ASC Structures, Structural Dynamics and Materials Conference and Exhibit, 37th, Technical Papers, Pt. 4, American Institute of Aeronautics and Astronautics, pp. 2470-2478, 1996.

[41] S.G. Lekhnitskii, Anisotropic Plates, 2nd ed., S. W. Tsai and T. Cheron, Trans., Gordon and Breach Science Publishers, pp. 157-217, 1968.

[42] C. Vlattas and C. Soutis, "Composites Repair: Compressive Behaviour of CFRP Plates with Reinforced Holes," 7th European Conference on Composite Materials, Realising Their Commercial Potential, 2, ECCM-7, Woodhead Publishing Ltd., pp. 87–92, 1996.

[43] C.N. Duong and C.H. Wang, Composite Repair, Theory and Design, Elsevier, 2007.

[44] L. Tong and C. Soutis, Eds., Recent Advances in Structural Joints and Repairs for Composite Materials, Kluwer Academic Publishers, 2003.

[45] A.A. Baker, L.R.F. Rose and R. Jones, Eds., Advances in the Bonded Composite Repair of Metallic Aircraft Structure, Vol.1 and 2, Elsevier, 2002.

[46] Composite Repair of Military Aircraft Structures, AGARD Conf. Proc. 550, AGARD, 1995.

[47] A.A. Baker and R. Jones, Eds., Bonded Repair of Aircraft Structures, Martinus Nijhoff Publishers, 1988.

[48] S-H. Ahn and G.S. Springer, "Repair of Composite Laminates," DOT/FAA/AR-00/46, FAA, 2000.

[49] L.P. Kollar and G.S. Springer, Mechanics of Composite Structures, Cambridge University Press, pp. 38-44, 2003.

[50] S.P. Timoshenko and J.N. Goodier, Theory of Elasticity, 3rd ed., McGraw-Hill, pp. 65-68, 90-95, 274-277, 1970.

[51] A.C. Ugural and S.K. Fenster, Advanced Strength and Applied Elasticity, 4th ed., Prentice Hall, pp. 99-102, 2003.

[52] H.J. Konish and J.M. Whitney, "Approximate Stresses in an Orthotropic Plate Containing a Circular Hole," Journal of Composite Materials, vol. 9, pp. 157-166, 1975.

[53] S.C. Tan, "Laminated Composites Containing an Elliptical Opening. I. Approximate Stress Analyses and Fracture Models," Journal of Composite Materials, vol.21, pp. 925-958, 1987.

[54] S.C. Tan, Stress Concentration Factors in Laminated Composites, Technomic Publishing Co., Inc., pp. 306-307, 1994.

[55] E.J. Barbero, Introduction to Composite Materials Design, Taylor and Francis, pp. 222-227, 1998.

[56] E. Sternberg and M.A. Sadowsky, "Three Dimensional Solution for the Stress Concentration Around a Circular Hole in a Plate of Arbitrary Thickness," Trans. ASME Appl. Mech. Sect., vol. 71, pp. 27-38, 1949.

[57] E.S. Folias and J.J. Wang, "On the Three-Dimensional Stress Field Around a Circular Hole in a Plate of Arbitrary Thickness," Computational Mechanics, vol. 6, pp. 379-391, 1990.

[58] J.B. Young and K.K. Lee, "Stress Concentration Factors in Countersunk Holes," Aeronautical Journal, vol. 97, 1993.

[59] W.D. Pilkey and D.F. Pilkey, Stress Concentration Factors, 3rd ed., John Wiley & Sons, Inc., pp. 239-240, 2008.

[60] A. Kotousov and C.H. Wang, "Three Dimensional Solutions for Transversally Isotropic Composite Plates," Composite Structures, vol. 57, pp. 445-452, 2002.

[61] J. Awerbuch and M.S. Madhukar, "Notched Strength in Composite Laminates: Predictions and Experiments – A Review," Journal of Reinforced Plastics and Composites, vol. 4, pp. 3-159, 1985.

[62] R.M. Jones, Mechanics of Composite Materials, 2nd ed., Taylor and Francis, pp.336-339, 1999.

[63] J.W. Bull, Numerical Analysis and Modelling of Composite Materials, Blackie Academic & Professional, pp. 34-35, 1996.

Appendix A

Approximate calculation of constitutive properties for glass fiber / vinyl ester woven roving

Due to the lack of a reference for the complete set of constitutive properties for **glass fiber / vinyl ester** woven roving (WR), an indirect approach is adopted for their estimation.

A.1 Calculation of constitutive properties for unidirectional glass fiber / vinyl ester composite material

The first step is to determine the constitutive properties of a unidirectional **glass fiber / vinyl ester** composite. Table A-1 summarizes the constitutive properties of a unidirectional glass fiber / epoxy composite [A1]. The unidirectional glass fiber / epoxy composite is considered orthotropic and thus has nine independent elastic constants: E_x', E_y', E_z' are the Young's moduli; G_{xy}', G_{xz}', G_{xz}' are the shear moduli; and ν_{xy}', ν_{xz}', ν_{yz}' are the Poisson's ratios. The properties of the unidirectional glass fiber / epoxy material presented in Table A-1 correspond to a 29.6% fiber volume fraction.

Table A-1: Constitutive properties for unidirectional glass fiber / epoxy composite material [A1].

Material	E_x' [GPa]	E_y' [GPa]	G_{xy}' [GPa]	ν_{xy}'	E_z' [GPa]	G_{xz}' [GPa]	G_{yz}' [GPa]	ν_{xz}'	ν_{yz}'
Glass fiber / Epoxy	38.61	8.27	4.14	0.26	8.27	4.14	3.45	0.26	0.34

The constitutive properties of the glass fiber / epoxy composite in Table A-1 are selected as the reference material for the subsequent calculations. The reason for this selection is that this composite has very similar constitutive properties to those of **glass fiber / vinyl ester** according to generic property data provided in the literature [A2].

The properties for the unidirectional **glass fiber / vinyl ester** corresponding to a 29.2% fiber volume fraction, can be seen in Table A-2.

Table A-2: Constitutive properties for unidirectional glass fiber / vinyl ester composite material.

Material	E_x'' [GPa]	E_y'' [GPa]	G_{xy}'' [GPa]	ν_{xy}''	E_z'' [GPa]	G_{xz}'' [GPa]	G_{yz}'' [GPa]	ν_{xz}''	ν_{yz}''
Glass fiber / Vinyl ester	38.60	8.23	8.86	0.26	8.23	8.86	7.38	0.26	0.34

In Table A-2, E_x'', E_y'', E_z'', G_{xy}'', G_{xz}'', ν_{xy}'', and ν_{xz}'' for **glass fiber / vinyl ester** were obtained directly from the literature [A2]. On the other hand, ν_{yz}'' was assumed to be the same as glass fiber / epoxy, since the values of ν_{xy}'' and ν_{xz}'' for **glass fiber / vinyl ester** match the respective properties of glass fiber / epoxy. Further, G_{yz}'' was approximated using the formula

$$G_{yz}'' = \frac{G_{xy}''}{G_{xy}} G_{yz} \tag{39}$$

A.2 Calculation of constitutive properties for glass fiber / vinyl ester woven roving (WR)

The next step is to calculate the constitutive properties for a **glass fiber / vinyl ester** woven roving (WR) for different types warp-weft configurations, based on the calculated properties of the unidirectional **glass fiber / vinyl ester** composite. These woven roving configurations vary in the percentage of **glass fibers** aligned with the warp and weft (or fill) directions, which in the present analysis are the x- and y- directions, respectively. In particular, the woven roving arrangement ranges from a balanced fabric, where the reinforcement in the warp direction is equal to the reinforcement in the weft direction (so-called 50% biased in the warp direction), up to a configuration of 100% biased in the warp direction, which corresponds to a unidirectional tape.

Smith [A3] proposed a treatment for the desired mechanical properties of WR materials. A bidirectional cloth ply was treated as a pair of equivalent, orthogonal, unidirectional plies. The elastic properties of each ply were appropriately reduced by being multiplied with a ply efficiency factor, corresponding to the percentage of fibers aligned with the warp (or weft) direction. The equivalent unidirectional plies of balanced

cloth material would, for example, have an efficiency of 0.5. In the case of a biased fabric, the uneven fiber distribution is represented by adopting different efficiencies in the orthogonal directions. Furthermore, for a typical WR laminate the effective through-thickness shear moduli was estimated by averaging the ply shear moduli G_{xz} and G_{yz}. Poisson's ratios v_{xz} and v_{yz} were found likewise.

Gay and Hoa [A4] suggested a similar approach as Smith [A3]. Their approach also considered the fabric as two unidirectional plies crossing each other orthogonally. The formulas proposed were [A4]

$$E_x = kE_x'' + (1-k)E_y'' \tag{40}$$

$$E_y = (1-k)E_x'' + kE_y'' \tag{41}$$

$$G_{xy} = G_{xy}'' \tag{42}$$

$$v_{xy} = \frac{v_{xy}''}{k + (1-k)\dfrac{E_x''}{E_y''}} \tag{43}$$

where k is the percentage of fibers in the warp direction, and E_x'', E_y'', G_{xy}'', and v_{xy}'' are the Young's modulus in x-direction, the Young's modulus in y-direction, the in-plane shear modulus, and the Poisson's ratio, respectively, of the unidirectional **glass fiber / vinyl ester** composite. According to Gay and Hoa [A4], this formulation provides stiffnesses that are higher than those of the physical WR by up to 15%. This error is the result of the curvature of the **glass fibers** introduced during the weaving process of the fabric [A4, A5]. This curvature "makes the woven fabric more deformable than two cross plies when subjected to the same loading" [A4]. The compressive stiffness of the glass fibers in WR is reduced compared to that of a similar unidirectional composite, because "when a compression load is applied, they are already buckled" [A5].

The calculated constitutive planar properties of the **glass fiber / vinyl ester** woven rovings using Equations (2)-(5) are provided in Table A-3.

Table A-3: Constitutive planar properties of glass fiber / vinyl ester woven roving (WR) laminates.

Material	k	E_x [GPa]	E_y [GPa]	G_{xy} [GPa]	ν_{xy}
Balanced WR	0.5	23.42	23.42	8.86	0.09
WR 60% biased	0.6	26.45	20.38	8.86	0.11
WR 70% biased	0.7	29.49	17.34	8.86	0.12
WR 80% biased	0.8	32.53	14.30	8.86	0.15
WR 90% biased	0.9	35.56	11.27	8.86	0.19
Unidirectional	1	38.60	8.23	8.86	0.26

A.3 References

[A1] J.N.Reddy, Mechanics of Laminated Composite Plates and Shells, 2nd ed., CRC Press, p. 88, 2004.

[A2] K. Galanis, "Hull Construction with Composite Materials for Ships over 100m in Length," Master Thesis, Massachusetts Institute of Technology, p. 52, 2002.

[A3] C.S. Smith, Design of Marine Structures in Composite Materials, Elsevier Science Publishers, pp. 55-57, 1990.

[A4] D. Gay and S.V. Hoa, Composite Materials Design and Applications, 2nd ed., CRC Press, pp. 41-43, 2007.

[A5] K.B Armstrong, L.G. Bevan and W.F. Cole II, Care and Repair of Advanced Composites, 2nd ed, SAE International, pp. 38-47, 2005.

Appendix B

Approximate calculation of constitutive properties for glass fiber / vinyl ester chopped strand mat (CSM)

B.1 Fiber and matrix volume fractions

The amounts of **glass fiber** and **vinyl ester** in **glass fiber / vinyl ester** composites utilized in marine applications are expressed as either a weight fraction or a volume fraction. The fiber volume fraction V_f and the matrix volume fraction V_m are calculated as a function of the matrix weight fraction R by [B1]

$$V_m = \frac{\frac{\gamma_f}{\gamma_m}}{\frac{1}{R} + \frac{\gamma_f}{\gamma_m} - 1} \tag{44}$$

$$V_f = 1 - V_m \tag{45}$$

where γ_f and γ_m are the specific gravities of the fiber and matrix, respectively. According to Smith [B1], the matrix weight fraction R in chopped strand mat (CSM) was 65% to 75%. In other words, the typical weight fraction of the glass content in a CSM is 25% to 35%.

Table B-1 provides a summary of **glass fiber** volume fractions calculated by using Equations (1) and (2), for **vinyl ester** matrix weight fractions varying from 40% to 100%, where γ_f and γ_m equal to 2.55 and 1.15, respectively.

Table B-1: Glass fiber volume fractions corresponding to various vinyl ester matrix weight fractions in glass fiber / vinyl ester composite.

Matrix weight fraction *R* [%]	100	95	90	85	80	75	70	65	60	55	50	45	40
Fiber weight fraction *1-R* [%]	0	5	10	15	20	25	30	35	40	45	50	55	60
Matrix volume fraction V_m [%]	100	98	95	93	90	87	84	80	77	73	69	64	60
Fiber volume fraction V_f [%]	0	2	5	7	10	13	16	20	23	27	31	36	40

B.2 Constitutive properties of unidirectional fiber reinforced composite

For a unidirectional fiber reinforced composite, the Young's modulus in the x-direction E_x, the Young's modulus in the y-direction E_y, the major Poisson's ratio v_{xy}, the minor Poisson's ratio v_{yx}, and the in-plane shear modulus G_{xy}, can be estimated by [B1]:

$$E_x = E_f V_f + E_m V_m \tag{46}$$

$$E_y = \frac{1+2\eta_1 V_f}{1-\eta_1 V_f} E_m \tag{47}$$

$$v_{xy} = v_f V_f + v_m V_m \tag{48}$$

$$v_{yx} = \frac{E_y}{E_x} v_{xy} \tag{49}$$

$$G_{xy} = \frac{1+2\eta_2 V_f}{1-\eta_2 V_f} G_m \tag{50}$$

$$V_f + V_m = 1 \tag{51}$$

where V_f and V_m are the fiber and the matrix volume fractions, respectively, E_f and E_m are the Young's moduli of the fiber and matrix, respectively, G_f and G_m are the shear moduli of the fiber and matrix, respectively, v_f and v_m are the Poisson's ratio for the fiber and matrix, respectively, and η_1, η_2 are parameters obtained from [B1]:

$$\eta_1 = \frac{\frac{E_f}{E_m} - 1}{\frac{E_f}{E_m} + 2} \tag{52}$$

$$\eta_2 = \frac{\frac{G_f}{G_m} - 1}{\frac{G_f}{G_m} + 1} \tag{53}$$

Typical values for E_f, E_m, G_f, G_m, v_f and v_m are given in Table B-2.

Table B-2: Typical constitutive properties of E- glass fiber and vinyl ester materials.

Material	E [GPa]	G [GPa]	ν
E-glass fiber	72	29.51	0.22
Vinyl ester	3.4	1.25	0.36

By substituting the properties from Table B-2 into Equations (3)-(10), we can obtain the constitutive properties of a unidirectional **glass fiber / vinyl ester** composite for various **glass fiber** volume fractions. The calculated constitutive properties for fiber volume fractions varying from 0% to 40% are summarized in Table B-3.

Table B-3: Constitutive properties of unidirectional glass fiber / vinyl ester composite.

Property	Fiber volume fraction V_f [%]												
	0	**2**	**5**	**7**	**10**	**13**	**16**	**20**	**23**	**27**	**31**	**36**	**40**
E_x **[GPa]**	3.40	4.99	6.67	8.46	10.35	12.36	14.51	16.80	19.26	21.89	24.72	27.78	31.08
E_y **[GPa]**	3.40	3.61	3.84	4.10	4.39	4.71	5.07	5.49	5.97	6.53	7.18	7.97	8.92
G_{xy} **[GPa]**	1.25	1.30	1.36	1.43	1.50	1.59	1.68	1.79	1.92	2.06	2.24	2.44	2.70
ν_{xy}	0.36	0.36	0.35	0.35	0.35	0.34	0.34	0.33	0.33	0.32	0.32	0.31	0.30
ν_{yx}	0.36	0.26	0.20	0.17	0.15	0.13	0.12	0.11	0.10	0.10	0.09	0.09	0.09

B.3 Constitutive properties for short fiber composites

Smith [B1] offered an analytical methodology for the calculation of constitutive properties of a composite with randomly oriented short fibers in a plane, such as **glass fiber / vinyl ester** chopped strand mat (CSM). Due to the random orientation of its fibers and the isotropic nature of its matrix (**vinyl ester**), the mechanical properties of CSM can be considered independent of direction. Thus, CSM is treated as an isotropic material in the x-y plane. The constitutive properties of CSM can be estimated by the following expressions [B1]:

$$E = \frac{(U_1 + U_4)(U_1 - U_4)}{U_1} \tag{54}$$

$$G = \frac{U_1 - U_4}{2} \tag{55}$$

$$\nu = \frac{E}{2G - 1} = \frac{U_4}{U_1} \tag{56}$$

where E, G and ν, are the Young's modulus, the shear modulus, and the Poisson's ratio of the planar isotropic CSM, respectively, and U_1 and U_4 are invariants defined by Tsai and Pagano [B2], and Halpin and Pagano [B3] as

$$U_1 = \frac{3C_{11} + 3C_{22} + 2C_{12} + 4C_{66}}{8} \tag{57}$$

$$U_4 = \frac{C_{11} + C_{22} + 6C_{12} - 4C_{66}}{8} \tag{58}$$

In Equations (14) and (15), C_{11}, C_{22}, C_{12} and C_{66}, are the stiffness coefficients provided by [B2, B3]

$$C_{11} = \frac{E_x}{1 - \nu_{xy}\nu_{yx}} \tag{59}$$

$$C_{22} = \frac{E_y}{1 - \nu_{xy}\nu_{yx}} \tag{60}$$

$$C_{12} = \frac{\nu_{xy}E_y}{1 - \nu_{xy}\nu_{yx}} \tag{61}$$

$$C_{66} = G_{xy} \tag{62}$$

where E_x, E_y, G_{xy}, ν_{xy}, and ν_{yx} are the Young's modulus in the x-direction, the Young's modulus in the y-direction, the in-plane shear modulus, the major Poisson's ratio, and the minor Poisson's ratio, respectively, of the unidirectional **glass fiber / vinyl ester** composite.

By substituting the constitutive properties of unidirectional **glass fiber / vinyl ester** given in Table B-3 into Equations (11)-(19), we obtain the constitutive properties of

the **glass fiber / vinyl ester** CSM for fiber volume fractions varying from 0% to 40%. These are summarized in Table B-4.

Table B-4: Constitutive properties of glass fiber / vinyl ester chopped strand mat (CSM).

Property	**Fiber volume fraction V_f [%]**												
	0	**2**	**5**	**6**	**10**	**13**	**16**	**20**	**23**	**27**	**31**	**36**	**40**
***E* [GPa]**	3.40	4.00	4.66	5.38	6.16	6.99	7.90	8.88	9.95	11.13	12.42	13.86	15.48
***G* [GPa]**	1.25	1.48	1.73	2.00	2.29	2.61	2.95	3.31	3.71	4.15	4.64	5.18	5.79
v	0.36	0.35	0.35	0.34	0.34	0.34	0.34	0.34	0.34	0.34	0.34	0.34	0.34

B.4 References

[B1] C.S. Smith, Design of Marine Structures in Composite Materials, Elsevier Science Publishers, pp. 52-53, 1990.

[B2] S.W. Tsai and N.J. Pagano, "Invariant Properties of Composite Materials," Composite Materials Workshop, S.W. Tsai, J.C. Halpin and N.J. Pagano, Eds., Technomic Publishing Co., p. 233, 1968.

[B3] J.C. Halpin and N.J. Pagano, "The Laminate Approximation for Randomly Oriented Fibrous Composites," Journal of Composite Materials, vol. 3, pp. 720-724, 1969.

Appendix C

C.1 Glass fiber / vinyl ester laminate of woven roving biased 60% in *x*-direction with circular hole filled with plug of glass fiber / vinyl ester chopped strand mat, subjected to tension in one direction

Figures C1 and C2 show the stresses σ_{xx} and σ_{yy}, respectively, around the hole boundary in a **glass fiber / vinyl ester** laminate of woven roving (WR) biased 60% in the *x*-direction, containing various plugs of **glass fiber / vinyl ester** chopped strand mat (CSM), and subjected to uniaxial tension σ_o in the *x*-direction. A biased WR is a fabric with an unequal distribution of fibers along the warp and weft directions. In a 60% biased woven roving, the reinforcement in warp direction is 60% of the total reinforcement, while the reinforcement in weft direction is 40% of the total reinforcement.

Figure C3 displays the effect of an increase of the percentage of **glass fiber** volume fraction in the CSM plug on the maximum tensile stress σ_{xx} around the edge of the hole in a laminate of WR biased 60% in *x*-direction. Figures C4 and C5 show the effect of an increase of the percentage of fiber volume fraction on the maximum stress σ_{yy} and the minimum stress σ_{yy}, respectively, around the edge of the hole in a laminate of WR biased 60% in *x*-direction.

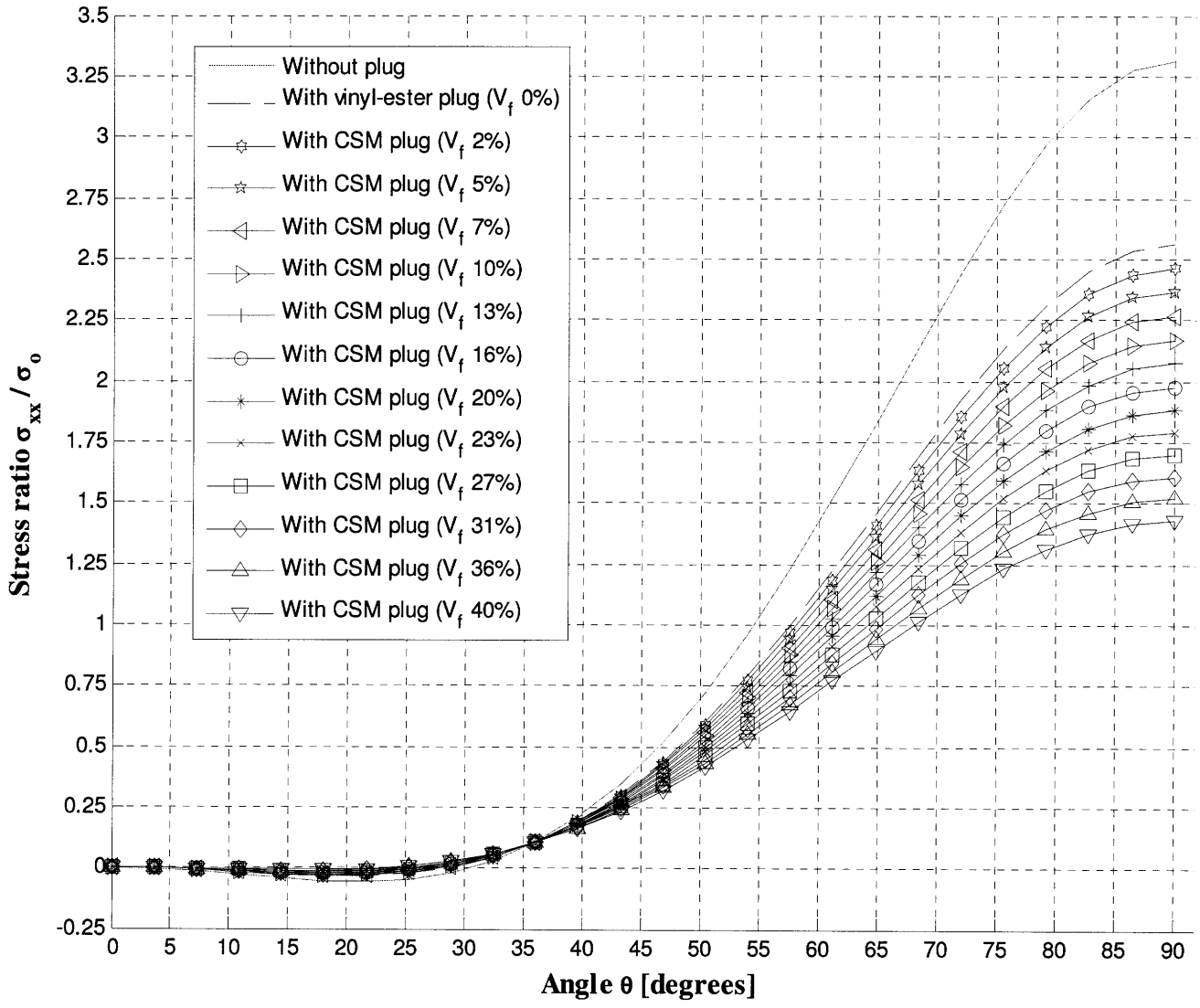

Figure C1: Stress σ_{xx} around hole in glass fiber / vinyl ester laminate of woven roving biased 60% in x-direction containing various plugs, and subjected to uniaxial tension σ_o in x-direction.

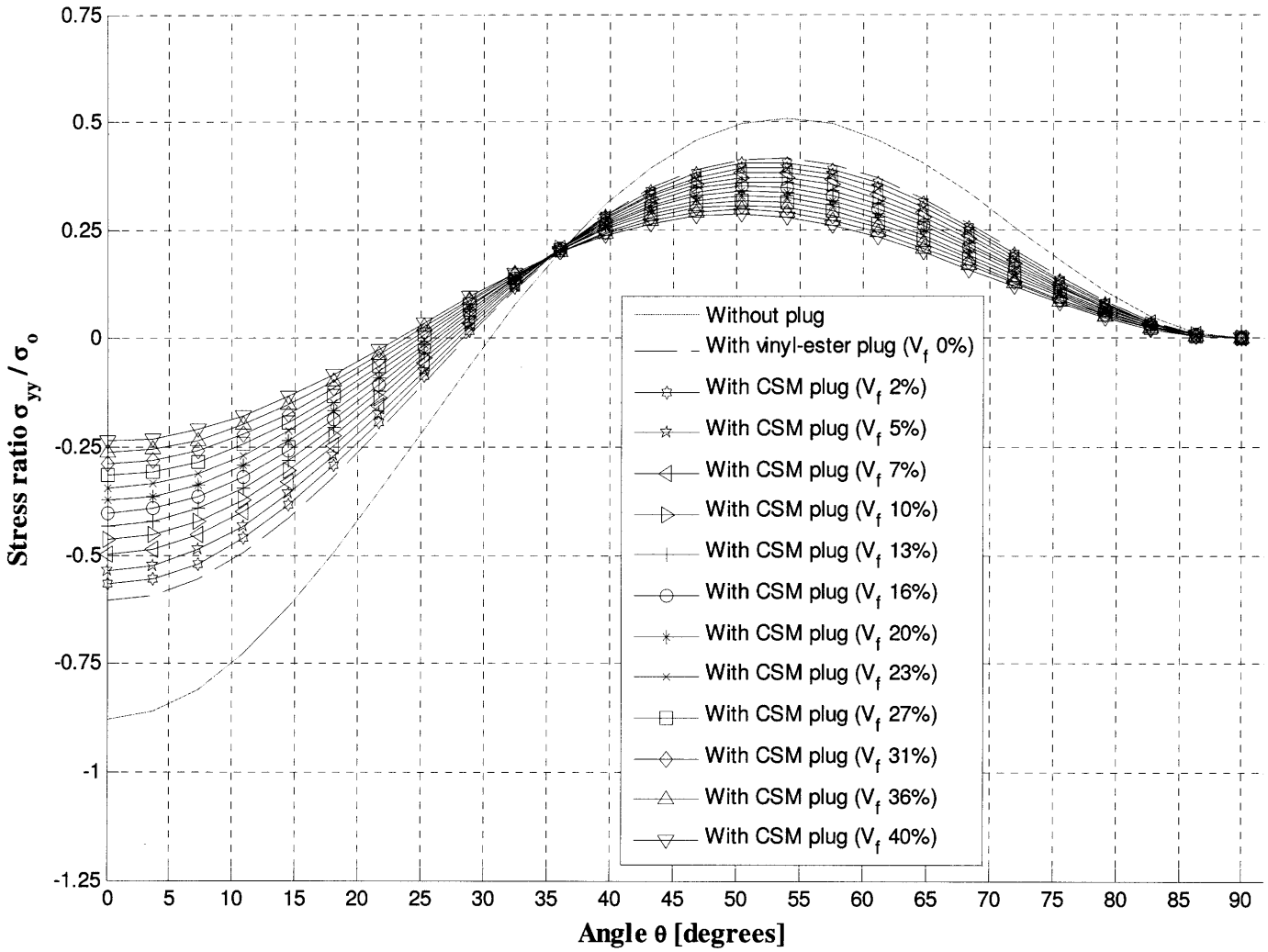

Figure C2: Stress σ_{yy} around hole in glass fiber / vinyl ester laminate of woven roving biased 60% in x-direction containing various plugs, and subjected to uniaxial tension σ_o in x-direction.

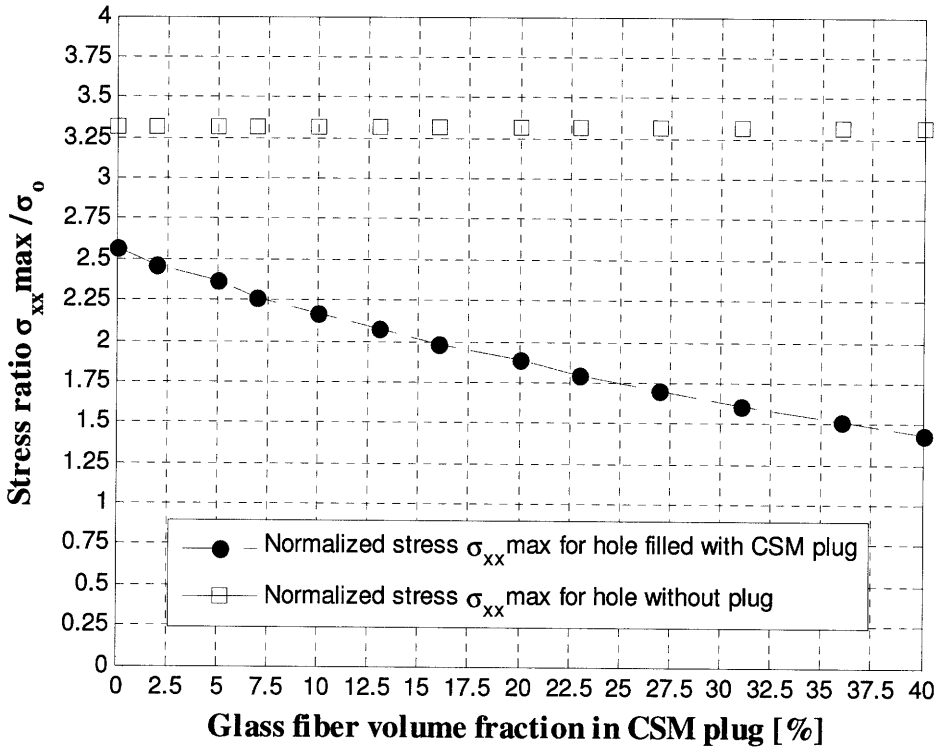

Figure C3: Normalized maximum stress σ_{xx} around edge of hole in laminate of glass fiber / vinyl ester woven roving (WR) biased 60% in x-direction for various chopped strand mat (CSM) plugs, and subjected to uniaxial tension σ_o in x-direction.

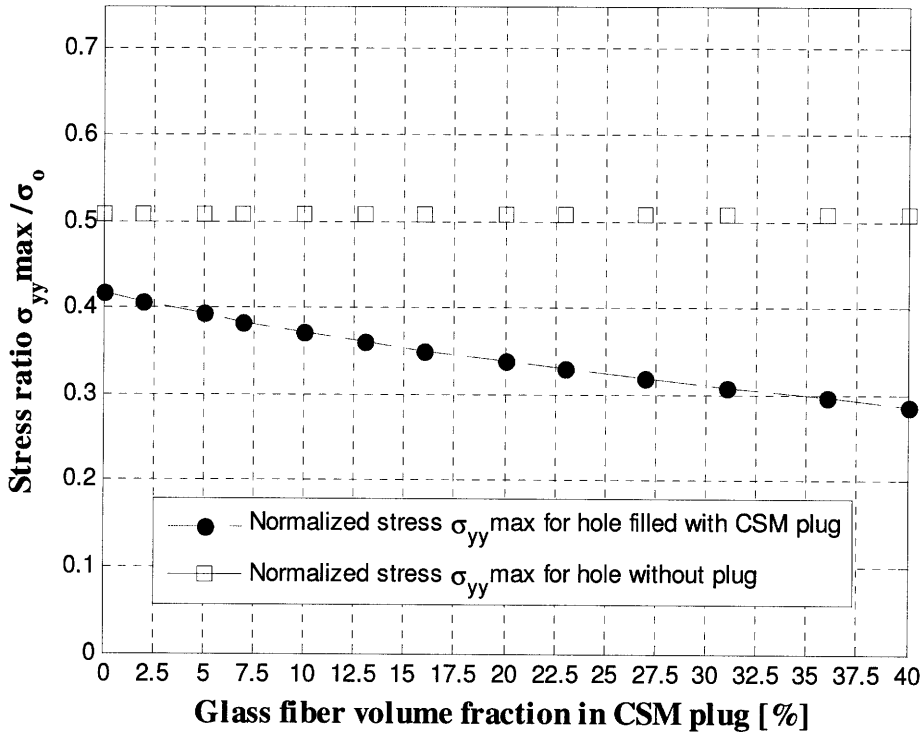

Figure C4: Normalized maximum stress σ_{yy} around edge of hole in laminate of glass fiber / vinyl ester woven roving (WR) biased 60% in x-direction for various chopped strand mat (CSM) plugs, and subjected to uniaxial tension σ_o in x-direction.

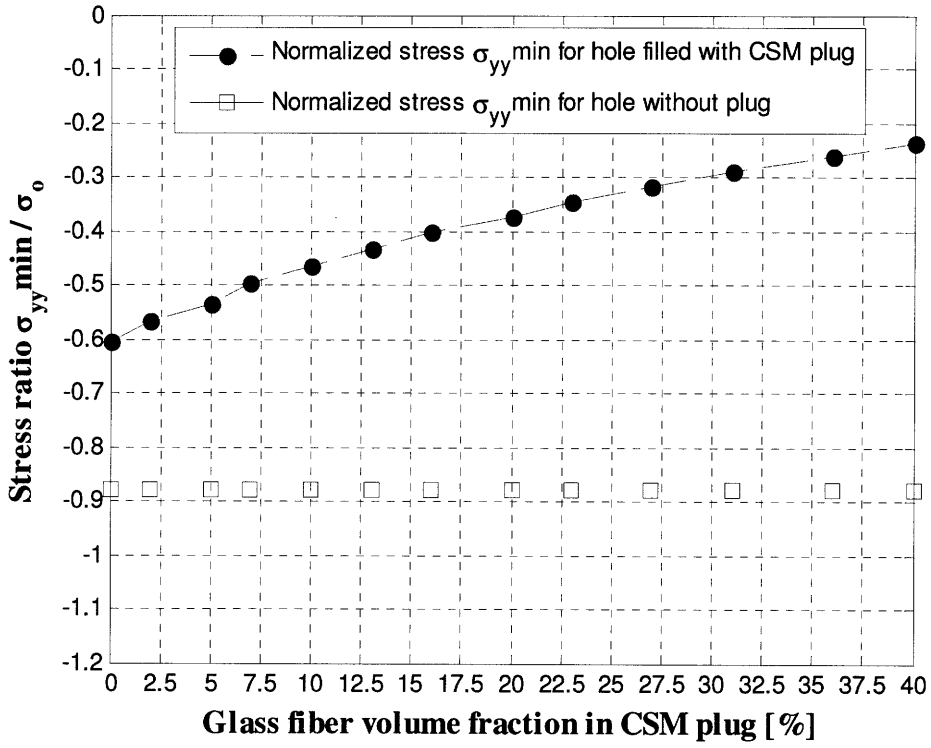

Figure C5: Normalized minimum stress σ_{yy} around edge of hole in laminate of glass fiber / vinyl ester woven roving (WR) biased 60% in x-direction for various chopped strand mat (CSM) plugs, and subjected to uniaxial tension σ_o in x-direction.

C.2 Glass fiber / vinyl ester laminate of woven roving biased 70% in x-direction with circular hole filled with plug of glass fiber / vinyl ester chopped strand mat, subjected to tension in one direction

Figures C6 and C7 show the stresses σ_{xx} and σ_{yy}, respectively, around the hole boundary in a **glass fiber / vinyl ester** laminate of woven roving (WR) biased 70% in the x-direction, containing various plugs of **glass fiber / vinyl ester** chopped strand mat (CSM), and subjected to uniaxial tension σ_o in the x-direction.

Figure C8 displays the effect of an increase of the percentage of **glass fiber** volume fraction in the CSM plug on the maximum tensile stress σ_{xx} around the edge of the hole in a laminate of WR biased 70% in x-direction. Figures C9 and C10 show the effect of an increase of the percentage of fiber volume fraction on the maximum stress σ_{yy} and the minimum stress σ_{yy}, respectively, around the edge of the hole in a laminate of WR biased 70% in x-direction.

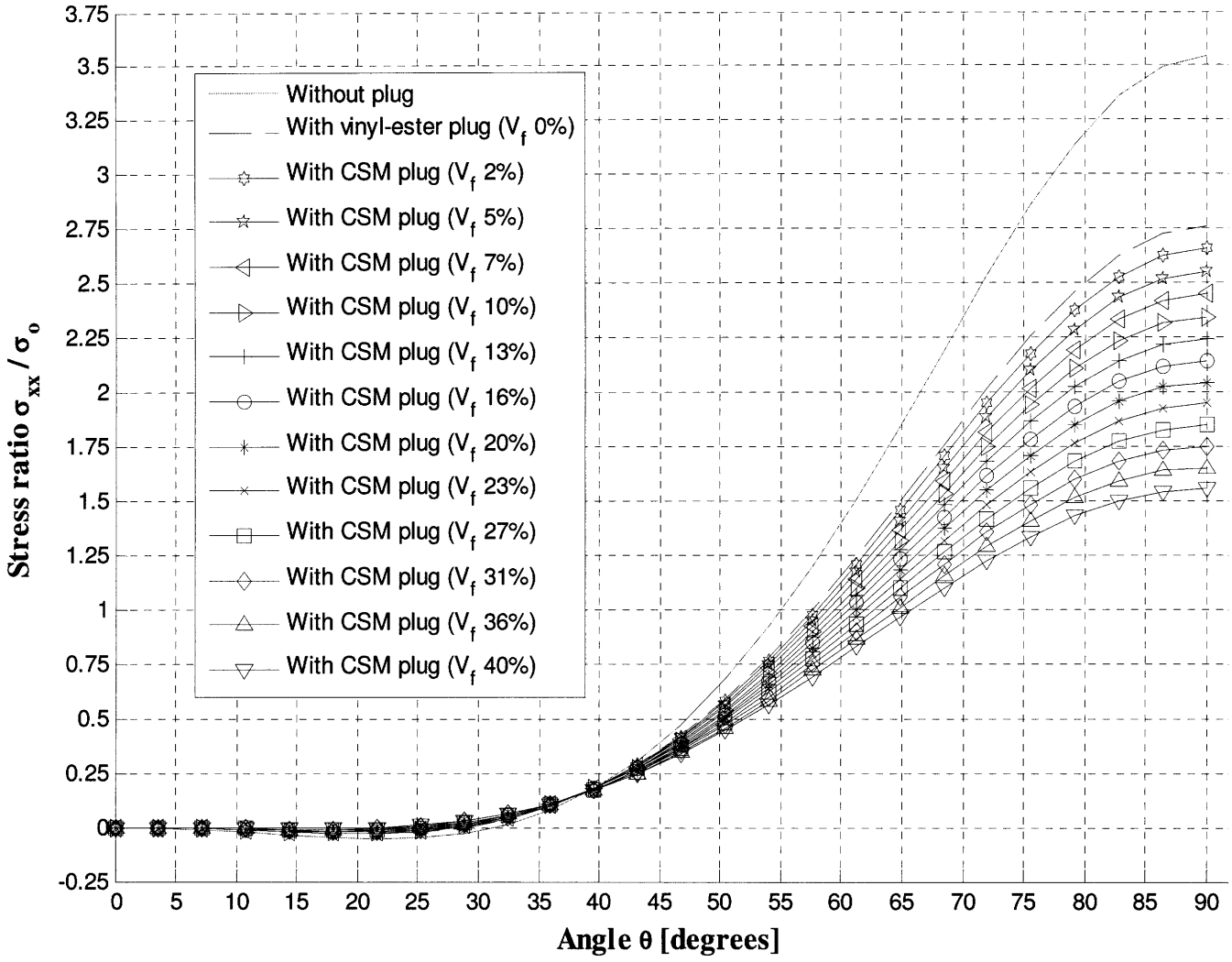

Figure C6: Stress σ_{xx} around hole in glass fiber / vinyl ester laminate of woven roving biased 70% in x-direction containing various plugs, and subjected to uniaxial tension σ_o in x-direction.

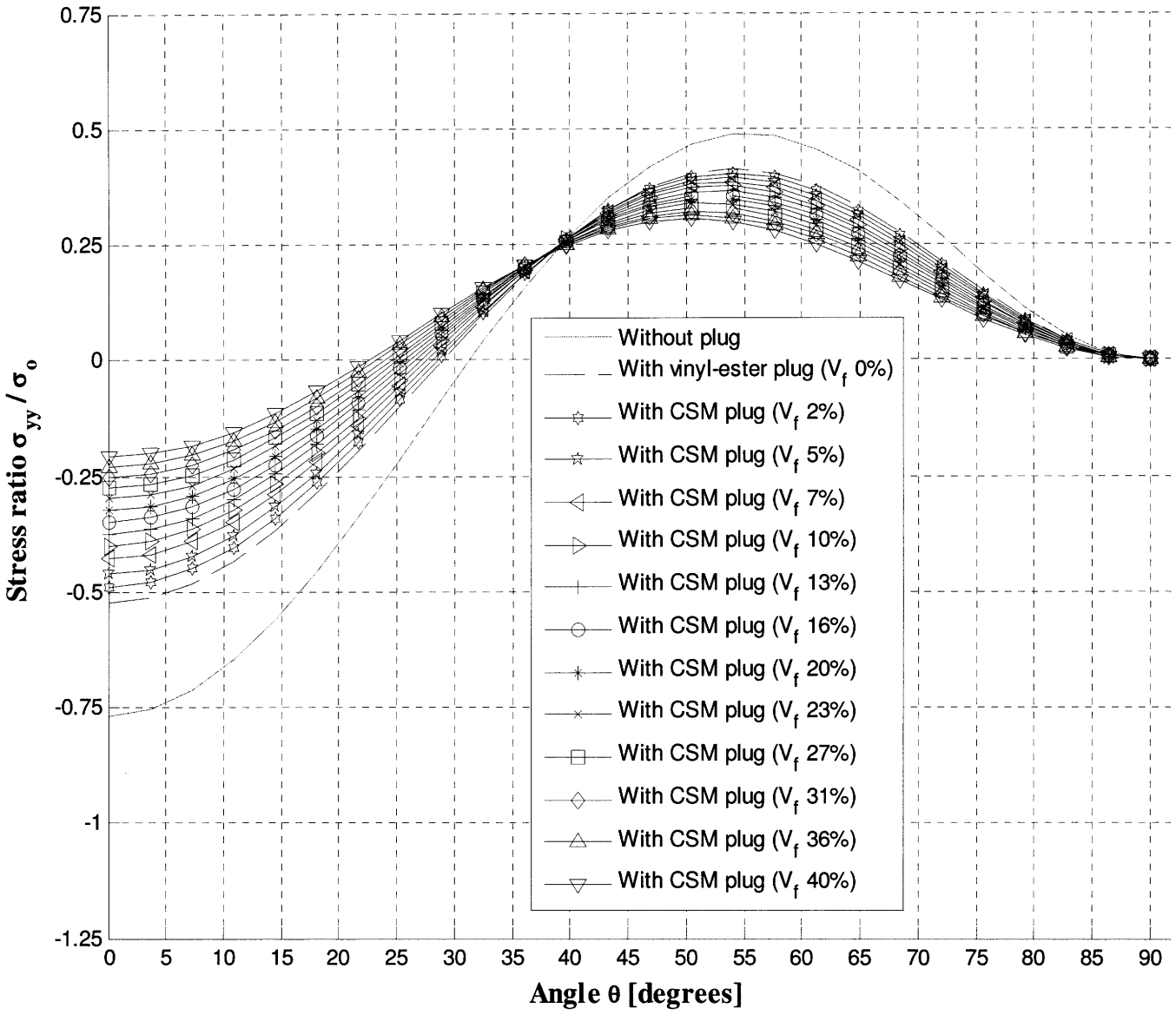

Figure C7: Stress σ_{yy} around hole in glass fiber / vinyl ester laminate of woven roving biased 70% in x-direction containing various plugs, and subjected to uniaxial tension σ_o in x-direction.

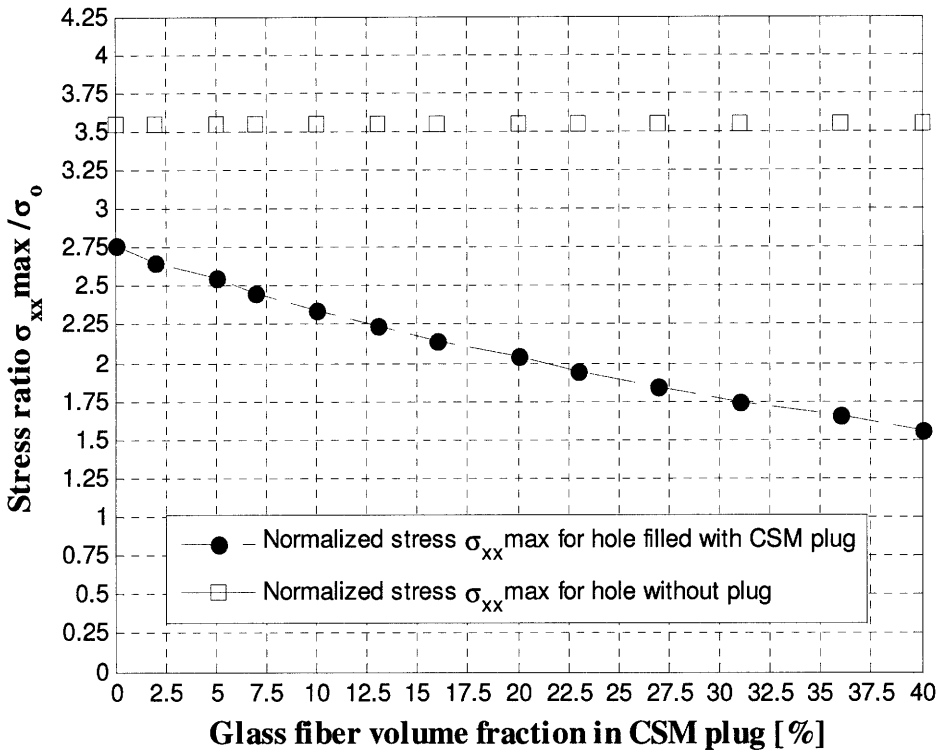

Figure C8: Normalized maximum stress σ_{xx} around edge of hole in laminate of glass fiber / vinyl ester woven roving (WR) biased 70% in x-direction for various chopped strand mat (CSM) plugs, and subjected to uniaxial tension σ_o in x-direction.

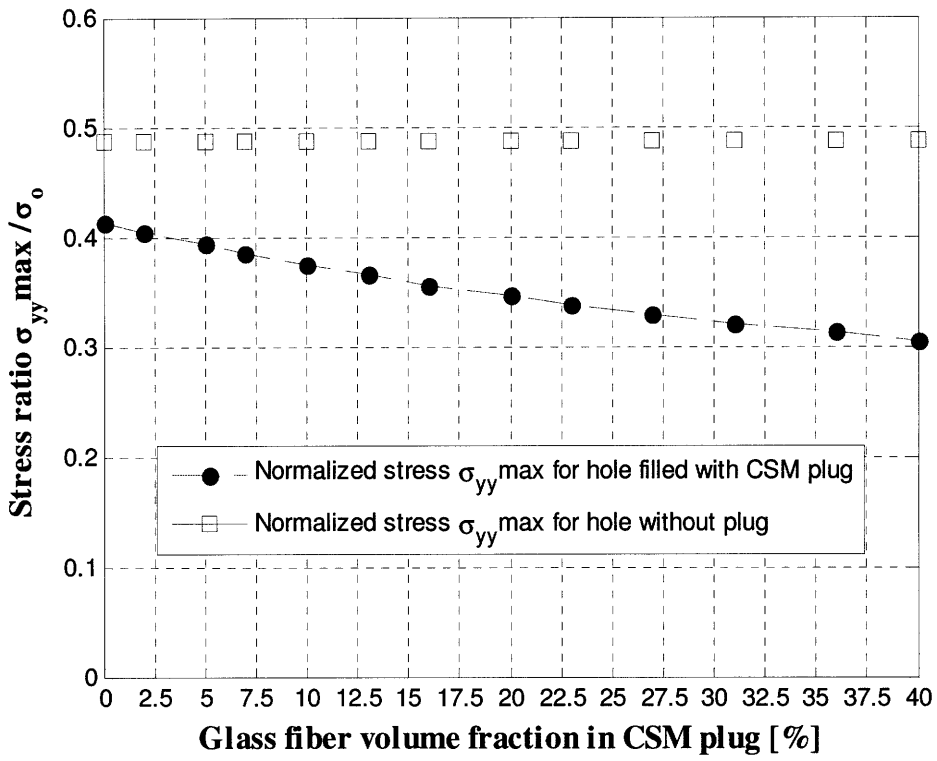

Figure C9: Normalized maximum stress σ_{yy} around edge of hole in laminate of glass fiber / vinyl ester woven roving (WR) biased 70% in x-direction for various chopped strand mat (CSM) plugs, and subjected to uniaxial tension σ_o in x-direction.

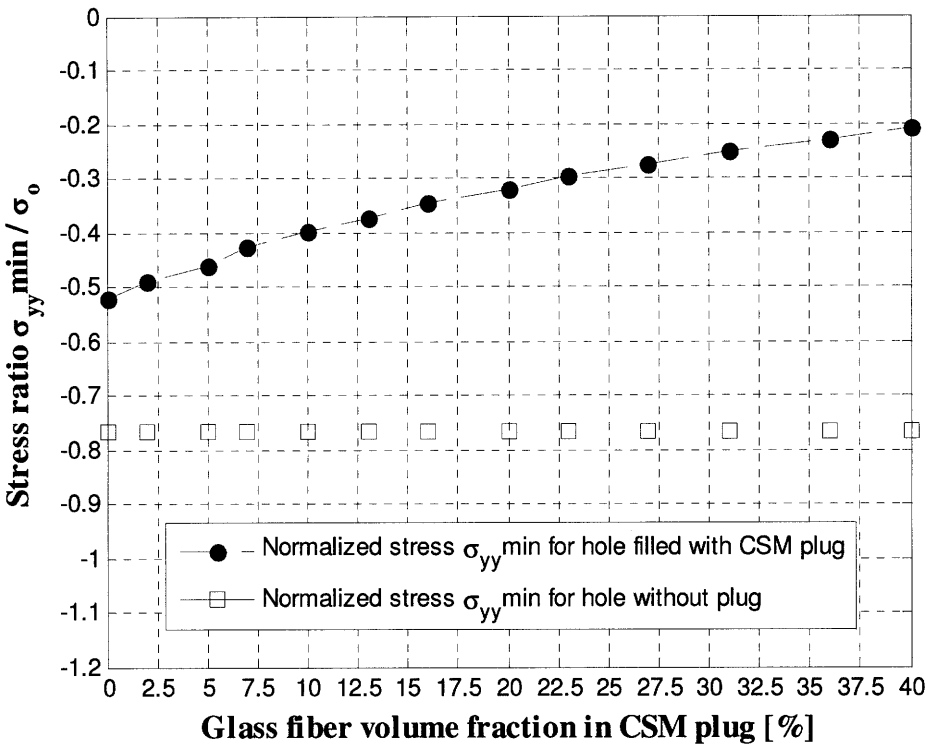

Figure C10: Normalized minimum stress σ_{yy} around edge of hole in laminate of glass fiber / vinyl ester woven roving (WR) biased 70% in x-direction for various chopped strand mat (CSM) plugs, and subjected to uniaxial tension σ_o in x-direction.

C.3 Glass fiber / vinyl ester laminate of woven roving biased 80% in *x*-direction with circular hole filled with plug of glass fiber / vinyl ester chopped strand mat, subjected to tension in one direction

Figures C11 and C12 show the stresses σ_{xx} and σ_{yy}, respectively around the hole boundary in a **glass fiber / vinyl ester** laminate of woven roving (WR) biased 80% in the *x*-direction, containing various plugs of **glass fiber / vinyl ester** chopped strand mat (CSM), and subjected to uniaxial tension σ_o in the *x*-direction.

Figure C13 displays the effect of an increase of the percentage of **glass fiber** volume fraction in the CSM plug on the maximum tensile stress σ_{xx} around the edge of the hole in a laminate of WR biased 80% in *x*-direction. Figures C14 and C15 show the effect of an increase of the percentage of fiber volume fraction on the maximum stress σ_{yy} and the minimum stress σ_{yy}, respectively, around the edge of the hole in a laminate of WR biased 80% in *x*-direction.

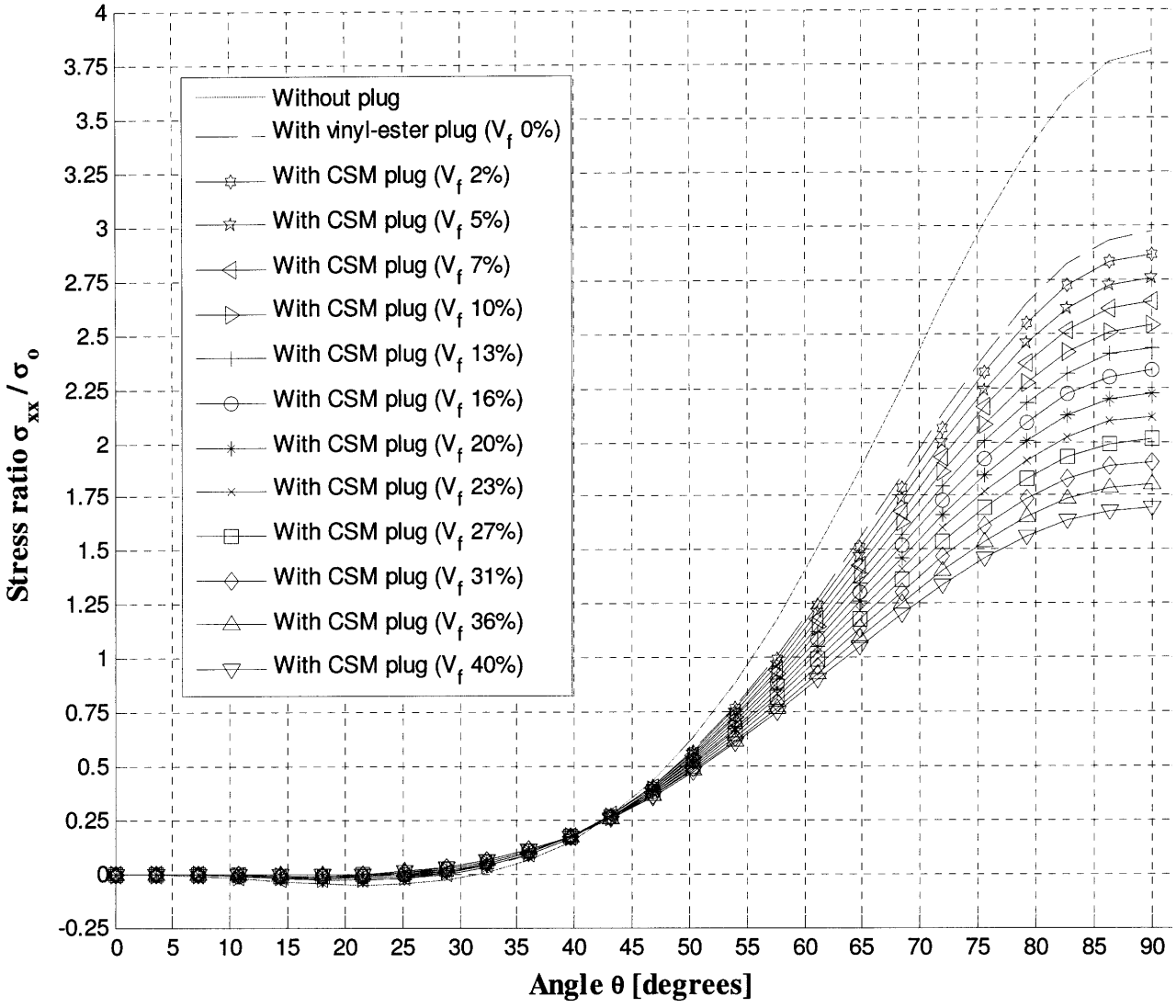

Figure C11: Stress σ_{xx} around hole in glass fiber / vinyl ester laminate of woven roving biased 80% in x-direction containing various plugs, and subjected to uniaxial tension σ_o in x-direction.

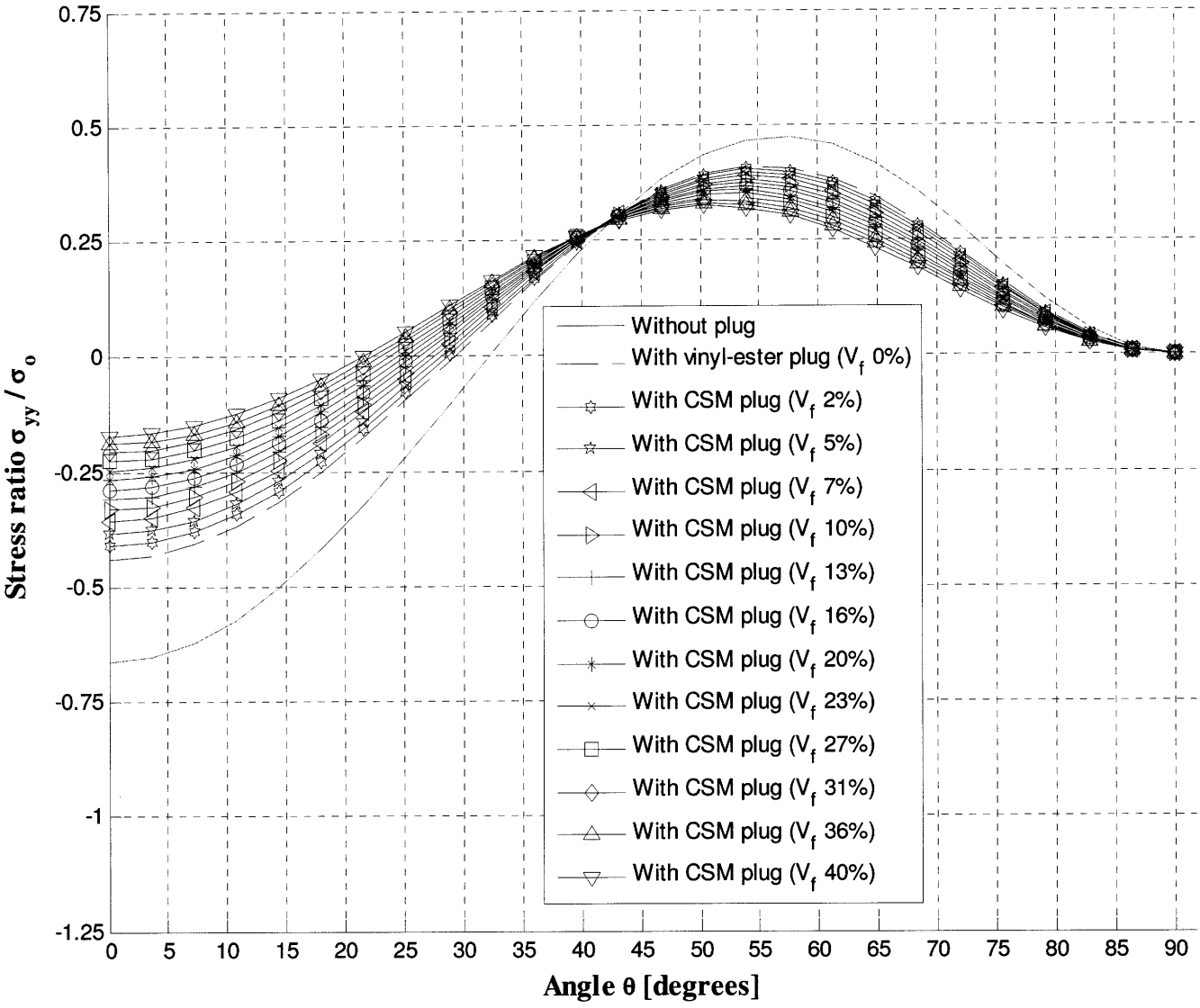

Figure C12: Stress σ_{yy} around hole in glass fiber / vinyl ester laminate of woven roving biased 80% in x-direction containing various plugs, and subjected to uniaxial tension σ_o in x-direction.

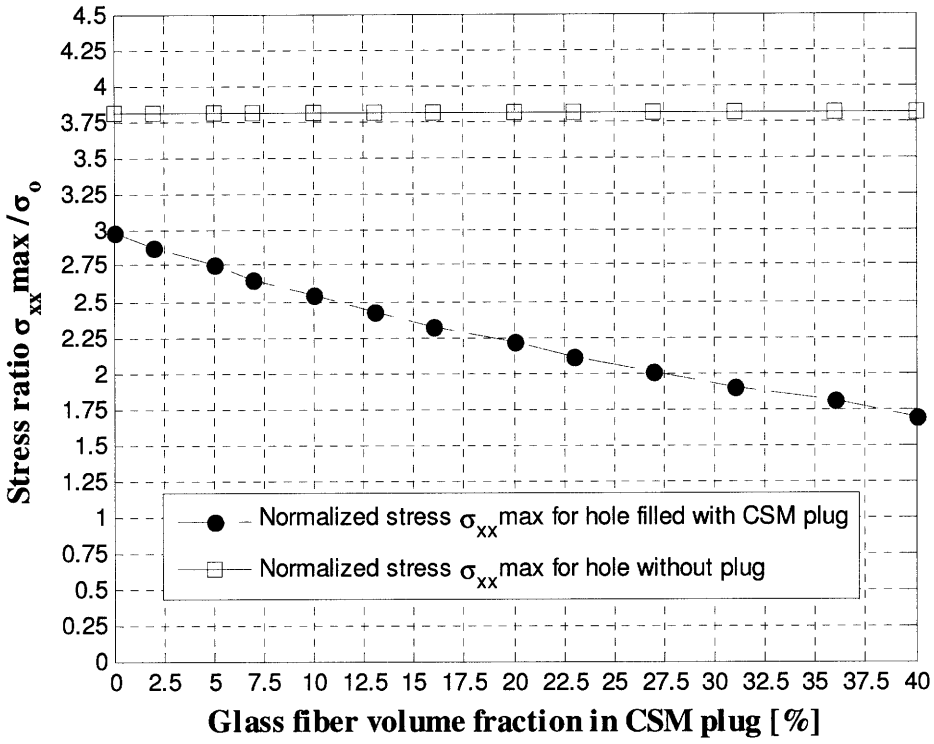

Figure C13: Normalized maximum stress σ_{xx} around edge of hole in laminate of glass fiber / vinyl ester woven roving (WR) biased 80% in x-direction for various chopped strand mat (CSM) plugs, and subjected to uniaxial tension σ_o in x-direction.

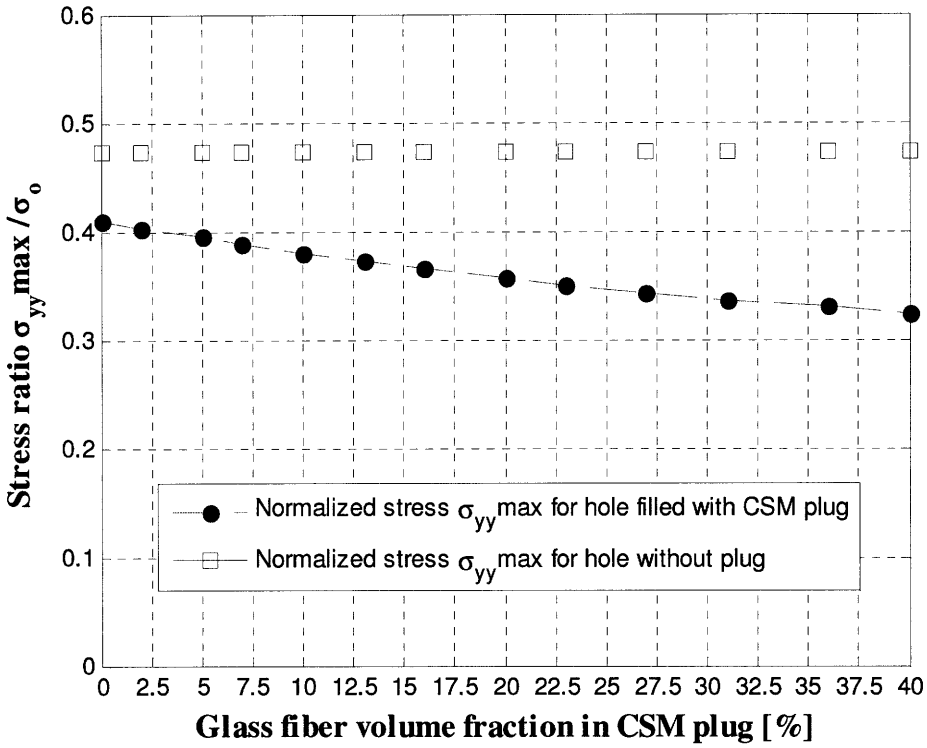

Figure C14: Normalized maximum stress σ_{yy} around edge of hole in laminate of glass fiber / vinyl ester woven roving (WR) biased 80% in x-direction for various chopped strand mat (CSM) plugs, and subjected to uniaxial tension σ_o in x-direction.

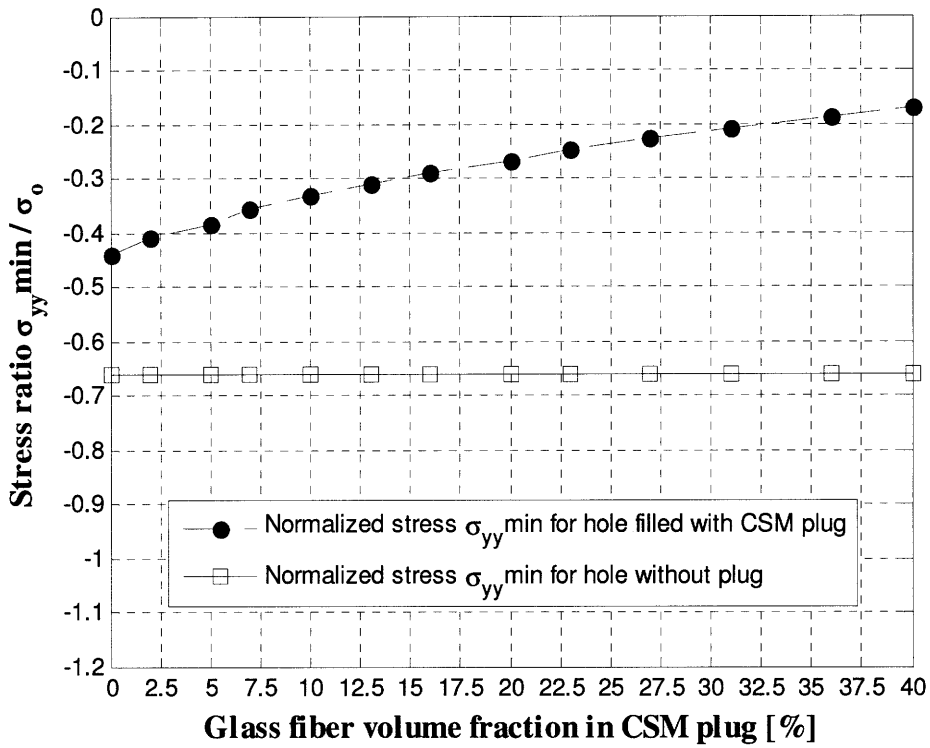

Figure C15: Normalized minimum stress σ_{yy} around edge of hole in laminate of glass fiber / vinyl ester woven roving (WR) biased 80% in x-direction for various chopped strand mat (CSM) plugs, and subjected to uniaxial tension σ_o in x-direction.

C.4 Glass fiber / vinyl ester laminate of woven roving biased 90% in *x*-direction with circular hole filled with plug of glass fiber / vinyl ester chopped strand mat, subjected to tension in one direction

Figures C16 and C17 show the stresses σ_{xx} and σ_{yy}, respectively, around the hole boundary in a **glass fiber / vinyl ester** laminate of woven roving (WR) biased 90% in the *x*-direction, containing various plugs of **glass fiber / vinyl ester** chopped strand mat (CSM), and subjected to uniaxial tension σ_o in the *x*-direction.

Figure C18 displays the effect of an increase of the percentage of **glass fiber** volume fraction in the CSM plug on the maximum tensile stress σ_{xx} around the edge of the hole in a laminate of WR biased 90% in *x*-direction. Figures C19 and C20 show the effect of an increase of the percentage of fiber volume fraction on the maximum stress σ_{yy} and the minimum stress σ_{yy}, respectively, around the edge of the hole in a laminate of WR biased 90% in *x*-direction.

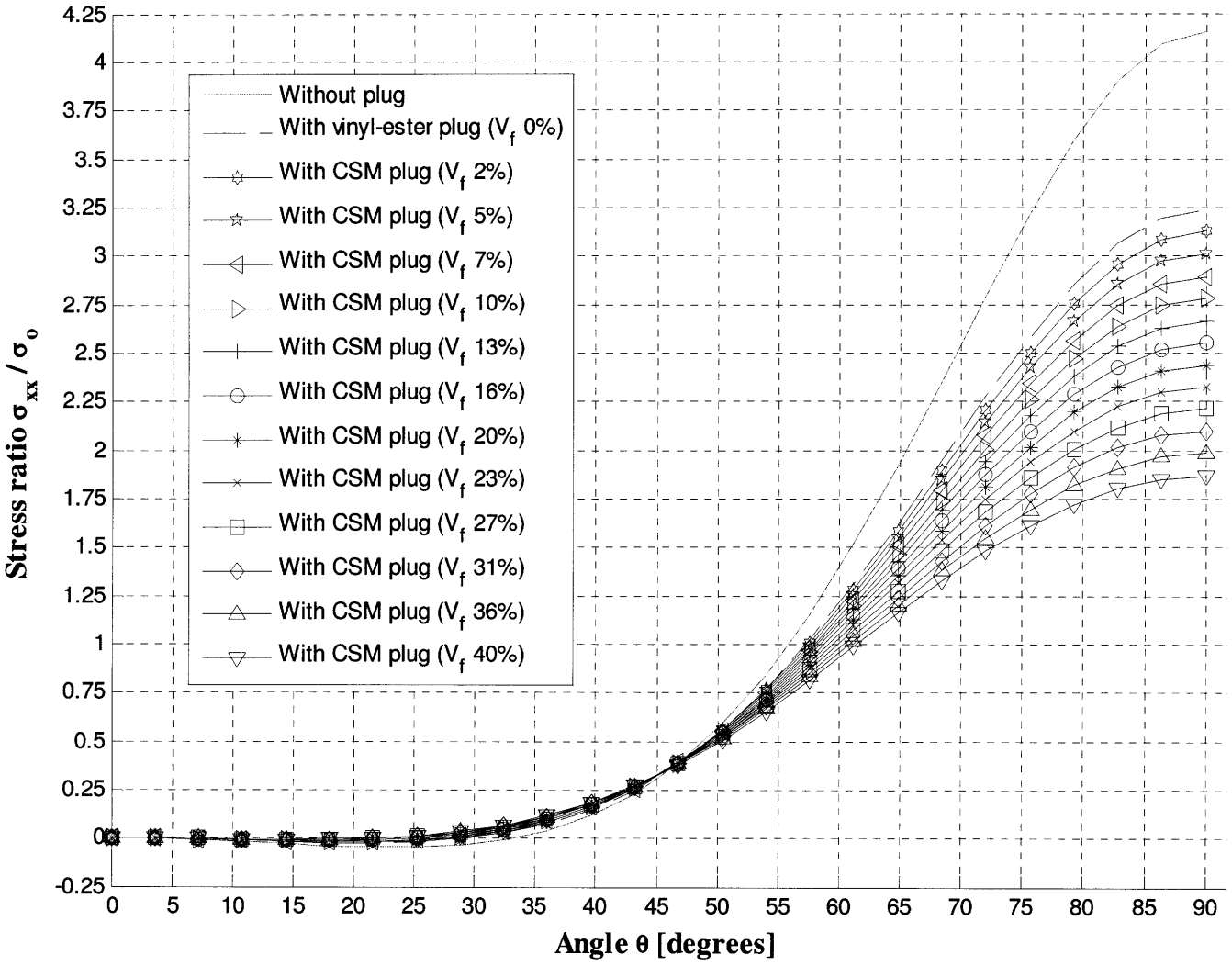

Figure C16: Stress σ_{xx} around hole in glass fiber / vinyl ester laminate of woven roving biased 90% in x-direction containing various plugs, and subjected to uniaxial tension σ_o in x-direction.

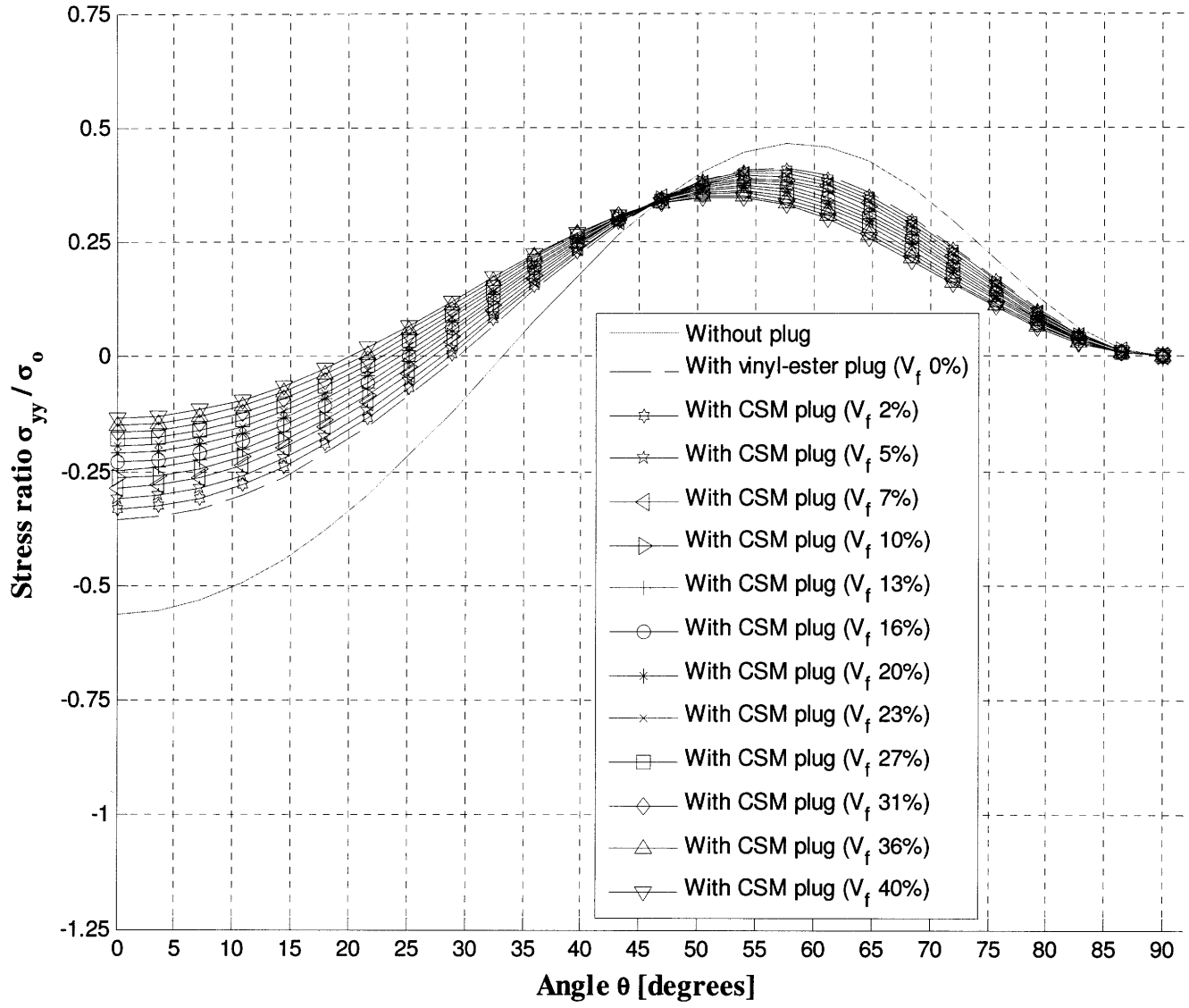

Figure C17: Stress σ_{yy} around hole in glass fiber / vinyl ester laminate of woven roving biased 90% in x-direction containing various plugs, and subjected to uniaxial tension σ_o in x-direction.

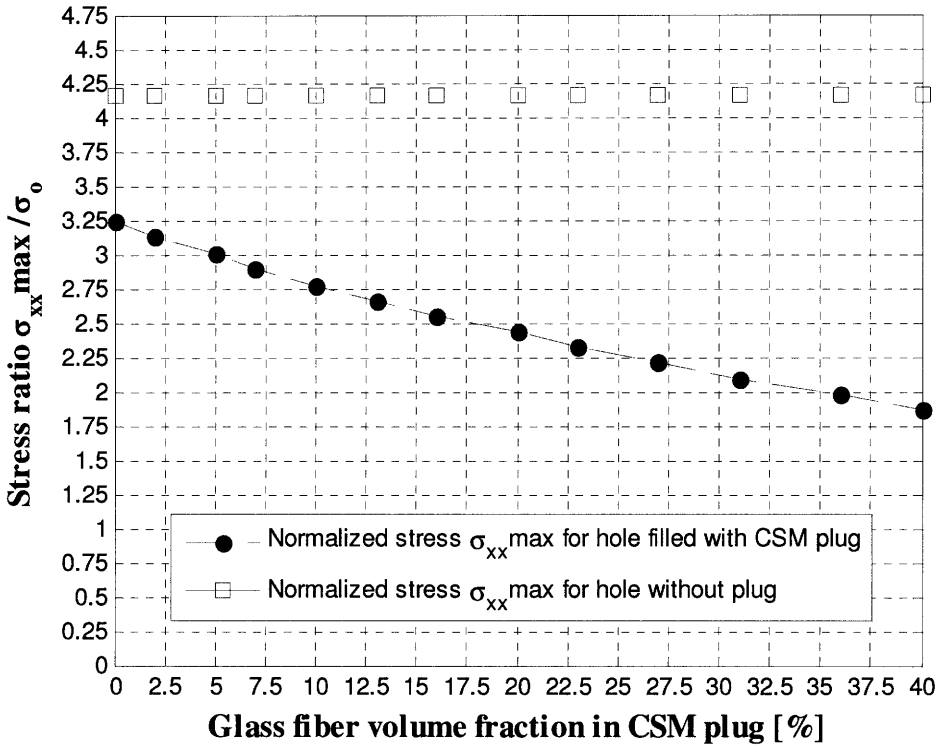

Figure C18: Normalized maximum stress σ_{xx} around edge of hole in laminate of glass fiber / vinyl ester woven roving (WR) biased 90% in x-direction for various chopped strand mat (CSM) plugs, and subjected to uniaxial tension σ_o in x-direction.

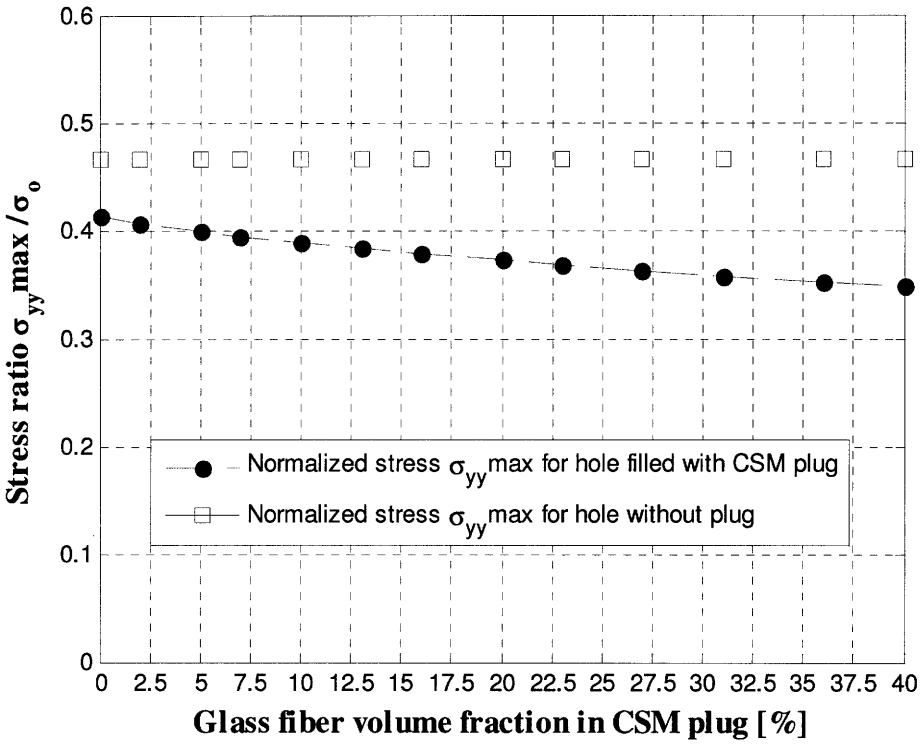

Figure C19: Normalized maximum stress σ_{yy} around edge of hole in laminate of glass fiber / vinyl ester woven roving (WR) biased 90% in x-direction for various chopped strand mat (CSM) plugs, and subjected to uniaxial tension σ_o in x-direction.

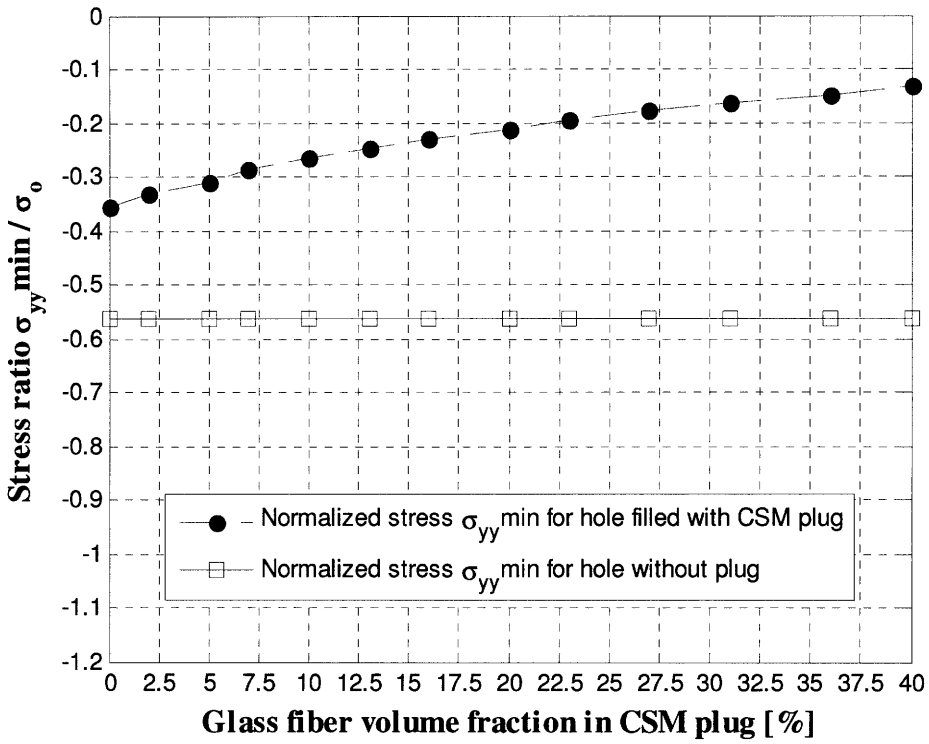

Figure C20: Normalized minimum stress σ_{yy} around edge of hole in laminate of glass fiber / vinyl ester woven roving (WR) biased 90% in x-direction for various chopped strand mat (CSM) plugs, and subjected to uniaxial tension σ_o in x-direction.

C.5 Glass fiber / vinyl ester laminate of unidirectional woven roving aligned with *x*-direction with circular hole filled with plug of glass fiber / vinyl ester chopped strand mat, subjected to tension in one direction

Figures C21 and C22 show the stresses σ_{xx} and σ_{yy}, respectively, around the hole boundary in a **glass fiber / vinyl ester** laminate of unidirectional woven roving aligned with the x-direction, containing various plugs of **glass fiber / vinyl ester** chopped strand mat (CSM), and subjected to uniaxial tension σ_o in the x-direction.

Figure C23 displays the effect of an increase of the percentage of **glass fiber** volume fraction in the CSM plug on the maximum tensile stress σ_{xx} around the edge of the hole in a laminate of unidirectional woven roving aligned with the x-direction. Figures C24 and C25 show the effect of an increase of the percentage of fiber volume fraction on the maximum stress σ_{yy} and the minimum stress σ_{yy}, respectively, around the edge of the hole in a laminate of unidirectional woven roving aligned with x-direction.

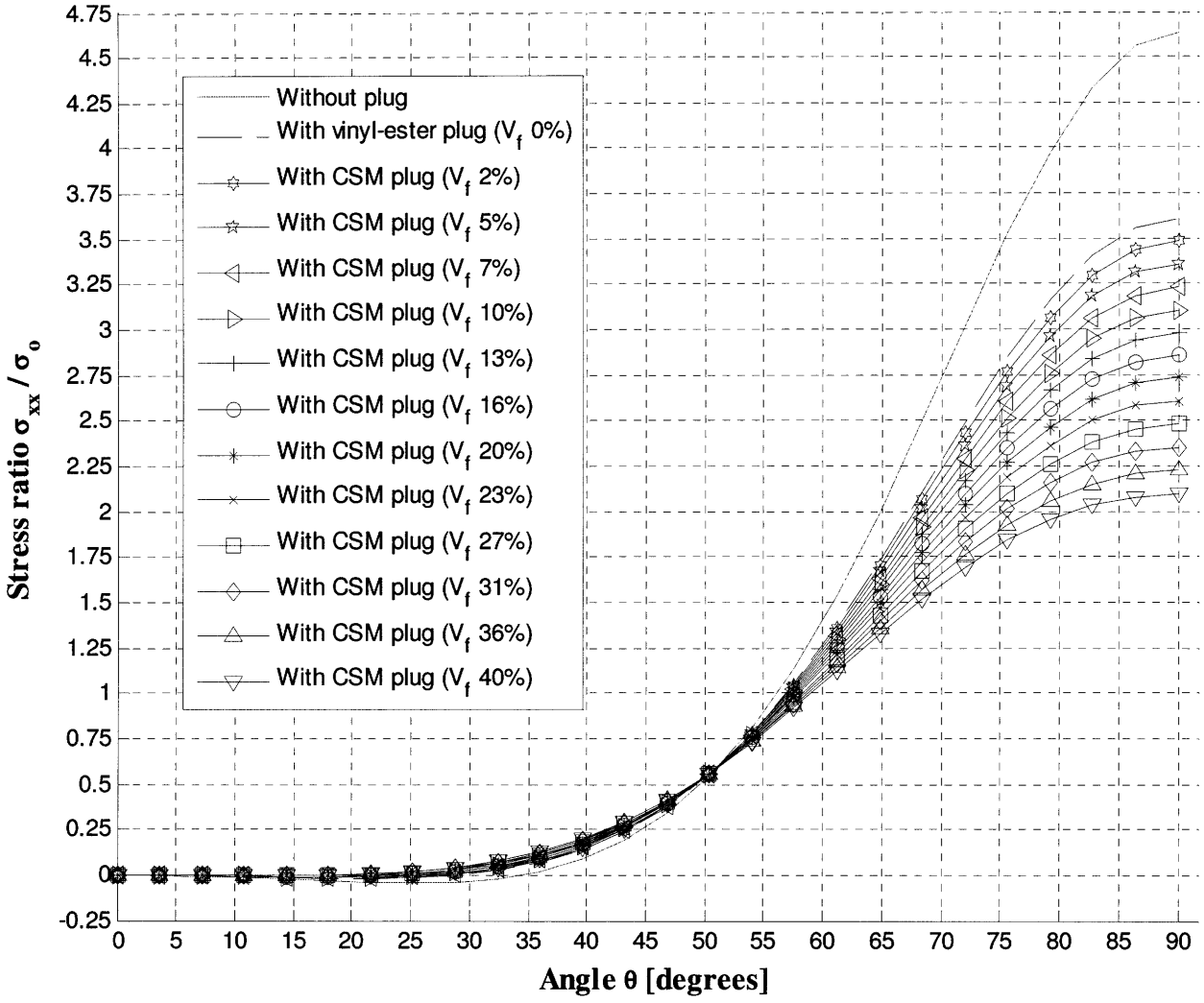

Figure C21: Stress σ_{xx} around hole in unidirectional glass fiber / vinyl ester laminate (aligned with x-direction) containing various plugs, and subjected to uniaxial tension σ_o in x-direction.

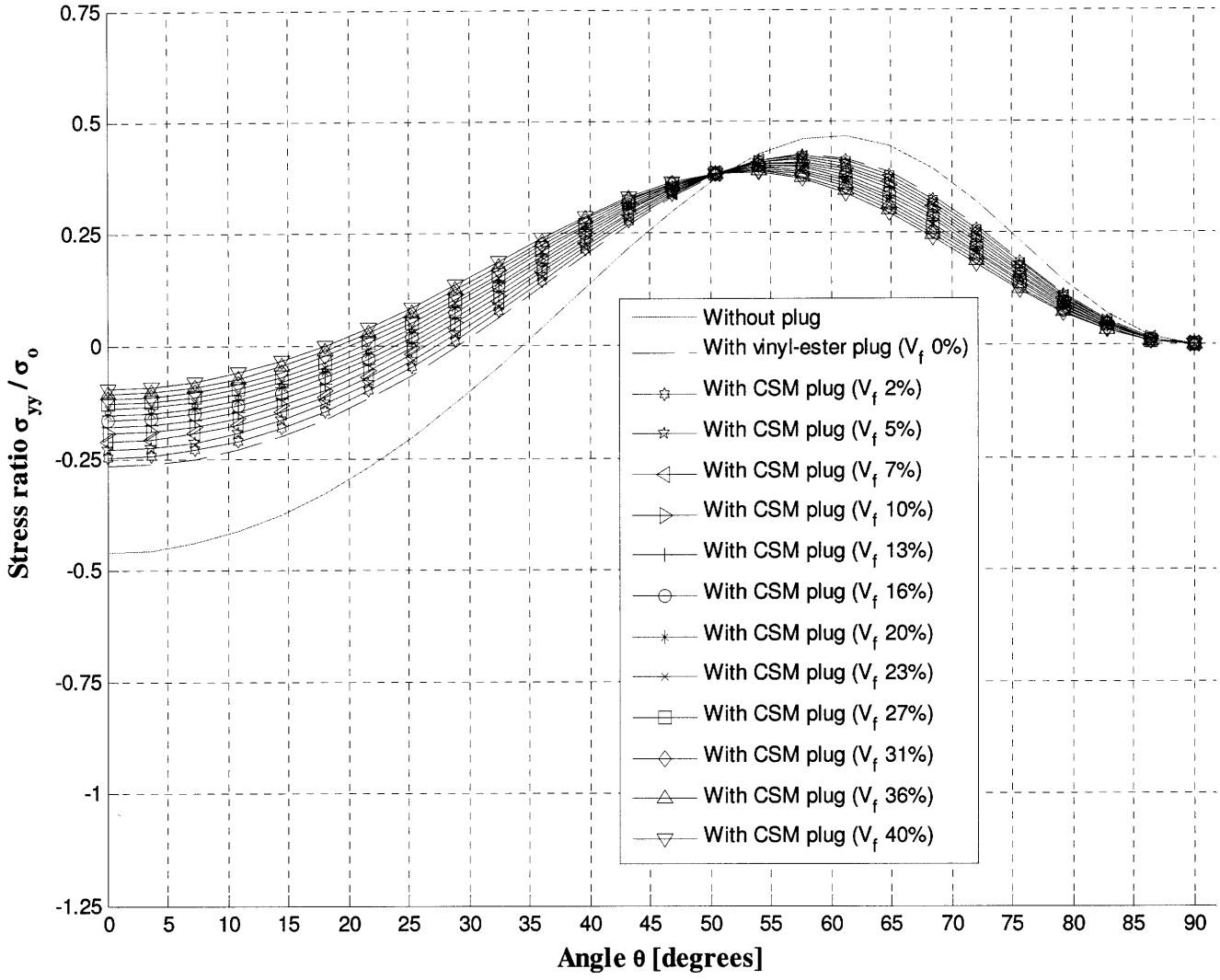

Figure C22: Stress σ_{yy} around hole in unidirectional glass fiber / vinyl ester laminate (aligned with x-direction) containing various plugs, and subjected to uniaxial tension σ_o in x-direction.

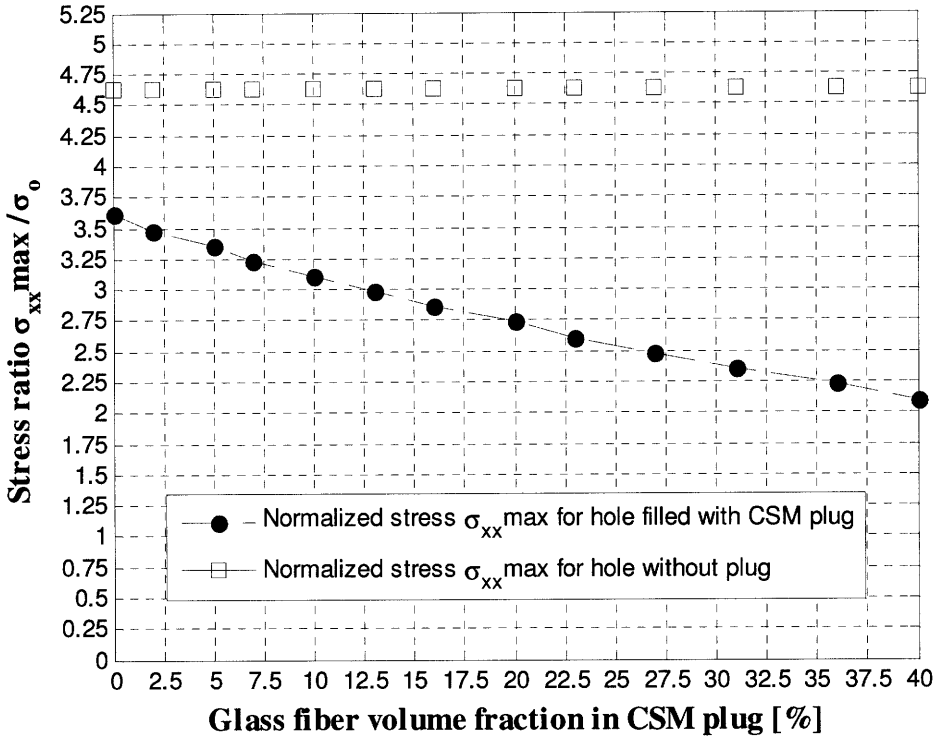

Figure C23: Normalized maximum stress σ_{xx} around edge of hole in unidirectional glass fiber / vinyl ester laminate (aligned with x-direction) for various chopped strand mat (CSM) plugs, and subjected to uniaxial tension σ_o in x-direction.

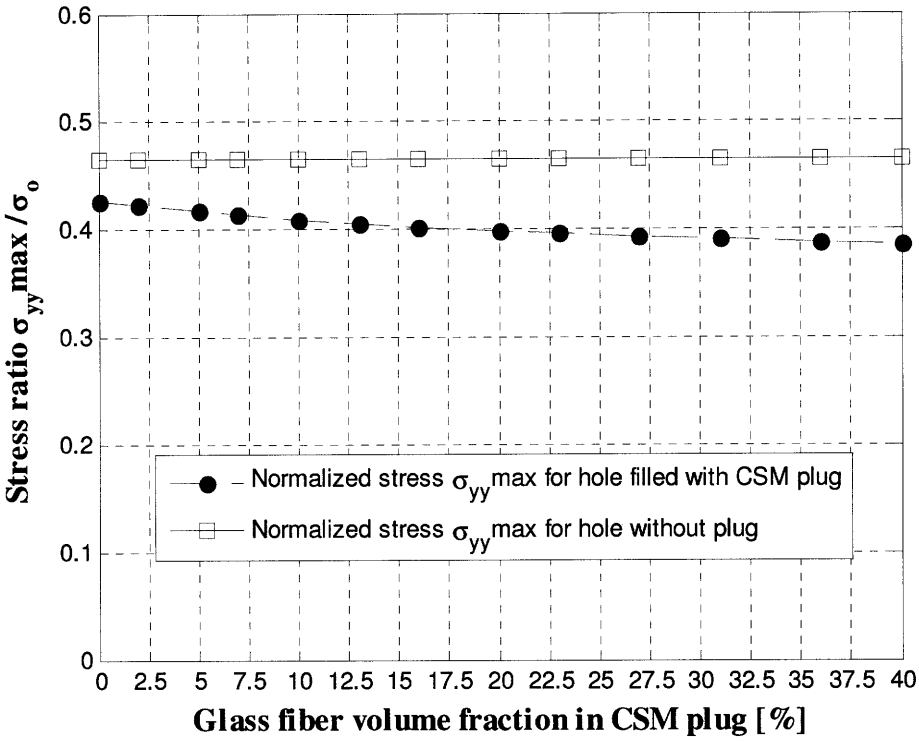

Figure C24: Normalized maximum stress σ_{yy} around edge of hole in unidirectional glass fiber / vinyl ester laminate (aligned with x-direction) for various chopped strand mat (CSM) plugs, and subjected to uniaxial tension σ_o in x-direction.

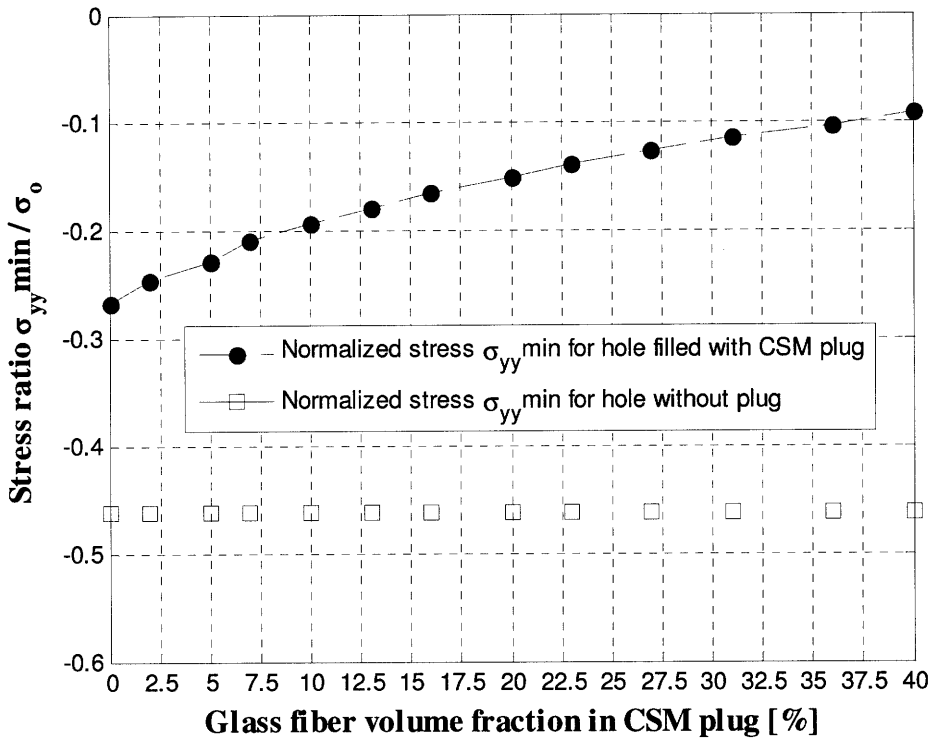

Figure C25: Normalized minimum stress σ_{yy} around edge of hole in unidirectional glass fiber / vinyl ester laminate (aligned with x-direction) for various chopped strand mat (CSM) plugs, and subjected to uniaxial tension σ_o in x-direction.